Master Thesis, Department of Geosciences

Reservoir quality preserving processes in Lower Jurassic Cook Formation of Veslefrikk area (Rigel prospect)

A petrophysical, sedimentological and petrographical perspective

Syed Moiz Hasnain

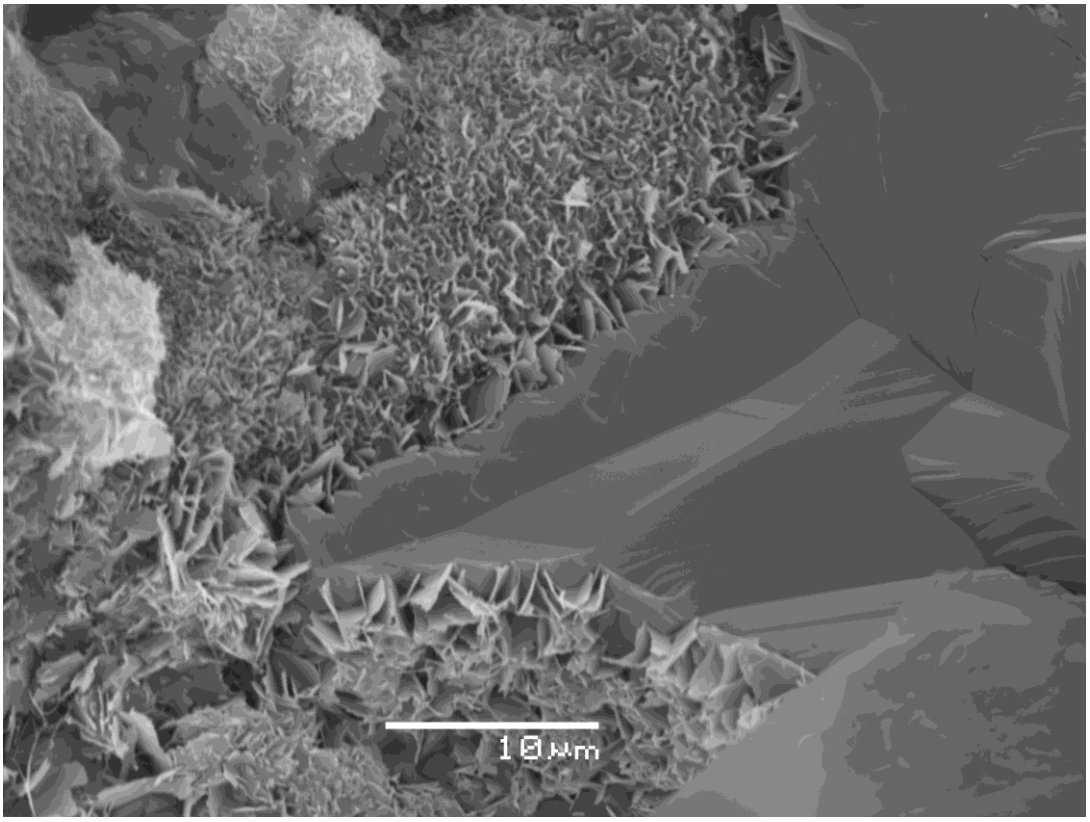

UNIVERSITY OF OSLO

FACULTY OF MATHEMATICS AND NATURAL SCIENCES

Reservoir quality preserving processes in Lower Jurassic Cook Formation of Veslefrikk area (Rigel prospect)

A petrophysical, sedimentological and petrographical perspective

Syed Moiz Hasnain

Master Thesis in Geosciences

Discipline: Sedimentology

Department of Geosciences

Faculty of Mathematics and Natural Sciences

University of Oslo

15.06.2015

Supervisors: Jens Jahren (UiO) and Richard Olstad (Tullow Oil)

This work is published digitally through DUO – Digitale Utgivelser ved UiO

http://www.duo.uio.no

It is also catalogued in BIBSYS (http://www.bibsys.no/english)

Acknowledgement

Thanks to Almighty ALLAH, the most Beneficent, the most Merciful.

First of all, I would like to thank my Supervisor Associate Professor Jens Jahren for his support, guidance and pleasant mood during this thesis. Thanks to Knut Bjørlykke and other teachers of the Geoscience Department and all the class fellows who will always remain in my affable memories. Thanks to Richard Olstad and Tullow Oil Norge AS for financing and organizing this study.

Thanks to Berit Løken for patience and guidance during long, cold days in SEM lab. Thanks to Kjemi, Beyene Girma Haile and Maarten Aerts for valuable discussions. Special thanks to Ásta Soffía for all the motivation, proofreading of this thesis and valuable feedback.

Special thanks to Saadullah Nisar, Uzair Naqvi, Asad Khan Khattak, Tauqeer Ahmed Saadi, and Abduljabbar for making this duration of study amazing and memorable.

Thanks to the most important people in my life and to whom I owe everything, my parents, I thank you for everything that I have now and for everything that I will achieve in the future. Thank you Ammi, Abbu, Yousra, Nabeel, Ebtehaj, Wahaj, and Abdullah for your love and positive expectations.

June 2015, Oslo

Syed Moiz Hasnain

Abstract

Lower Jurassic Cook Formation is an important hydrocarbon reservoir in northern North Sea due to its anomalously high porosity at depths around 3000 meters. This study presents information about the depositional environment, petrographic and petrophysical properties, and reservoir quality of Cook Formation in Oseberg and Veslefrikk area.

Reservoirs of Brent and Dunlin groups have been studied by examination of cores from three wells. Reservoir intervals are studied by electrical logs, sedimentological core description, quantitative bulk and clay XRD analysis, optical point counting and SEM analysis. The main goal has been to study the relation between depositional environment, diagenesis, quartz cementation and formation of chlorite precursor.

The Cook Formation consists of several depositional settings because of its extensive lateral distribution. In Veslefrikk area it has been interpreted as prograding delta deposit, while in Oseberg are, it is observed as upper shoreface deposit. Sandstones in Cook Formation have overall quartz dominant mineralogy with some carbonate cemented intervals. Kaolinite, chlorite and illite are major clay minerals found.

Well developed and extensive chlorite grain coats were observed in Veslefrikk area causing quartz inhibition and porosity preservation. Reservoir quality of Cook Formation is moderate to good in Veslefrikk area. In Oseberg area, sandstones are observed to be more porous and cleaner indicating good reservoir quality.

The formation of iron-rich clay precursor in Veslefrikk area has been suggested mainly by mechanical infiltration of clay suspensions and by minor possible contribution from bioturbation. Chlorite coating or precursor was not observed in Oseberg area, possibly due to the erosion during reworking.

Prediction of chlorite coating in deeply buried reservoirs is difficult. If the relation between depositional environment and formation of chlorite precursor is understood, then prediction and mapping of chlorite coatings in intermediate to deeply buried reservoirs can become possible.

Table of Contents

1. Introduction 1
   1.1 Introduction 2
   1.2 Methodology and purpose 3
   1.3 The Study Area 4
2. Geological setting of the area 5
   2.1 Stratigraphy 8
   2.2 Cook Formation 10
   2.3 Depositional environments of Cook Formation 10
3. Processes effecting reservoir characteristics 13
   3.1 Introduction 14
   3.2 Near surface diagenesis 14
   3.3 Mechanical compaction 15
   3.4 Chemical compaction 15
4. Porosity preserving processes 17
   4.1 Introduction 18
   4.2 Authigenic Chlorite 18
   4.3 Illite or Illite/Chlorite Coatings 20
   4.4 Micro-Quartz 20
   4.5 Hydrocarbon emplacement 21
5. Methodology 23
   5.1 Introduction 24
   5.2 Petrographic analysis 24
      5.2.1 Point counting and Grain size analysis 24
      5.2.2 Scanning Electron Microscope (SEM) 24
      5.2.3 XRD Analysis 25
      5.2.4 Limitations of petrographic analysis 25
   5.3 Petrophysical analysis 26
      5.3.1 Well correlation and interpretation of well logs 26
      5.3.2 Cross plotting and histogram 26

5.3.3 Limitations of petrophysical evaluation....26
5.4 Core description....26
6. Petrophysical results....27
6.1 Well correlation and producing formations....28
6.1.1 Well 30/3-4....28
6.1.2 Well 30/3-5S....29
6.1.3 Well 30/6-17A....29
6.2 Petrophysical properties....29
7. Sedimentological analysis and results....35
7.1 Introduction....36
7.2 Facies analysis of Cook Formation....36
7.3 Facies association....40
7.3.1 Tidal channel deposits (B1/C1/C2)....40
7.3.2 Shoreface sandstones (A1/A2)....40
7.3.3 Mouth bar deposits (B2)....41
7.3.4 Tidal Sand flat (B3)....41
7.3.5 Tidal mud flat (B4)....41
8. Petrographic results....43
8.1 Introduction....44
8.2 Texture and composition....44
8.3 Grain size and Sorting....46
8.4 Intergranular volume....54
8.5 SEM Petrography....58
9. Discussion....67
9.1 Introduction....68
9.2 Depositional environment of Cook Formation....68
9.3 Petrography....69
9.3.1 Porosity observations....70
9.3.2 Grain size....71
9.4 Mineralogy....72

9.5 Clay mineralogy 72
9.5.1 Chlorite 72
9.5.2 Kaolinite 76
9.5.3 Illite 77
9.6 Cook Formation as a reservoir 77
9.6.1 Depositional environment 77
9.6.2 Mechanical compaction 78
9.6.3 Diagenetic processes 79
10. Conclusions 81
11. References 83
12. Appendices 91
Appendix A: Sedimentological logs 92
Appendix B: Chlorite composition and TVD for samples from well 30/3-5S 94

1. Introduction

1.1 Introduction

This thesis is a part of collaboration between University of Oslo and Tullow Oil Norge AS. The aim of this report is to improve the understanding and prediction of reservoir quality in deep Jurassic sandstones in Veslefrikk area of northern North Sea.

Highly porous and permeable sandstones at depths between 2000 to 4000 metres below sea floor are considered significantly important for hydrocarbon exploration. Such sandstones have proved to be very good reservoirs worldwide. Sandstones are not always easy for exploration until their properties as a reservoir rock are fully understood.

A subsurface rock having effective porosity and permeability to produce commercially feasible quantities of petroleum is considered a 'Reservoir'. Reservoir characterization is a process in which the quality of reservoir is determined by utilizing various geological methods. For a quality reservoir, porosity and permeability are the properties of prime importance. Porosity is interstitial void space in the rock and permeability is the property of rock which determines the ease to fluid flow. Porosity plays its part in storing the fluid and permeability plays its role in transmitting the fluid through the rock in response to applied pressure. Capillary pressure is another property which can be defined as the attraction between the surfaces of solids and liquids in a rock, resulting in the resistance to flow of fluid (Slatt, 2013).

The amount of porosity and permeability varies significantly depending upon the mineralogical composition of rock, grain size, depositional environment, and post deposition conditions which includes depth of burial, compaction, and temperature. Compaction is a porosity reducing phenomenon which takes place in two ways i.e. mechanical and chemical (which includes quartz cementation) (Bjørlykke and Jahren, 2010). Mechanical compaction takes place simply due to the burden of overlying rocks. In mechanical compaction brittle grains are broken in small fragments and adjacent pore spaces are occupied by these broken pieces. After sometime, grains find more contact points and achieve a more robust setting making the rock harder for further mechanical compaction.

Chemical compaction resulted by quartz cementation is considered the most common phenomenon for porosity reduction. Sandstone reservoirs located deeper than 2 kilometres in sedimentary basins with normal geothermal gradients are affected by quartz cementation (Bjørlykke and Jahren, 2010).

1.2 Methodology and purpose

The purpose of this study is to improve the understanding of controlling factors of chlorite coatings in deep Jurassic sandstones in northern North Sea. This will help in prediction of the reservoir quality of sandstone in Veslefrikk area. A total of 328 meters of cores from two wells in Veslefrikk area (30/3-4 and 30/3-5S) and one well in Oseberg area (30/6-17A) (Figure 1.1) were selected for study. 28 samples were selected from the study interval and these samples were studied through point-counting, X-ray diffraction (XRD), sedimentological core description, and Scanning Electron Microscope (SEM).

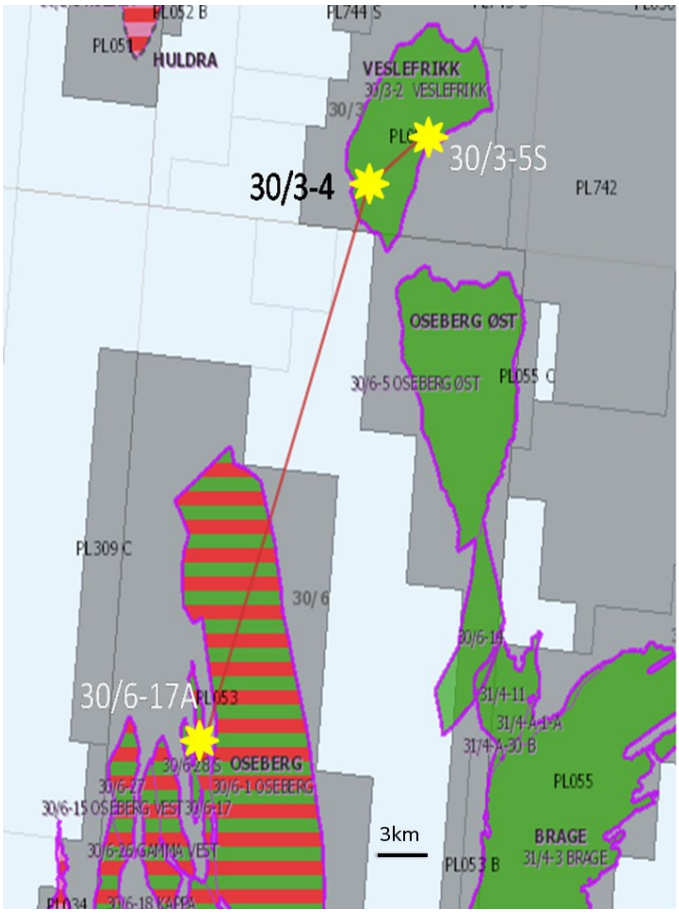

Figure 1.1 Location of Study wells in Veslefrikk and Oseberg Area.

1.3 The Study Area

On the eastern side of North Viking graben, Veslefrikk field is situated at blocks 30/3 and 30/6 of Norwegian sector. It is located around 30 km north of Oseberg in Northern part of North Sea (Figure 1.3).Production licence was awarded in 1979. Originally it contained 54.1 million Sm^3 oil and 5.7 billion Sm^3 gas. Reservoir rocks in this area are mostly Jurassic Sandstones from Dunlin group, Brent group, and Statfjord Formation.

Around 80% of the reserves are contained in Brent group making it the main reservoir. The depth of reservoirs ranges between 2800 to 3200 meters. Water depth in this area is about 185 metres. Reservoir quality is variable in places from moderate to excellent. Production in this field is taking place by the help of pressure support from water alternating gas injection in Dunlin and Brent reservoirs, whereas with gas injection in Statfjord Formation (Norwegian Petroleum Directorate, 2014).

Veslefrikk field occurs in Jurassic sandstones. This area consists of normal faults. Major faulting was ceased by the end of Jurassic. This field is located on the crest of a tilted horst block (Lundegard, 1994). Oil production is declining from Veslefrikk but gas production is expected to increase in future (Figure 1.2). New development wells are being planned and drilling rig has been upgraded (Norwegian Petroleum Directorate, 2014).

Figure 1.3 Location of Veslefrikk oil field (Statoil, 2013)

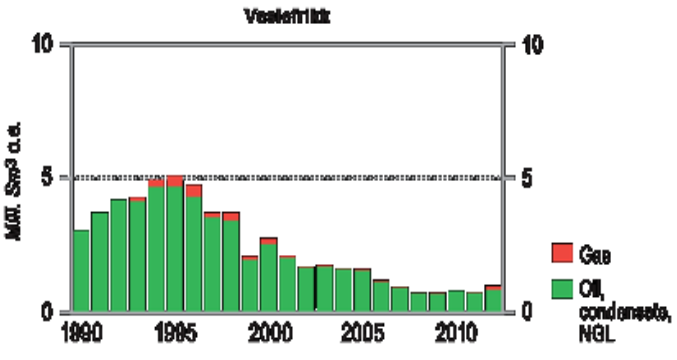

Figure 1.2 Production from Veslefrikk oil field (Norwegian Petroleum Directorate, 2014).

2. Geological setting of the area

On May 20, 1964 German consortium initiated the drilling of first offshore well called Nordsee B-1andmarked the beginning of exploration in North Sea (Brennand et al., 1998). Until December 2013, recoverable resources were estimated around 9.3 billion Sm^3 of oil equivalents (Norwegian Petroleum Directorate, 2013).

Northern North Sea is north-south oriented and 150-200 km wide zone of extended crust (Fjeldskaar et al., 2004). According to Faleide and Berge (2000) crustal architecture of the area is generally the result of two lithospheric extension events and their related thermal subsidence episodes. The area is characterised by the features that are related with thinning and extension of crust such as, sedimentary basins in asymmetric half grabens and large rotated fault blocks (Fjeldskaar et al., 2004).

North Sea is an area with complex tectonic history. The main trend of the region is transformation of an area with massive mountain belts into an area of extensive rifting. Salt tectonics is another feature of the area which is quite important for hydrocarbon accumulation in southern North Sea (Lyngsie et al., 2006). North Sea experienced the collision of three plates during Caledonian orogeny in middle Palaeozoic. As suggested by Lyngsie et al. (2006) this area is influenced by four major tectonic events since Cambrian i.e., (1) Caledonian collision between Late Ordovician to Early Silurian, (2) following rifting and basin formation mainly during Carboniferous to Permian, (3) Mesozoic rifting, (4) inversion from Late Cretaceous to Early Tertiary.

Architectural framework of the northern North Sea was first shaped by major Permo-Triassic rifting event. In present days its rift axis is thought to be under Horda Platform. Many of the master faults produced during first episode (Permo-Triassic) were reactivated during the second episode of rifting. This episode was initiated around late Middle Jurassic and its centre was under present day Viking Graben (Christiansson et al., 2000). Second phase of rifting was triggered by the thinning of lithosphere beneath North Sea caused by a mental head plum during Middle Jurassic. Rifting initiated in the South and then propagated towards the North (Glennie and Underhill, 1998). Permo-Triassic episode of rifting and subsidence had not reached to equilibrium before the second episode initiated (Badley et al., 1988, Gabrielsen et al., 1990).

A very important feature of the North Sea with respect to hydrocarbons is Viking Graben. It is a Mesozoic rift system but rifting in this area predates the Caledonian orogenic extensional collapse and is characterized by two main rifting phases since Devonian (Rupke et al., 2008). Viking Graben is better understood now due to the advancements in understanding of rift basin formation along with increased availability of seismic and well data across this area. On these basis two rifting episodes have been recognised, i.e., Late Permian to Early Triassic and Bathonian (Middle Jurassic) to Ryazanian (Early Cretaceous). Major unconformities are primarily considered of tectonic origin instead of eustatic. These unconformities mark the border between these episodes of rifting. During Late Permian to Early Triassic, extension about N-S axis took place followed by Triassic to Mid Jurassic thermal subsidence which produced steep faults. Thermal subsidence followed by rifting episode of Triassic-Early Jurassic provided accommodation space for the sediments of Brent and Dunlin group. Overlying Viking group was deposited during Middle Jurassic-Early Cretaceous (Badley et al., 1988). Structural traps and rotated faults blocks were formed during Late Jurassic-Early Cretaceous (Glennie and Underhill, 1998). Existence of a third tectonic event during Tertiary period is suggested by Rupke et al. (2008), although, major tectonic activity is generally thought to have ceased after the Late Jurassic rifting (Lundegard, 1994).

Climax of rifting was reached during Upper Jurassic when fault activity was focused only on a few faults along the margins of Viking Graben. This made the relief of graben more pronounced and created graben topography including platforms and platform marginal heights (Gabrielsen et al., 1990). Rifting during Late Jurassic was followed by post rift subsidence because of cooling (Marcussen et al., 2010).

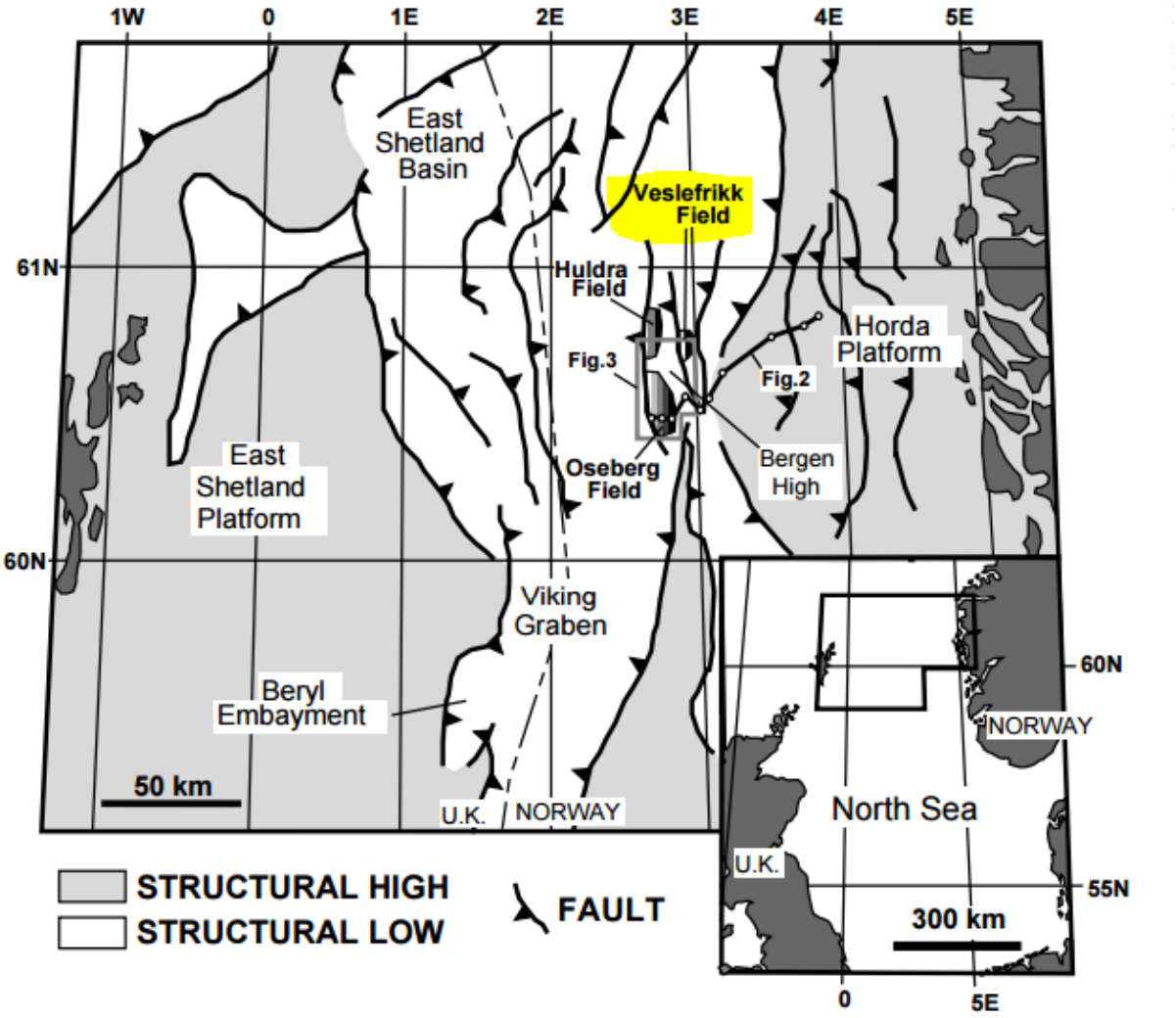

Figure 2.1 Structural setting of the North Sea (Muto and Steel, 1997).

2.1 Stratigraphy

Norwegian continental shelf is rich with hydrocarbon reservoirs, around 50% of these reserves are contained in sediments of Jurassic age. The Jurassic sediments of the North Sea were deposited in an intraplate tectonic setting. This region was in the south of weakly linked Greenland, Laurentia, and Fennoscandian shield areas, located in north of Tethyan Ocean. Tethyan Ocean was going through an active extension around that time. During early Jurassic, sediments were provided to epeiric sea from shield areas and transient or permanent

land areas. The epeiric sea consisted of complex array of shallow marine shelves separated by deeper troughs (Underhill, 1998).

Triassic - Jurassic period faced several changes in tectonic, climatic and sea level changes (Steel, 1993). Non marine Triassic basins transformed into a thoroughly marine basin due to transgression during Early Jurassic (Ziegler, 1982). Facies of ephemeral fluvial system changed to alluvial sandstones, shale and coals, related to more humid and developed river systems. This indicates a Late Triassic - Early Jurassic climate change (from arid to humid) in North Sea (Roe and Steel, 1985).

Vollset and Doré (1984) summarized the lithostratigraphic nomenclature for Triassic and Jurassic of Norwegian North Sea. Lower Jurassic of Norwegian North Sea comprises Statfjord group and Dunlin group, which is underlain by Middle Jurassic Brent group.

The distribution of Lower Jurassic sandstones is dependent upon the accommodation space, tectonic subsidence and variation in sediment supply. Therefore, it is represented by repeated retrogradation and progradation (Charnock et al., 2001).

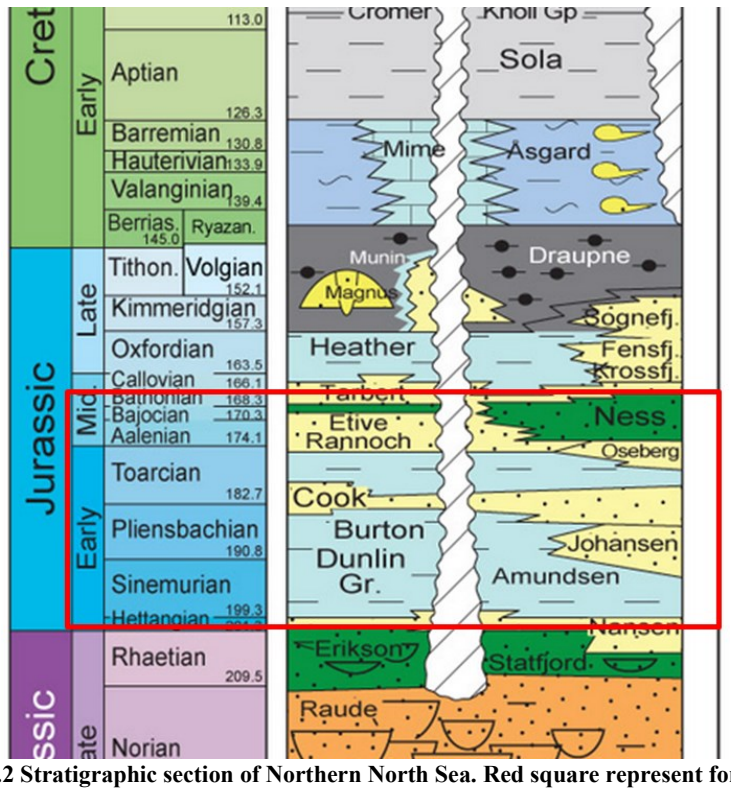

Figure 2.2 Stratigraphic section of Northern North Sea. Red square represent formations encountered in study area (modified after Norlex (2015)).

2.2 Cook Formation

Cook Formation is a part of Dunlin group which has formations of age ranging from Hettagian to Bajocian. In northern North Sea, Dunlin group is subdivided into five formations i.e. Amundsen (at bottom of the group), Johansen, Burton, Cook, and Drake formations (at the top of group). Cook Formation (Age: Pliensbachian to Toarcian) is 63.5 meters thick in type well (UK well 211/29-3 (Shell)) where it is dominantly a marine siltstone with some silty claystone intercalations of grey colour. These claystones and siltstones contain sandy streaks which become more prominent in Norwegian waters. Sandstones become dominant lithology on Horda Platform and its western margin. The sandstones are subangular to subrounded, greyish brown to white and very fine to fine grained, with occasional thin layers of coarse to medium grained sandstones. Cook Formation can be distinguished from Drake (overlying) and Amundsen or Burton (underlying) formations on wireline logs by increase in sonic velocity and decrease in gamma ray count (Vollset and Doré, 1984).

Cook Formation is only sand dominated interval that extends to Oseberg area and which occurs in most of northern North Sea areas. Base of Cook Formation (in cores recovered from Oseberg area) rests on a mudstone bed that covers a thin bed consisting of calcitic, sideritic, and phosphatic peloids and cements. This calcitic bed is interpreted as condensed sequence and it makes the top of the Burton Formation (Livbjerg and Mjøs, 1989).

2.3 Depositional environments of Cook Formation

Cook Formation is extensively distributed in northern North Sea and it has been reported in literature with different depositional environments at different locations. Going from north to south; in Snorre Field it has been identified as offshore mudstone by Nystuen and Fält (1995), as well as by Underhill (1998). In Statfjord Field it is classified as marine shoal sand deposits by Dalrymple (2001). In Gulfaks Field, lower part of Cook Formation represents offshore to lower shoreface environment on distal parts of a wave influenced shelf, while its upper part is interpreted as marginal to shallow marine deltaic setting, characterized by tidal activity (Livbjerg and Mjøs, 1989, Dreyer and Wiig, 1995, Marjanac and Steel, 1997, Folkestad et al., 2012).

In Oseberg Field, Cook Formation is subdivided into three units i.e. Cook A, Cook B and Cook C. Cook A was characterised as prograding subtidal sand body. Cook B is comprised of mud and siltstones with thin lenses of sandstones and it separates Cook A from Cook C. Cook C unit was deposited as an offshore sand ridge (Livbjerg and Mjøs, 1989). At Horda platform, Cook Formation is identified as estuarine and marine shoreface sandstone deposited during lowstand incision, transgression and progradation (Charnock et al., 2001).

3. Processes effecting reservoir characteristics

3.1 Introduction

The properties of sandstone reservoirs are controlled primarily by mineralogical composition, texture, grain size, sorting, and diagenesis. Diagenesis starts taking place after the deposition of sediments and it continues during burial of the rock. Properties of reservoir rock remain variable throughout the burial and uplift due to the effect of chemical and mechanical compaction which results in the dissolution and precipitation of minerals. Bjørlykke and Jahren (2010) suggested following main process of diagenesis:

3.2 Near surface diagenesis

Near surface diagenesis involves the reaction of minerals in sediments with ground water (fresh or saline depending upon the dry or wet climates). Sands can be cemented by carbonates near the seafloor. Dissolved solids can be more mobile by fluid flow close to surface. Sediments are also more vulnerable to chemical change at shallow depths compared to deep burial. When under saturated meteoric water seeps down into the soil, it dissolves unstable minerals (mica and feldspar) and precipitates kaolinite (Bjørlykke and Jahren, 2010).

Equation 1

$$2K\ (Na)\ AlSi_3O_8 + 2H^+ + 9H_2O \rightarrow Al_2Si_20_5\ (OH)_4 + 4H_4SiO_4 + 2K^+\ (2Na^+)$$

K-Feldspar Kaolinite Dissolved silica

Equation 2

$$2KAl_3Si_3O_{10}\ (OH)_2 + 2H^+ + 3H_2O \rightarrow 3Al_2Si_20_5\ (OH)_4 + 2K^+$$

Muscovite Kaolinite cation

Meteoric water dissolves feldspar and mica, precipitates authigenic clay minerals such as kaolinite. This dissolution produces secondary porosity, while at the same time precipitation of clay minerals reduces porosity. As the result of this dissolution and precipitation little gain in porosity is achieved. Kaolinite can also reduce permeability by filling up the pores. Usually authigenic kaolinite occurs as cluster and oil can flow between and around kaolinite cemented pores. At greater depths with temperatures around 130°C, kaolinite can be altered to illite if K^+ ions are available in the system. Authigenic illite has a

fibrous form which can damage the reservoir more severely by reducing its permeability (Bjørlykke and Jahren, 2010).

3.3 Mechanical compaction

During mechanical compaction, close packing of grains, fracturing and grain deformation take place. These processes increase the mechanical stability of grains. Initially at shallow depths 0-2 kilometres, well sorted sands can still be loose if not cemented by carbonate. This is when mechanical compaction plays a very important role. It has been observed during experimental compaction of loose sand (porosity 40% to 42%) that mechanical compaction can reduce the porosity from 35% to 25% at 20 to 30 MPa pressure. This compaction also depends upon grain size and grain strength. This experimental data also showed that coarse grain sand is more prone to lose porosity than fine grain sand (Chuhan et al., 2002). It should also be considered that in basins with normal geothermal gradient (80-100 °C at 2 kilometres) quartz cementation can provide stability to grain framework preventing mechanical compaction after 2 kilometres depth. Quartz cementation can start around 4-6 kilometres depth in cold sedimentary basins, until then mechanical compaction can remain effective resulting in intense grain crushing at pressures around 50 MPa.

Carbonate grains are more ductile under pressure than quartz, due to which grain contacts are enlarged and overburden stress is distributed to the larger area on each grain (Shinn and Robbin, 1983). Biogenic carbonate is unstable under redox boundary, it dissolves and precipitates as cement (Saigal and Bjørlykke, 1987). This cementation makes the rocks denser and primary velocity increases in such rocks which can be observed in seismic and electrical logs. Detrital carbonate grains can dissolve in later stages of diagenesis and produce cement (Morad, 2009).

3.4 Chemical compaction

In basins similar to North Sea, quartz cementation can start around 2-3 kilometres depth (80-100 °C), strengthening the grain framework of rocks. Poorly sorted and lithic sands lose their large proportions of porosity at shallower depths (1-2 kilometres). Usually only 2% quartz cement is sufficient to strengthen the grain framework to prevent further mechanical

compaction. Once quartz cementation starts, it does not stop until it occupies all the available pore spaces or the temperature drops down below 70-80 °C. Generally, feldspathic sandstones and quartz arenites loses porosity by the process of quartz cementation. Amount of quartz cement is favoured in the basins with slow subsidence rate and high geothermal gradients (Bjørlykke and Jahren, 2010). An example of quartz cementation can be seen in Figure 3.1.

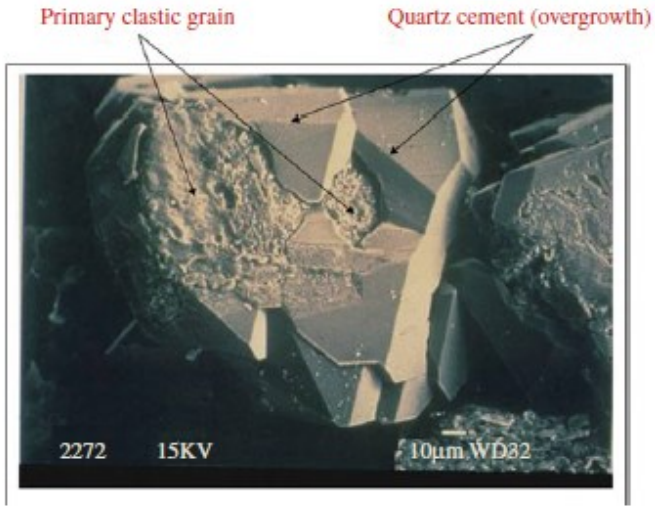

Figure 3.1 - Quartz cement overgrowths can be seen in this SEM acquired image (Bjørlykke and Jahren, 2010).

4. Porosity preserving processes

4.1 Introduction

The history of sandstone diagenesis from shallow to deep burial determines the reservoir quality. Quartz cementation and mechanical compaction are found to be the most effective porosity reducing processes. Deeply buried sandstones still show effective porosity which advocate for porosity preserving processes. There are three porosity preserving process mentioned in literature (Bloch et al., 2002, Bjørlykke and Jahren, 2010) i.e. grain coating, fluid over pressure and early hydrocarbon emplacement. The scope of this thesis is limited to grain coating porosity preserving process.

Grain coating minerals like authigenic chlorite and micro-quartz have been observed acting as porosity preserving mechanism in various sandstone reservoirs found deeper than 4 kilometres (Ehrenberg, 1993, Aase et al., 1996, Bloch et al., 2002, Chuhan et al., 2002, Storvoll et al., 2002, Berger et al., 2009, Ajdukiewicz and Lander, 2010, Taylor et al., 2010, Dowey et al., 2012, Sun et al., 2014).

Heald and Larese (1974) cited in Bloch et al. (2002), comprehensively enlisted different types of coatings on detrital quartz grains. In addition to chlorite and micro-quartz, they described the occurrences of carbonate specks rimming quartz grains and iron oxide coats. Quartz overgrowths are forced by carbonate specks on detrital quartz gains to form isolated crystals, which is a slower process than continuous overgrowth. On the other hand, iron oxide coats are not effective in preventing quartz cementation.

4.2 Authigenic Chlorite

Chlorite is most widely found grain coating mineral in worldwide settings e.g., Jurassic Tilje, Tofte, Statfjord, Garn and Dunlin Formation in North Sea and Haltenbanken area (Ehrenberg, 1993), the Sawan gas field in Pakistan (Berger et al., 2009), Sichuan Basin in Western China (Sun et al., 2014) are few examples. Sandstone deposited in a range of sedimentary environments contains chlorite coatings most commonly in delta related environments (44%) and secondly in fluvial environments (19%). Iron rich chlorite implies coastal environment whereas, magnesium rich and iron rich mixed chlorite are found in marine and terrestrial environments (Dowey et al., 2012).

Precipitation of chlorite requires a source of iron which can be formed in a fluvio-deltaic setting. As the river water reaches to the mouth, increased salinity causes Fe to flocculate and deposit in amorphous state which makes it highly reactive. It makes a clay-rich gel like layer which can form ooids at points of high current energy. Sedimentary facies architecture and paleo-river discharge pattern in the architecture, determines the geometry of chlorite distribution (Ehrenberg, 1993). Burrowing organisms produce faecal material which can form into smectite-rich clays which may further transform into chlorite coatings. Formation of coatings on quartz grains in early diagenetic stage is essential to preserve porosity at greater depths (Bjørlykke and Jahren, 2010).

Quartz cementation models suggest that coating is a vital factor in retardation of quartz overgrowths. Chlorite as a grain coating mineral can reduce the available nucleation area for overgrowths of quartz (Lander et al., 2008). Variations in porosity of clean sand are usually correlated with abundance of chlorite grain coating and lack of quartz cementation (Ehrenberg, 1993). The presence of authigenic chlorite coatings can restrict mechanical compaction. Inter-crystalline pores in chlorite may contribute to the micro-porosity of sandstone (Sun et al., 2014).

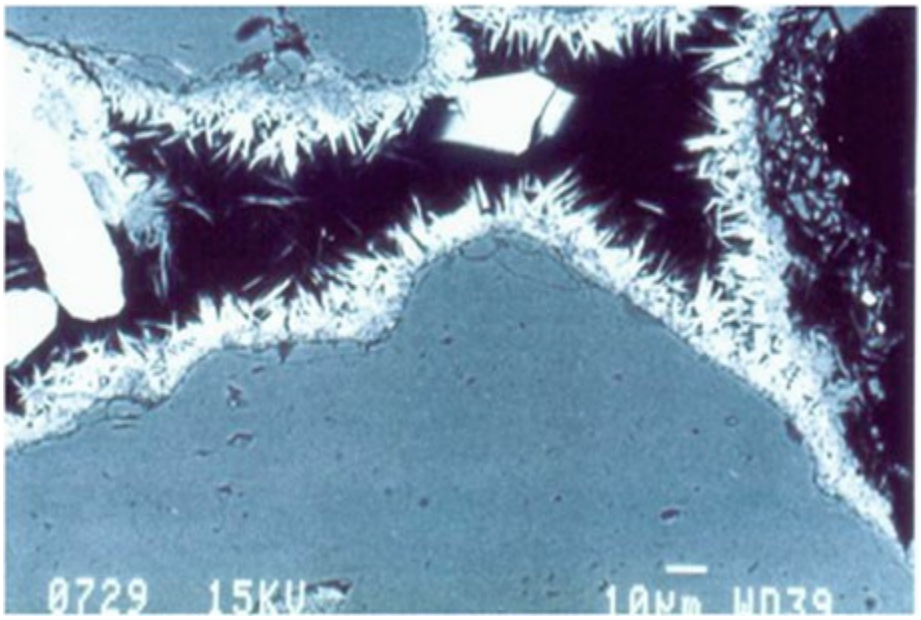

Figure 4.1 - Needle like structure is chlorite coating over quartz grains (Bjørlykke and Jahren, 2010).

4.3 Illite or Illite/Chlorite Coatings

Observations of Storvoll et al. (2002) showed that illite and illite/chlorite coatings can also be effective in resisting quartz precipitation and preserving porosity. Illite coatings are generally thick (6 to 8 μm) possibly due to its fibrous and flaky appearance. Presence of illite can be explained by two mechanisms (1) by the replacement of smectite or (2) by replacement of kaolinite (Bjørlykke et al., 1992). Illite coatings are expected to be found in rocks with smectite as clay matrix and/or with high K-feldspar content at the time of deposition.

4.4 Micro-Quartz

Occurrence of micro-quartz coating is underreported (Aase et al., 1996, Bloch et al., 2002). These coats are not as prominent as chlorite coats under petrographic examination and they are sometimes overlooked or mistaken by leaching of detrital quartz grains. Micro-quartz form coatings on the surface of detrital quartz grains (like chlorite coating) and retards the pore-filling quartz overgrowths (Bloch et al., 2002). Micro-quartz precipitates at lower temperature (60-65 °C) than quartz cementation (80-100 °C) (Bjørlykke and Jahren, 2010).

Quartz overgrowth takes place by mergence and/or overlapping of incipient overgrowths with same crystallographic configuration as underlying detrital quartz grain. The random orientation of micro-quartz crystals attached to detrital quartz grains interfere with formation of quartz cement. Micro-quartz may also resist the pressure solution by solidifying contacts between quartz grains (Bloch et al., 2002).

The presence of siliceous sponge spicules (Rhaxella) controls the distribution of microcrystalline quartz coatings. Amorphous silica sponge spicules are considered as the source of cryptocrystalline and microcrystalline quartz. These quartz morphologies proposes rapid crystallization from locally saturated silica solutions (Aase et al., 1996).

Excess of micro-quartz affects permeability more than porosity. Generally, micro-quartz aggregates are intergrown with diagenetic, illite forming clusters with micro-porosity and secondary porosity by dissolution of sponge spicules. Total porosity can be high but

permeability is reduced due to blockage of pore throats by micro-quartz aggregates (Aase et al., 1996).

4.5 Hydrocarbon emplacement

The effect of hydrocarbon emplacement with quartz cementation is debatable. Marchand et al. (2002) showed in their study of the Miller and Kingfisher fields in United Kingdom North Sea, that oil emplacement retarded the rate of quartz cementation in Brae Formation, due to which porosity was preserved even at the depth of 4 km and temperature around 120°C. In most of the cases quartz grains are water wet and quartz cementation can take place on these water wet contacts. Hydrocarbons can be effective in porosity preserving if quartz grains are oil wet (Walderhaug, 1990).

5. Methodology

5.1 Introduction

The focus of this thesis has been on reservoir characterization and processes affecting reservoir quality. To understand the properties of reservoir, techniques like core description, analysis of thins sections under optical and scanning electron microscope, and quantitative mineralogical analysis through XRD was employed. These techniques helped in understanding the reservoir quality, depositional environment and diagenetic processes. These methods are of different resolution and measurement errors are possible.

5.2 Petrographic analysis

During this study 28 thin sections and stubs from three wells in Veslefrikk area of northern North Sea were analyzed. Point counting and textural analysis were performed to understand the depositional environment and estimating the bulk mineralogical composition.

5.2.1 Point counting and Grain size analysis

Grain size analysis and point counting were done by utilizing optical microscope. A total of 300 points per thin sections were counted on 28 samples (8,400 points in total). A Swift automatic counter was used on the turning disc stage of optical microscope and each thin section was analyzed trough it. The credibility of this analysis depends up on the quality and polish of thin sections, resolution of microscope and experience of operator who performed the point count.

Visual scan of whole thin section was acquired to analyze textural features and grain size measurements were obtained with the help of software ScopeView. Grain size analysis was performed by measuring 50 grains from each thin section (1400 hundred grains in total).

5.2.2 Scanning Electron Microscope (SEM)

Scanning Electron Microscope (SEM) is powerful equipment which can be used to look into the pores and identify minute mineral particles and examine their distribution in pores. The Scanning Electron Microscope type JEOL JSM-6460L V, with LINK INCA Energy 300 (EDS) from Oxford Instruments was utilized with a standard wolfram filament of 15 kV. The

SEM is able to examine rough surfaces at a magnification range from 20X to 200,000X. Stubs for SEM were made from core pieces by breaking and exposing fresh surfaces. These rock pieces were then glued to aluminum stubs and then coated with gold to make the surface electrically conducting. These stubs were analyzed in secondary electron image (SEI) mode of SEM. Thin sections (carbon coated) were analyzed in backscattered (BEC) mode. The analysis was performed to observe micro level features such as chlorite coatings, quartz overgrowths, porefilling clay, dissolved feldspars, and their distribution. Different mineral were identified by the help of peaks in spectrum obtained through SEM. The SEM petrology atlas (Welton, 2003) was consulted frequently to match and identify spectra.

5.2.3 XRD Analysis

X-ray powder diffraction (XRD) analysis was performed on 28 rock samples taken from cores stored at NPD head office, Stavanger. The samples were crushed and micronized for 12 minutes by McCrone Mill in silicon carbide cylinder filled with 8 ml ethanol, 3 gm rock powder and agate crushing micronizers. XRD diffractograms were first processed through Diffrac Eva 4.0 and mineral phases were identified based upon their peak position. This information was then used for further processing of data by Profex (version 3.5.0) in BGMN software suit (4.2.22) to calculate proportion of existing mineral phases in each sample. The results obtained through XRD can be used to compare with point count and SEM mineralogy.

5.2.4 Limitations of petrographic analysis

Even though petrographic analysis is a powerful tool, it has some limitations:

- For a good point count, 300 points are only a rough estimate of overall composition, moreover, mistaken identity of minerals during thin section analysis and point counting may occur.
- Fine material can be washed away during thin section preparation and polishing which ultimately may result in overestimation of porosity during point count.
- Grain size can be overestimated due to quartz overgrowths and/or cementation. It can also be underestimated due to because of dissolution of grains.
- Preparation of stubs can produce artificial features which can be mistaken as natural features.

5.3 Petrophysical analysis

5.3.1 Well correlation and interpretation of well logs

Two of the three wells in this study were correlated with the third well 30-3/4 to understand the vertical and lateral distribution of sand stones. The software Interactive Petrophysics was used for correlation. Wellbore information was taken from NPD website (www.npd.no). Formations were correlated by comparing the similar curves (in terms of shape and magnitude) generated by wireline logs, comparing core photos and well top information from NPD Factpages. Through the same software, lithology logs and porosity logs were generated and compared with logs made from cores. Different wells have different well log sets but caliper, gamma, resistivity and density are common.

5.3.2 Cross plotting and histogram

Cross plots are quite good tool in representing relations between different plotted quantities. By this method generally, scattered plot is produced which can be used for the interpretation of hydrocarbon zone, mineralogy, lithology etc. Generally, two types of cross plots exist i.e. compatible logs like porosity and density to define lithology; cross plots of incompatible logs like gamma ray and resistivity to quantify fluid content and lithology. Cross plots used in this study were generated by softwares like Microsoft Excel and Interactive Petrophysics.

5.3.3 Limitations of petrophysical evaluation

Even though high tech softwares are used, it is still possible to misinterpret logs. If the information about lithology is incomplete then log interpretation can be difficult or misleading. To address all those possible uncertainties cross plots can be used as quality check parameter.

5.4 Core description

Cores from wells (30/3-4, 30/3-5 and 30/6-17A) were described in terms of grain size, texture, structure and bioturbation in two days at NPD head office Stavanger. The logs were made by the help of cores and their images at NPD website. Furthermore, wireline logs were compared and matched with lithology logs to act as quality check and interpretation tools. It also helped to complete lithology logs at depths where cores were not available.

6. Petrophysical results

6.1 Well correlation and producing formations

In Table 6.1 water depth, bottom hole temperature and average estimated temperature in corresponding formations is mentioned. Different geothermal gradients were calculated for each well considering 4 °C at sea floor and according bottom hole temperatures. A stratigraphic correlation plot can be seen in Table 8.2.

Parameters/well	30/3-4	30/3-5S	30/6-17A
Water Depth (m)	164	175	110
Kelly Bushing elevation (m)	23	56	25
Total Depth (MD, mRKB)	3287	4724	2686
True Vertical Depth (TVD, mRKB)	3285	3340	2528
Maximum inclination (°)	6	69.4	2.8
Bottom hole Temp. (°C)	152	120	104
Calculated Geothermal gradient (°C/m)	0.047	0.037	0.041
Avg. Temp. in Ness (°C)	127	102	*
Avg. Temp. in Etive (°C)	129	104	*
Avg. Temp. in Oseberg (°C)	**	105	*
Avg. Temp. in Drake (°C)	133	**	*
Avg. Temp. in Cook (°C)	138.2	111	100
Avg. Temp. in Amundsen (°C)	*	*	101

*Not included in study interval, **Not encountered in study interval.

Table 6.1 Summary and temperature history of studied wells.

6.1.1 Well 30/3-4

Well 30/3-4 is an oil/gas appraisal well, completed in 1985. This well was drilled in Veslefrikk Field to investigate possible oil accumulations in Ness and Etive formations and to determine the oil/water contact. Its secondary objective was to explore the sandstones of Dunlin Group. Hydrocarbons were encountered in Ness, Etive, and Cook Formation and oil/water contact was determined at 2930 meters (NPD Factpages).

6.1.2 Well 30/3-5S

Well 30/3-5S was drilled in the east side of Veslefrikk Field and was completed in 1992. Its primary and secondary targets were Brent Group and Statfjord Group, respectively. Below the depth of 4050 meters, fully developed Brent group was penetrated. The well encountered hydrocarbons and Brent Group and Cook Formation. This well was completed in July 1992 and was converted into development well 30/3-A-14 (NPD Factpages). This is a deviated well and data is obtained in measured depth (mMD), due to which all the samples and readings from this well will be kept in measured depth. True vertical depth of the samples can be seen in Appendix B.

6.1.3 Well 30/6-17A

Well 30/6-17A was an exploration well, located on the western side of Oseberg Field. Cook Formation acted as a gas bearing reservoir in this well and developed as a coarsening upward sequence with average porosity around 24%. The well was completed in 1986 (NPD Factpages).

6.2 Petrophysical properties

Primary wave or P-wave velocities (Vp) can reveal the information about the cementation and density of subsurface rocks. Typically high density rocks exhibit high p-wave velocities. Rocks with same type of composition can exhibit different velocities depending upon the density of fluid content and cementation. For example, typical velocity for dry sand ranges between 400-1200 m/s, whereas, for wet sands it is between 1500-2000 m/s. These velocity zones can also overlap e.g., saturated shales and clays can have velocity range between 1100-2500 m/s and porous and saturated sandstones can exhibit a velocity range of 2000-3500 m/s. Highest P-wave velocities are typically displayed by carbonates, evaporites, igneous and metamorphic rocks which can vary from 3500 to 6500 m/s.

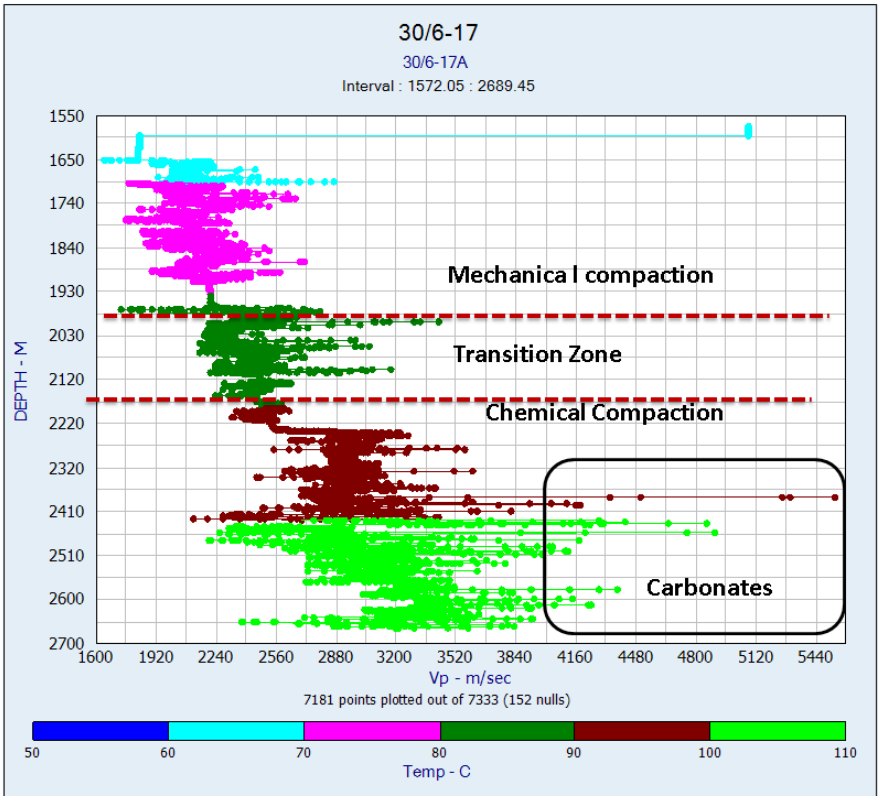

Figure 6.1 P-wave velocities for well 30/6-17A are plotted against depth (temperatures are approximates).

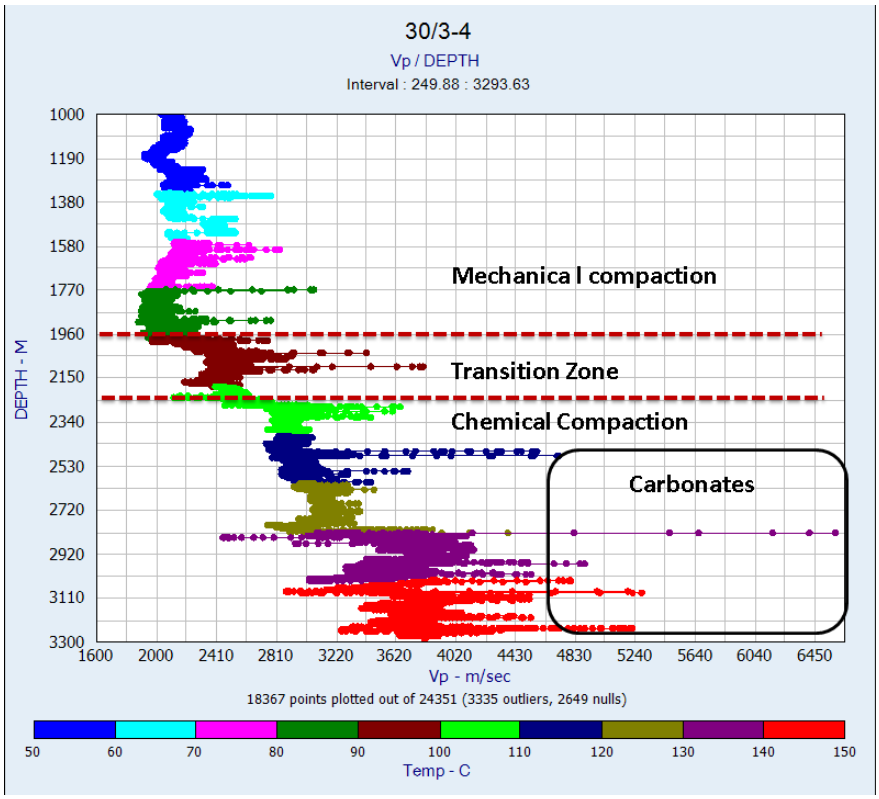

Figure 6.2 P-wave velocities for well 30/3-4 are plotted against depth (temperatures are approximates).

Primary velocity data of well 30/6-17A and 30/3-4 is plotted against depth in Figure 6.1 and Figure 6.2, respectively. An increase in velocity trend can be observed below the mechanical compaction zone. This increase in velocity can be indicative of transition zone where both processes like mechanical and chemical compaction are active. This interval has already entered into chemical compaction regime (70+ °C). As the temperature keeps on rising (80+ °C) with depth we can see a progressive increasing velocity trend in deeper intervals. This is most likely because of quartz cementation; however, abnormally high velocities are possibly sandstones with carbonate cements.

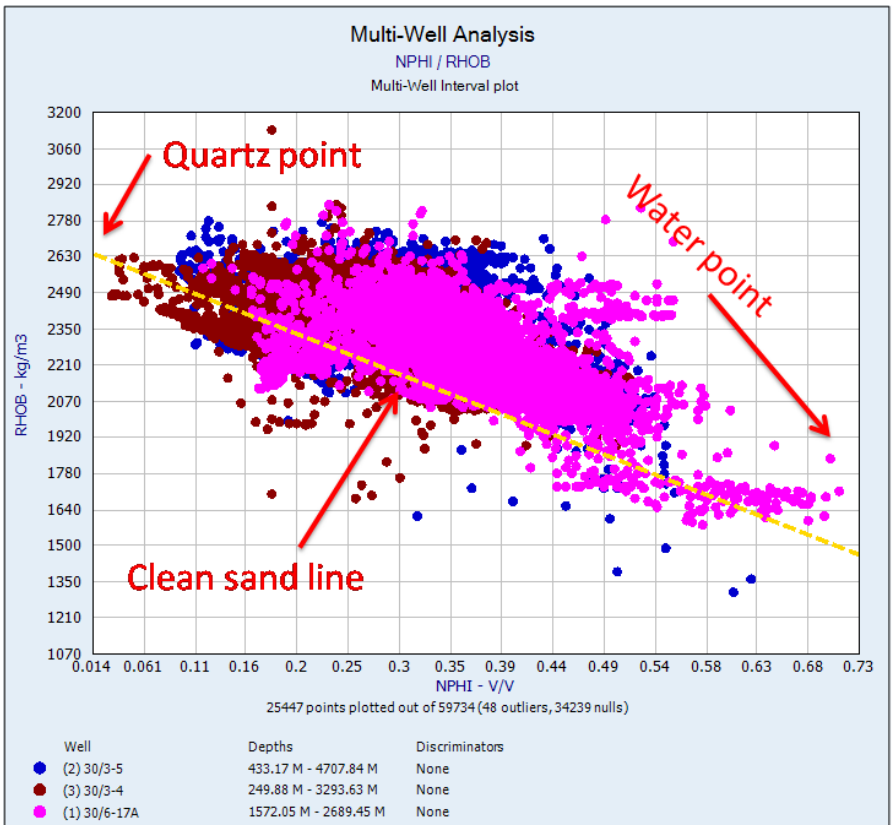

Figure 6.3 Cross plot between Neutron porosity (NPHI) and density (RHOB) logs.

A cross plot between density and neutron porosity (Figure 6.3) is used to separate clean sand data points from rest of the lithologies. Clean sand line can be drawn by connecting the quartz point at 2650 kg/m^3 density and zero neutron porosity with water point at 1kg/m^3 and 1 neutron porosity (Heslop and Heslop, 2003).

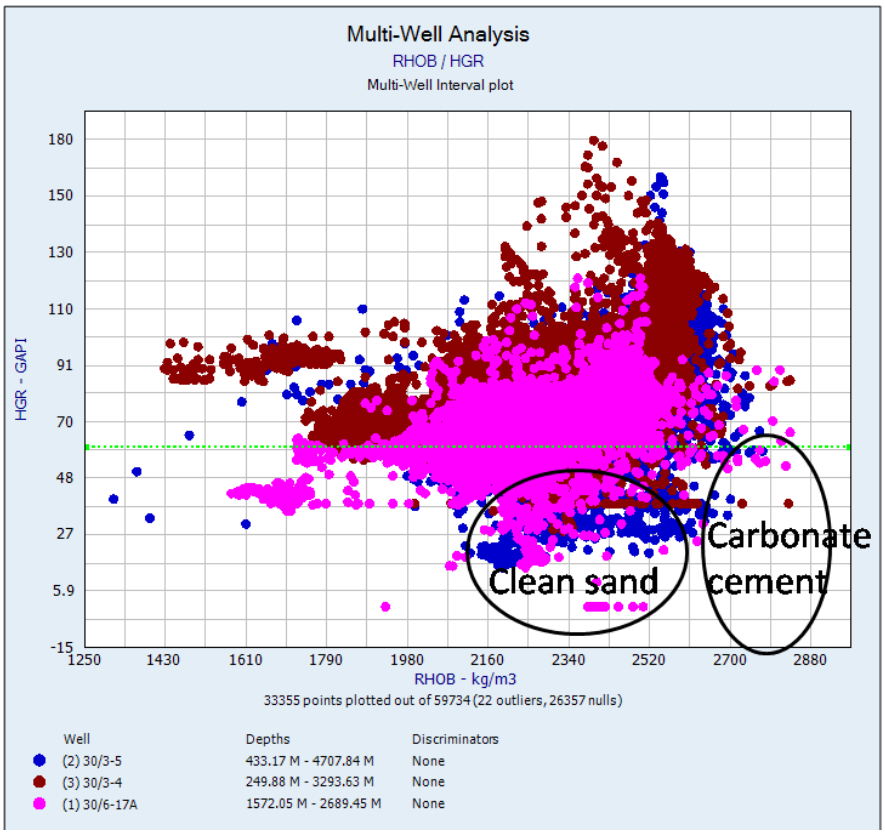

Figure 6.4 Cross plot between gamma ray (HGR) and density (RHOB) logs. Green line marks sand/shale boundary.

Cross plot of gamma ray and density logs of all three wells is presented in Figure 6.4. The sand/shale boundary is created at 60 API of gamma ray value. Below 60 API all the data is considered sand and above 60 API data is considered shale. Increasing shale content is indicated by increasing gamma ray values and increasing density values. Equal to or higher than 2650 kg/m^3 values indicate pure sand with zero or very low porosity or quartz and/or carbonate cementation in sandstone pores. These situations are not good for a petroleum reservoir. However, moderate values of density (less than 2400 kg/m^3) and lower than 60 API of gamma ray are reasonable for a possible petroleum reservoir.

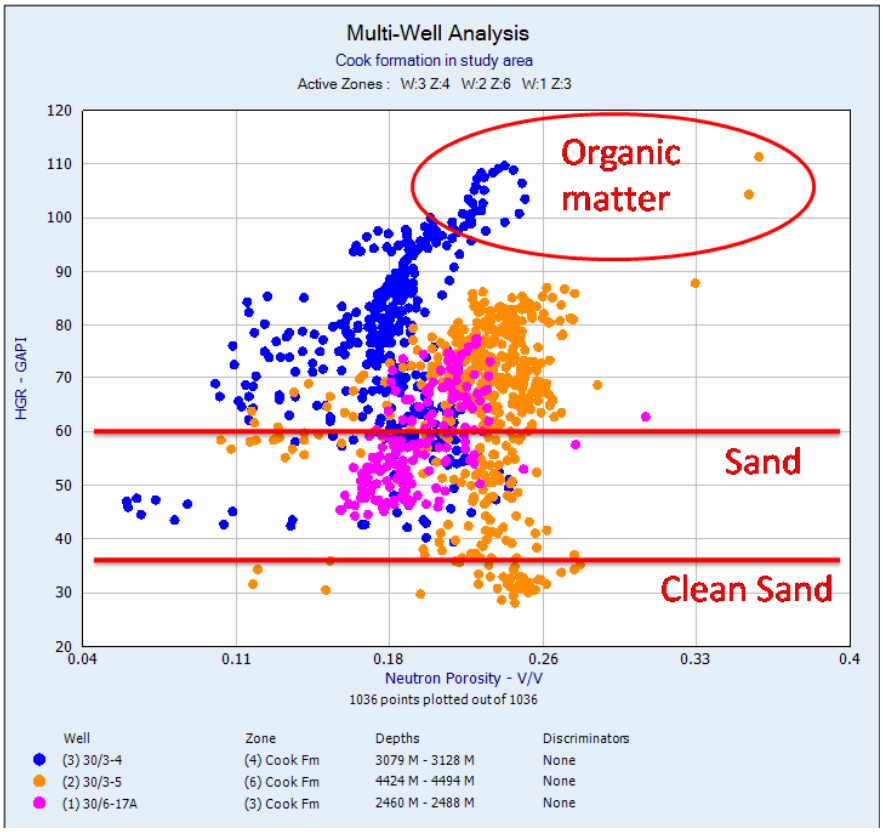

Figure 6.5 Gamma ray (HGR) values of Cook Formation in three wells are plotted against Neutron porosity.

Neutron porosity logs provide information about the estimated porosity of rocks by measuring apparent concentration of hydrogen atoms per unit volume. Practically, it gives information about bound fluid and free fluid in the formation without differentiating them (Rider, 2002). Thus porosity of water bearing shales can be overestimated. A cross plot of gamma ray and neutron porosity logs (Figure 6.5) can be used to differentiate between shale and sandstone. Gamma ray log considers natural radioactivity of the formation and it is not affected by porosity. High gamma ray (shale content) and high neutron porosity (hydrogen content) values break the general trend of the cross plot and expose the zone of hydrocarbons (Heslop and Heslop, 2003).

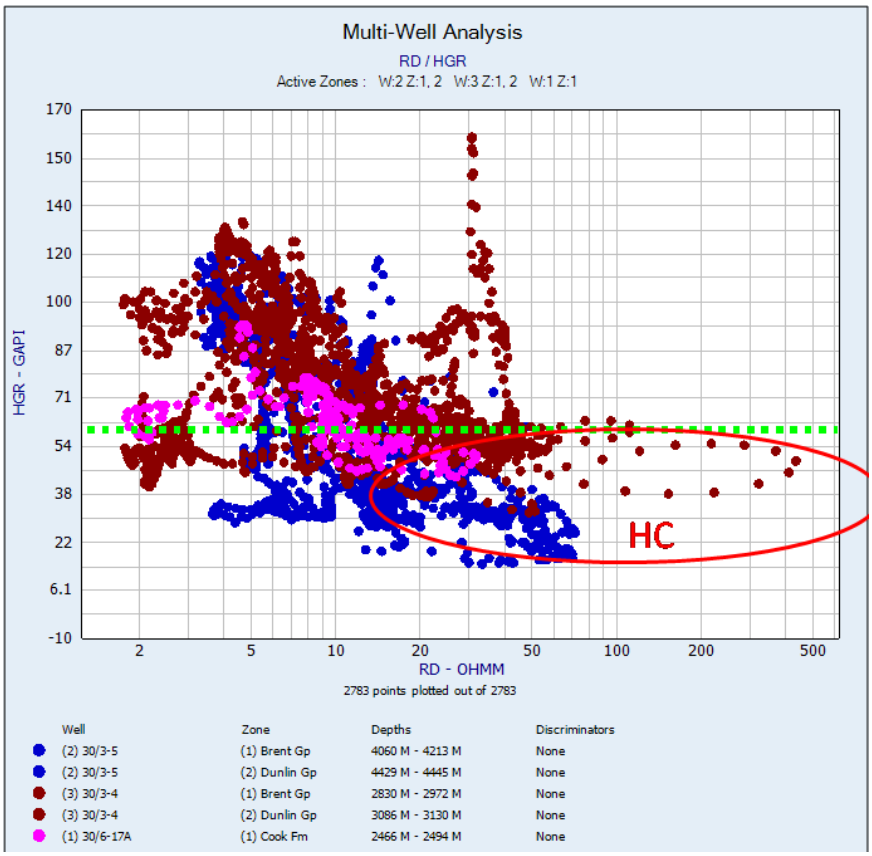

Figure 6.6 Gamma ray (HGR) values of Cook Formation in three wells are plotted against deep resistivity (RD) values. Green line at 60API is sand/shale boundary.

Gamma ray and deep resistivity values of the study intervals are plotted in a cross plot, shown in Figure 6.6. Most of the rock materials are insulators but fluids contained within formation are conductors. Hydrocarbons are exceptional fluids which are infinitely resistive to electricity. Porous and hydrocarbon bearing intervals display very high resistivity (Rider, 2002). Cross plot of resistivity and gamma ray separate hydrocarbon bearing sands due to their significantly high resistivity.

7. Sedimentological analysis and results

7.1 Introduction

Core description and sedimentological interpretation was performed partially at NPD head office Stavanger, and by utilising core images and wire line logs. Three days were utilised to interpret grain size, texture, and sedimentary structures to understand depositional environments. A brief description of Cook Formation and its distribution in different wells is given in Table 7.1. Facies are characterised on the basis of texture, lithology, and sedimentary structures. Active processes during the deposition of sediments can be understood by the utilisation of these characteristics.

Cook Formation				
	Top (m)	Bottom (m)	Thickness (m)	Study interval (m)
30/3-4	3079	3128	49	2830-2972 & 3086-3130
30/3-5S	3188	3233	45	2951-3052 & 3191-3202
30/6-17A	2460	2488	28	2466-2494

Table 7.1 Distribution of Cook Formation in the study area (depths are given in TVD).

7.2 Facies analysis of Cook Formation

Gamma ray response is extremely sensitive to grain size and clay content. Fining upward, coarsening upward sequences or other changes in grain size or clay content affect gamma ray, which results in a change-related shape on the log. This phenomenon makes it very useful in identifying lithology and subsequently interpreting depositional environment. In Figure 7.1, few examples of some common facies associations and their corresponding gamma ray responses can be seen. Identified facies and their location in the well can be seen in Figure 7.3 and 7.4. It is quite obvious that high proportion of fine material caused high gamma ray counts.

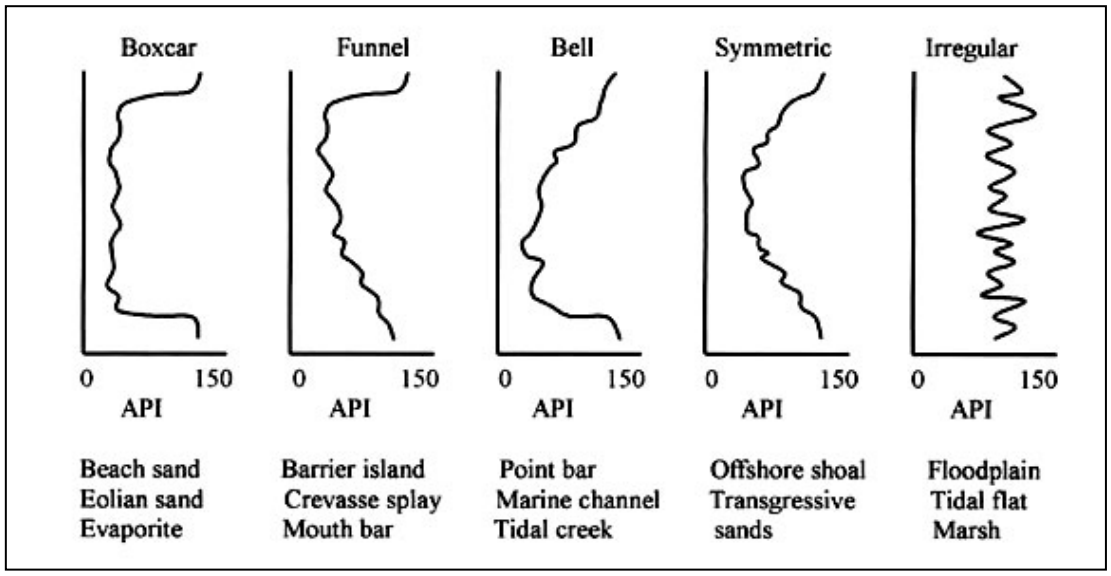

Figure 7.1 Facies associations with gamma ray response (Cant, 1992).

Depositional facies were first identified on the basis of their gamma ray response (Figure 7.1), after that a detailed analysis of texture and grain size was performed. On the basis of this set of information facies were classified into eight categories (Figure 7.5). In Well 30/3-5S and 30/6-17A two facies were identified. Facies were more diverse in well 30/3-4 than others. Four depositional facies are identified in this well. Sedimentary structures such as, lenticular, flaser and wavy beddings, ripple marks, wave ripples, mud drapes, slump (soft sediment deformation), and bioturbation were encountered during facies analysis. In all three wells Cook Formation maintained coarsening upward trend (Figure 7.2).

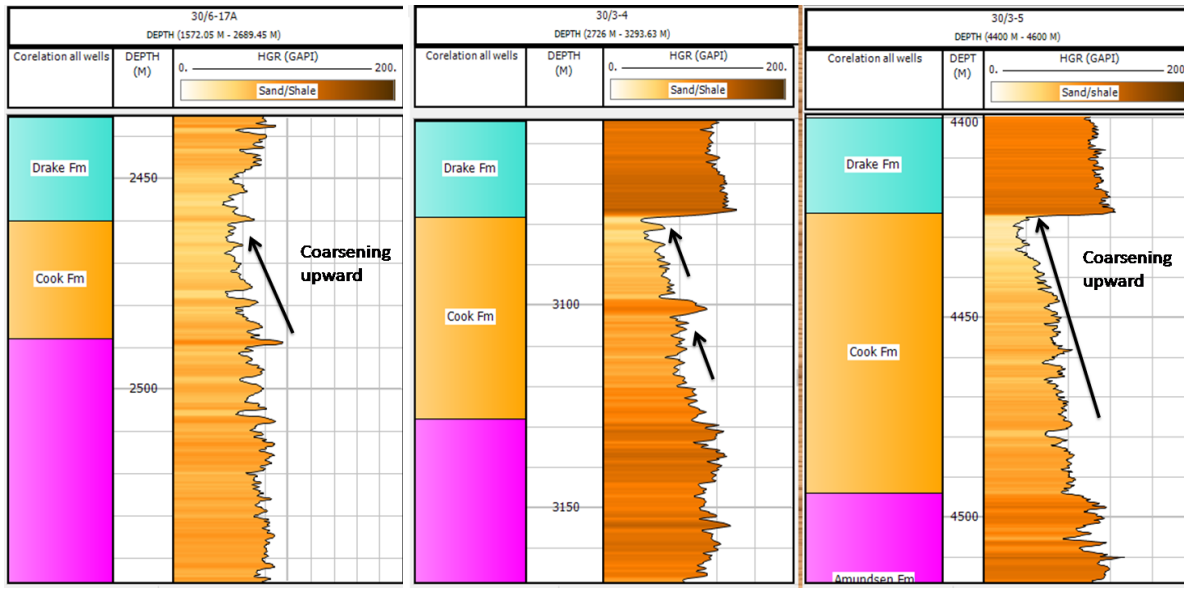

Figure 7.2 Prominent coarsening upward trend of Cook Formation in study wells, from left to right: 30/6-17A, 30/3-4 and 30/3-5S (true thickness of Cook is 49m in 30/3-5S).

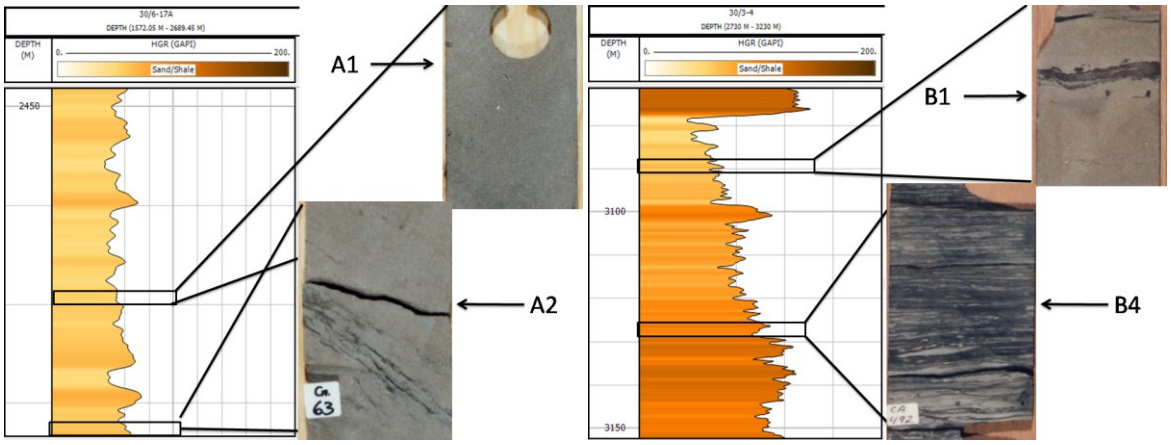

Figure 7.3 Facies location in well 30/6-17A (left) and 30/3-4 (right).

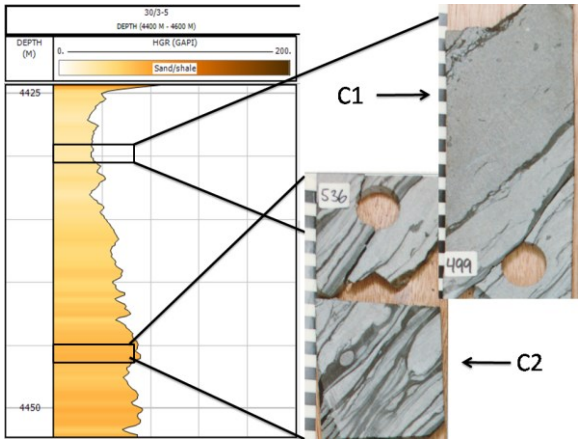

Figure 7.4 Facies location in well 30/3-5S.

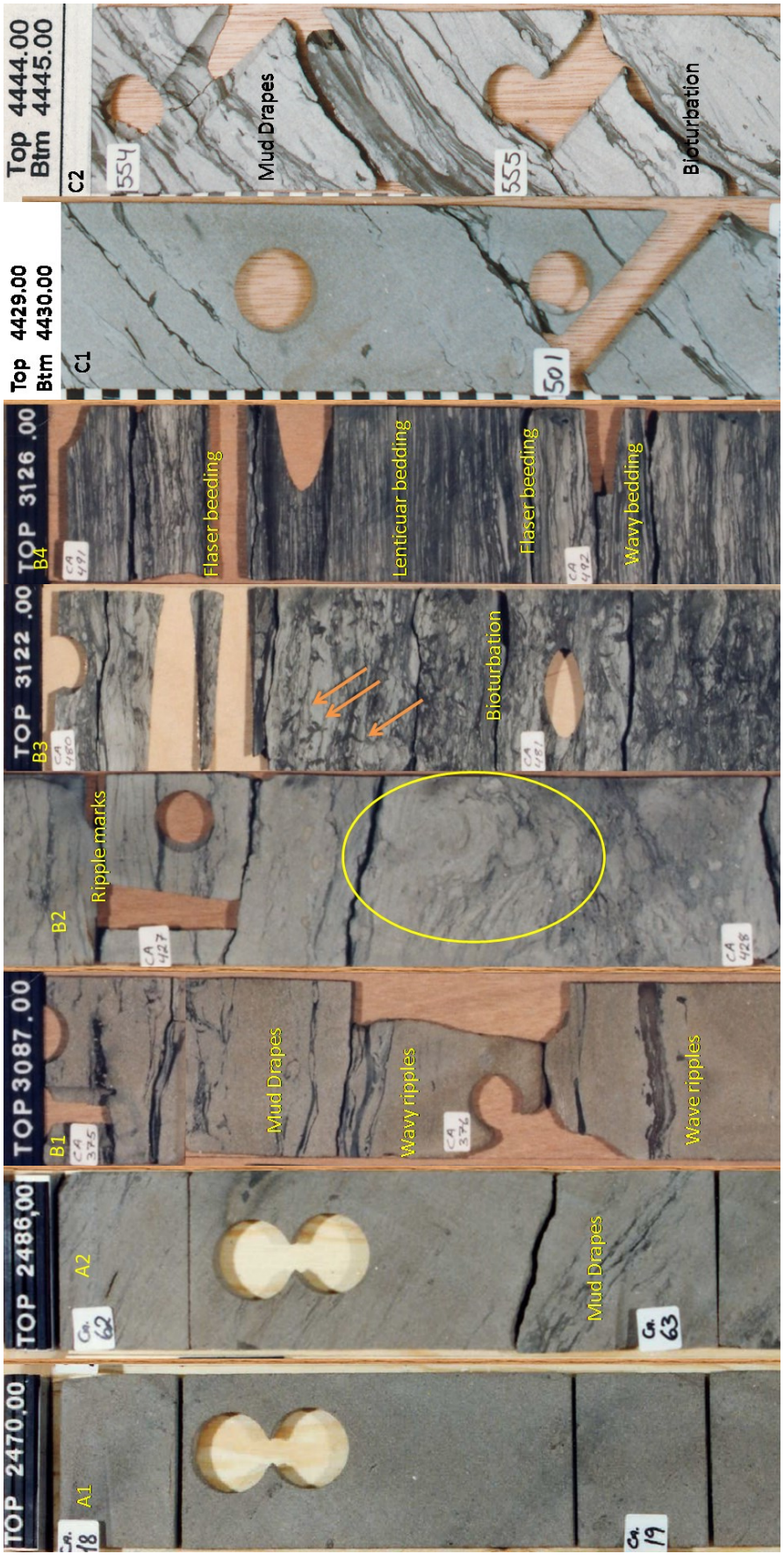

Figure 7.5 A1: Sandstone relatively clean (well 30/6-17A, 2470m), A2: Sandstone (well 30/6-17A, 2486m), B1: Sandstone (well 30/3-4, 3087m), B2: Sandstone (well 30/3-4, 3104m), B3: Shaly sandstone (well 30/3-4, 3122m), B4: Mudstone (well 30/3-4, 3126m), C1: Sandstone (well 30/3-5S, 4429m), C2: Sandstone (well 30/3-5S, 4444m).

7.3 Facies association

Facies encountered in this study appear to have conformable association with underlying shaly strata and sharp contact with overlying shale (Drake Formation) except in well 30/6-17A of Oseberg Area, where the contact was gradational (Figure 7.2). Abundance of mud drapes, wavy ripples in lower part and coarsening upward trend in upper part of Cook Formation, suggest that these sediments were deposited in tidally influenced deltaic and shoreface environment. Over all coarsening upward sequence with cyclic repetition of silty-shaly laminae in the lower part indicates a prograding delta setting. A description of facies association is provided in Table 7.2.

7.3.1 Tidal channel deposits (B1/C1/C2)

Channel deposits generally characterised by upward fining sandstones. Coarse material is deposited in a channel before the deposition of suspended fine material and clays. Multiple fining upward cycles, cross-lamination and cross stratification are commonly observed structures in this setting (Coleman and Prior, 1982). Facies B1, C1 and C2 are considered to be related to this environment. Facies B1 is found at the upper most part of Cook Formation in well 30/3-4 whereas, facies C1 and C2 are parts of Cook Formation in well 30-3/-5S.

7.3.2 Shoreface sandstones (A1/A2)

Shoreface sandstones are generally clean, well sorted quartz rich sand with occasional mud laminae occurences. Because of the constant reworking of sediments due to wave action, plant fragments, clay and other lighter materials are sparse in these sandstones (McCubbin, 1982). Facies A1 and A2 (Figure 7.5) are characterised in this sedimentary environment due to paralel bedding and not many apparent sedimentary structures. These facies are found in well 30/6-17A and show a transition from mud drapes and send lense dominated grey coloured sandstone (A2) in the lower part of Cook Formation towards a cleaner, coarser and more porous sandstone. Gamma ray trend in this area interval is also indicative of this transition (Figure 7.2).

7.3.3 Mouth bar deposits (B2)

In Mouth bar deposits fine grain sand with mud and slump structures at the bottom can be seen. Mouth bar deposits are formed due to the positive feedback between deposition and flow divergence. When channel flow diverges near ocean, it deposits sediments creating a bar-like feature in the middle of channel, which in return reduces the speed of flowing water and more sediments are deposited (Edmonds and Slingerland, 2007). Facies B2 was found in 30/3-4 below facies B1.

7.3.4 Tidal Sand flat (B3)

Facies B3 (Figure 7.5) can be characterised into tidal sand flat environment. This facies consists of micaceous, very fine grains, medium to dark grey sandstone (Weimer et al., 1982). Intense bioturbation was observed, it is considered to be deposited during high energy marine flooding or by storm currents and later bioturbated. This facies encountered in Cook Formation in well 30/3-4 and ranged from 1 to 3meters in thickness.

7.3.5 Tidal mud flat (B4)

Tidal mud flats can be characterised by interbedded sand and mud which result in lenticular and flaser bedding. These are common in subtidal environments and forms due to the fluctuation of energy. Sand is deposited during wave induced or tidal current flow, whereas mud is deposited during slack tide periods. These alternations of sand and mud can range from few centimetres to less than 1 millimetre (Weimer et al., 1982). Facies B4 (Figure 7.5) is closely related to this environment. However, this facies was found only in 30/3-4 at the lower part of Cook Formation. High gamma ray readings were observed at this interval. This facies gradually transformed into Facies B3.

Facies association	Facies Units	Lithology	Depositional setting	Description	Reservoir quality
TC	B1, C1, C2	Sandstone	Tidal channel	Deposited in intertidal to subtidal wave dominating environment zone (gamma ray response: Boxcar)	Moderate-poor
SF	A1, A2	Sandstone	Shoreface deposits	Deposited in shoreface and transition zone (gamma ray response: funnel)	Good
MB	B2	Sandstone	Mouth bar deposits	Deposited in tidal and transition zone (gamma ray response: Funnel)	Moderate-poor
TF	B3, B4	Sandstone& mudstone	Tidal sand and mud flat	Deposited in subtidal zone (gamma ray response: Irregular)	Poor

Table 7.2 Facies association with facies and depositional environment interpretation.

8. Petrographic results

8.1 Introduction

Petrographic analysis was performed to obtain a detailed description of reservoir intervals of the three study wells. The focus of petrographic analysis was examination of texture, mineral composition, and distribution of porosity. Texture and composition of sand units influences the amount of chlorite coatings and their distribution. Reasonable understanding of controlling factors of authigenic chlorite and its formation is required to predict high porosity and limited quartz cementation at depths falling under chemical compaction domain.

8.2 Texture and composition

Petrographic analysis including point counting and grain size analysis was performed on all 28 thin sections. Point counting was performed to gather information about matrix, authigenic clays, porosity, and intergranular volume (IGV). A summary of point counting results is given in Table 8.1. Some of the IGV values were unusually high, which could be due to the presence of high amount of authigenic clays and carbonate cement. The average calculated IGV value lies around 32% (Figure 8.6). Bulk mineralogical composition was acquired through XRD analysis (Table 8.5). Point counting mineralogical estimates and XRD estimates are more or less in agreement.

During Point counting very little or no lithic fragments were observed in sandstones. Petrographic results plotted in QFL diagram of Folk (1980) shows that sandstones are mostly quartzarenite and subarkosic in composition (Figure 8.1). Sandstone composition plotted on QFL diagram of Dickinson et al. (1983) shows cratonic interior and transitional continental provenance of sandstone (Figure 8.2).

Maturity of sandstones was calculated by textural maturity criteria developed by Folk (1951) which is summarised as:

I. *Immature stage:* Angular and poorly sorted grains, with considerable amount of clay and fine mica.
II. *Submature stage:* Angular and poorly sorted grains, with very little or no clay.
III. *Mature stage:* Subangular but well sorted grains, with no clay.

IV. *Supermature stage:* Rounded and well sorted grains, with no clay.

According to above mentioned criteria, most of the samples having subangular and well sorted grains, fall in mature stage (stage III), but few samples have high amount of clays which can be classified as immature sandstones (stage I).

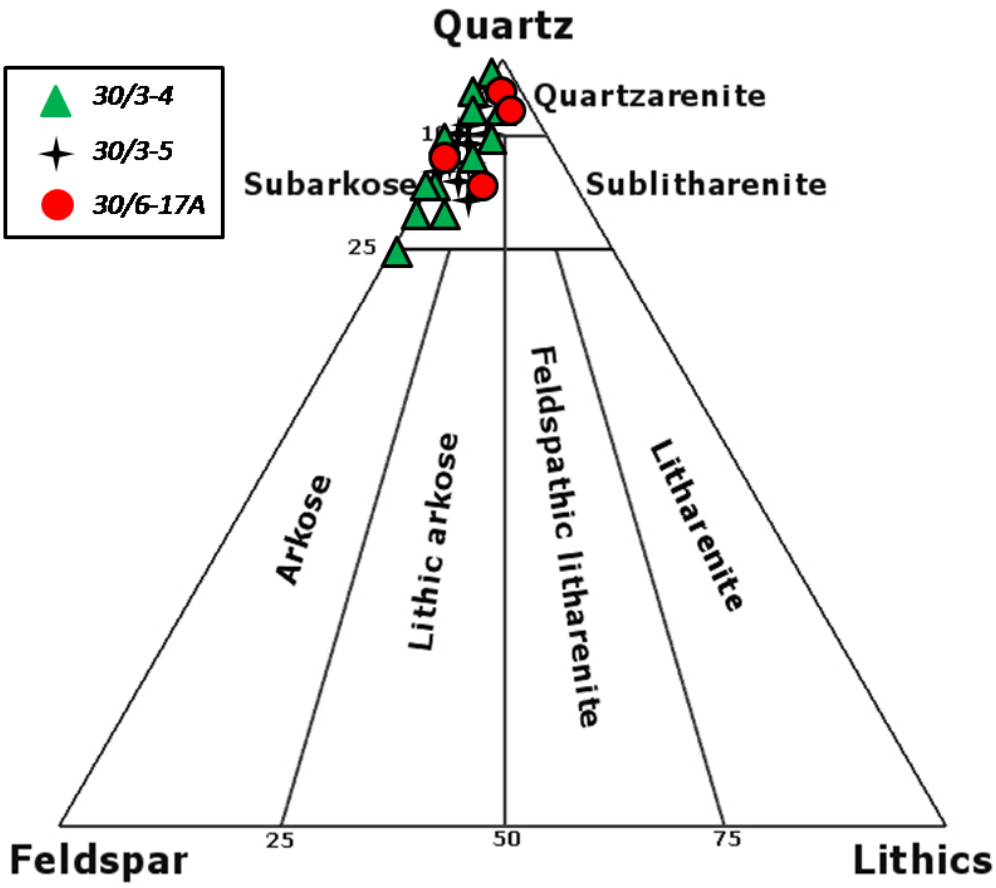

Figure 8.1Classification of sandstones according to Folk (1980) shows sandstones falls in subarkose to quartzarenite category.

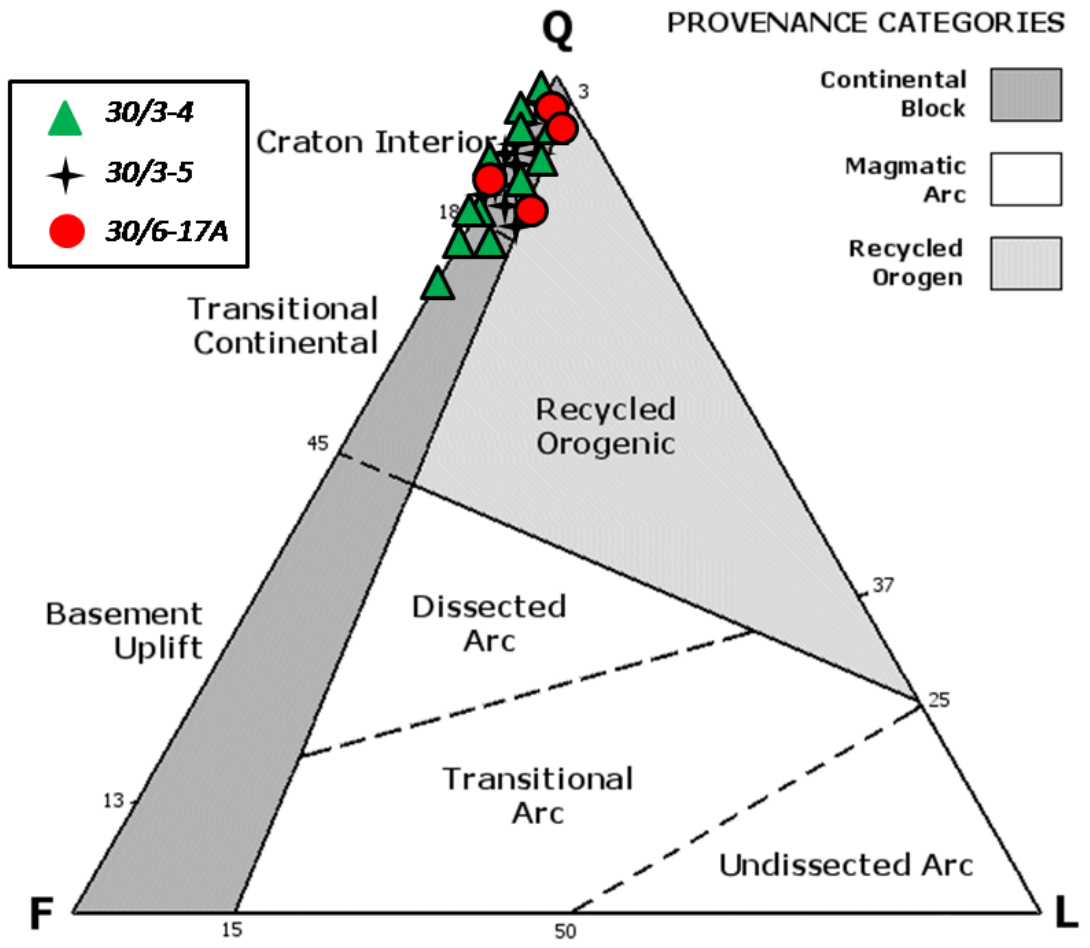

Figure 8.2 Sandstone composition is plotted over Sandstone provenance diagram ((Dickinson et al., 1983) suggesting a cratonic interior and transitional continental provenance.

8.3 Grain size and Sorting

Grain size analysis was performed by using petrographic microscope and ScopeView software (details are mentioned in section 5.2.1). The acquired grain size data was calculated in an Excel spreadsheet called GRADISTAT by Blott and Pye (2001). This spread sheet calculates grain size statistics in several methods but for this study Folk and Ward (1957) method is used. Grain size results are split in two parts, in Table 8.3 results for wells 30/6-17A and 30/3-4 is given with true vertical depths, whereas in Table 8.4 results for well 30/3-5S are given with measured drilling depth to keep it consistent with other petrophysical data.

Well	Formations	Depth	Rock forming minerals					Authigenic Clays		Cement						
			Quartz	Feldspar	Rock Fr.	Calcite	Acc. min.	Kaolinite	Chlorite	Quartz	Cement	Carbonate	Matrix	oal/organic	Porosity	IGV
30/6/17A	Cook	2466.5	65.3	3.1	0.0	6.1	2.0	5.8	2.0	3.1	1.0	0.0	0.0	0.0	11.3	23.3
		2475.8	43.3	3.3	0.0	22.0	2.7	10.7	0.7	4.0	0.0	0.0	0.0	0.0	13.3	28.7
		2487.3	64.7	0.0	0.0	4.7	2.0	8.7	0.7	5.3	0.0	0.0	0.0	0.0	14.0	28.6
	Amundsen	2492.3	56.0	2.7	0.0	3.3	4.7	9.0	0.0	5.0	2.7	0.0	0.0	0.0	16.7	33.3
30/3-4	Ness	2833.7	62.0	2.0	0.0	6.0	2.0	6.0	0.0	3.3	0.0	0.0	0.0	0.0	18.7	28.0
		2867.6	65.2	4.8	2.9	0.0	0.0	6.4	1.3	1.4	1.9	1.4	0.0	0.0	14.7	27.1
	Etive	2874.8	70.2	6.2	0.0	2.3	1.9	9.5	0.0	0.5	0.0	0.0	0.0	0.0	9.5	19.4
		2888.8	59.2	9.0	1.3	1.1	2.6	10.8	4.5	1.5	0.0	3.8	0.0	0.0	6.3	26.8
	Drake	2951.7	55.4	8.1	0.0	8.7	4.7	6.5	1.0	1.8	0.0	4.9	0.0	0.0	9.0	23.1
		2958.6	22.0	2.7	0.0	0.0	0.0	1.3	1.3	4.7	0.0	61.3	0.0	0.0	6.7	75.3
		2959.8	55.5	4.6	0.0	1.1	2.2	3.7	2.3	1.8	0.0	22.2	0.0	0.0	6.5	36.5
	Cook	3088.6	62.7	4.3	0.0	0.0	1.3	3.4	0.4	1.1	0.0	18.2	0.0	0.0	8.6	31.8
		3102.2	51.5	6.1	0.0	0.0	1.4	1.5	0.6	1.4	0.0	37.4	0.0	0.0	0.0	41.0
		3108.6	66.1	7.8	0.0	0.0	2.6	7.8	3.4	1.5	2.4	0.6	0.0	0.0	7.8	23.5
		3113.9	63.0	4.4	0.0	0.0	1.8	7.1	0.9	9.5	0.0	7.1	0.0	0.0	6.2	30.8
		3126.9	60.8	9.8	0.0	0.0	2.9	9.8	6.9	1.3	0.7	0.0	0.0	0.0	7.8	26.5
30/3-5	Ness	4061.80	65.1	2.3	0.0	0.0	0.0	9.3	0.0	0.0	0.0	9.3	0.0	0.0	14.0	32.6
		4086.60	62.3	2.9	0.0	0.0	0.0	8.6	0.0	2.2	0.0	0.0	0.0	0.0	24.0	34.8
		4112.43	65.0	6.5	0.4	0.0	0.0	4.1	0.0	2.1	14.6	0.0	0.0	0.0	7.3	28.1
	Etive	4137.60	60.9	10.2	1.5	0.0	0.0	6.1	0.0	0.0	0.0	10.2	0.0	0.0	11.2	27.4
	Oseberg	4181.43	58.1	8.7	0.7	0.0	0.0	6.2	0.0	3.1	0.0	12.6	0.0	0.0	10.7	32.5
		4210.34	42.4	6.5	0.0	17.3	5.8	7.2	0.0	6.5	1.4	0.0	0.0	0.0	12.9	28.1
	Cook	4429.40	63.0	6.7	0.8	0.0	1.7	13.4	3.4	0.8	0.0	0.8	0.0	1.7	7.6	27.7
		4435.65	65.0	5.7	1.2	0.0	0.8	14.6	5.7	0.0	0.0	0.4	0.0	0.0	6.5	27.2
		4440.75	65.1	4.3	0.9	0.0	1.7	14.8	2.7	5.3	0.0	0.0	0.0	0.0	5.2	27.9
		4441.65	58.8	6.1	0.0	0.0	1.8	14.0	3.5	2.6	0.0	1.3	0.0	0.0	11.8	33.3
		4442.35	59.8	5.6	0.0	0.0	3.4	14.3	4.8	4.9	0.0	1.6	0.0	0.0	5.6	31.2
		4444.70	58.7	3.6	0.3	0.0	2.7	15.1	4.4	3.7	0.0	1.8	0.0	0.0	9.8	34.8

Table 8.1Point counting results of all 28 thin sections.

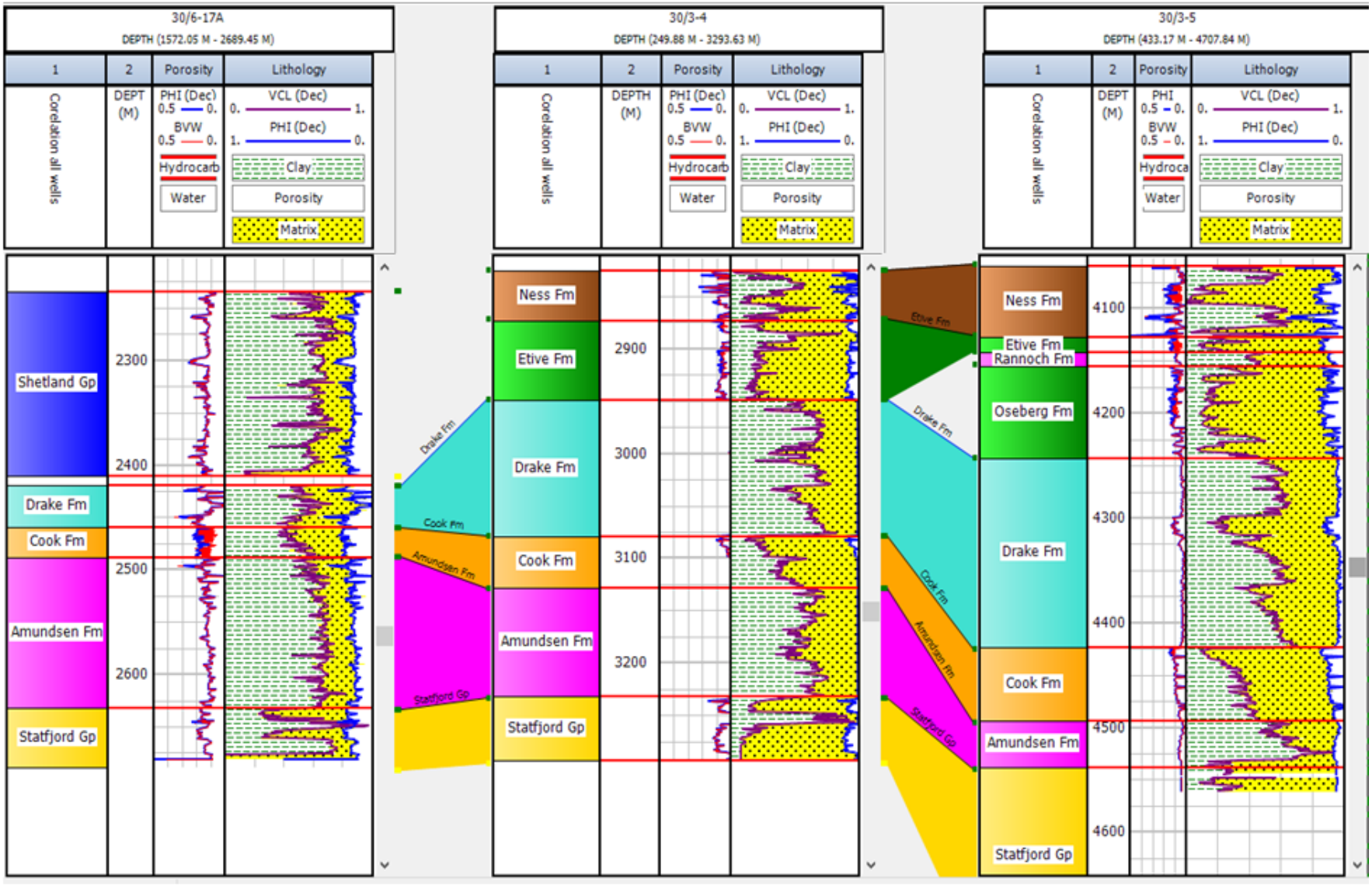

Table 8.2 Stratigraphic correlation of three wells.

Well	Formations	Depth (SSTVD)	Grain sizre (avge)	FOLK AND WARD METHOD 1957				V.COARSE SAND %	COARSE SAND%	MEDIUM SAND%	FINE SAND%	V. FINE SAND%	TOTAL SILT%
				MEAN	SORTING	SKEWNESS	KURTOSIS						
30/6/17 A	Cook	2466.50	156.23	Fine Sand	Moderate	Fine	Platy	0.0	1.9	31.5	42.6	24.1	0.0
		2475.80	193.27	Fine Sand	Moderately Well	Symmetrical	Meso	0.0	3.5	49.1	43.9	1.8	1.7
		2487.32	158.92	Fine Sand	Moderately Well	Fine	Lepto	0.0	0.0	40.0	48.0	12.0	0.0
	Amundsen	2492.33	149.74	Fine Sand	Moderately Well	Fine	Meso	0.0	0.0	30.0	53.3	16.7	0.0
30/3-4	Ness	2833.70	141.88	Fine Sand	Moderately Well	Symmetrical	Lepto	0.0	0.0	21.1	70.2	7.0	1.8
		2867.55	211.54	Fine Sand	Moderately	Fine	Meso	1.8	3.5	43.9	36.8	12.3	1.8
	Etive	2874.80	214.98	Med. Sand	Moderate	Fine	Lepto	0.0	6.7	51.7	33.3	6.7	1.7
		2888.75	109.90	Fine Sand	Moderately Well	Fine	Meso	0.0	0.0	5.1	66.1	27.1	1.7
	Drake	2951.71	234.04	Med. Sand	Poor	Fine	Platy	0.0	25.0	36.5	19.2	17.3	1.9
		2958.60	160.46	Fine Sand	Poorl	Fine	Platy	0.0	6.3	30.2	27.0	25.5	11.0
		2959.80	201.85	Fine Sand	Moderate	Symmetrical	Meso	0.0	9.3	37.0	40.7	11.1	1.9
	Cook	3088.55	150.42	Fine Sand	Moderate	Symmetrical	Meso	0.0	1.8	26.3	47.4	22.8	1.8
		3102.22	137.73	Fine Sand	Moderately Well	Fine	Meso	0.0	0.0	18.9	58.5	20.8	1.9
		3108.55	80.72	V.Fine Sand	Moderately Well	Coarse	Platy	0.0	0.0	3.6	30.4	62.5	3.6
		3113.87	70.18	V.Fine Sand	Well	Coarse	Platy	0.0	0.0	0.0	16.3	79.6	4.1
		3126.90	120.68	Fine Sand	Moderately Well	Fine	Platy	0.0	0.0	14.3	53.1	30.6	2.0

Table 8.3 Grain size results for well 30/6/17 in Oseberg area and 30/3-4 in Veslefrikk area.

Well	Formations	Depth (mMD.)	Grain sizre (avge)	FOLK AND WARD METHOD 1957				V.COARSE SAND %	COARSE SAND%	MEDIUM SAND%	FINE SAND%	V. FINE SAND%	TOTAL SILT%
				MEAN	SORTING	SKEWNESS	KURTOSIS						
30/3-5	Ness	4061.80	47.11	V.Fine Sand	Moderate	Fine	Lepto	0.0	0.0	0.0	11.5	50.4	38.1
		4086.60	272.04	Med. Sand	Poor	Fine	Meso	0.0	27.8	37.0	14.8	14.9	5.5
		4112.43	97.85	Fine Sand	Moderate	Coarse	Meso	1.6	1.6	7.9	34.9	49.2	4.7
	Etive	4137.60	97.27	Fine Sand	Moderately Well	Symmetrical	Meso	0.0	0.0	1.6	50.8	45.9	1.6
		4181.43	235.45	Fine Sand	Poor	Symmetrical	Meso	3.3	13.3	31.7	31.7	18.3	1.7
	Oseberg	4210.34	213.35	Fine Sand	Poor	Coarse	Meso	2.0	13.7	27.5	33.3	23.5	0.0
	Cook	4429.40	110.52	Fine Sand	Moderately Well	Symmetrical	Meso	1.6	1.6	9.8	52.5	32.8	1.6
		4435.65	122.88	Fine Sand	Moderately Well	Symmetrical	Platy	0.0	0.0	13.0	55.6	29.6	1.9
		4440.75	162.48	Fine Sand	Moderately Well	Fine	Meso	0.0	0.0	35.1	55.4	9.5	0.0
		4441.65	191.99	Med Sand	Moderately Well	Fine	Meso	0.0	1.8	52.7	41.8	3.6	0.0
		4442.35	76.70	V.Fine Sand	Moderately Well	Fine	Meso	0.0	0.0	2.0	29.4	60.9	7.8
		4444.70	106.96	Fine Sand	Moderately Well	Coarse	Platy	0.0	1.9	5.7	41.5	49.1	1.9

Table 8.4 Grain size results for well 30/3-5.

Well	Formations	Depth	Quartz	Albite	K-felsd	Calcite	Siderite	Ankerit	Ill/Musc	Chlorite	Kaolid	Pyrite	Rutile	Marcasite
30--6-17A	Cook	2466.5	66.29	6.94	8.59	0.369	2.452	0.384	2.42	0.884	9.5	1.631	0.55	0
		2475.8	51.71	5.4	8.78	0.46	20.36	0.99	1.77	0.89	6.29	3.298	0.045	0
		2487.32	62.11	4.25	10.8	0.777	1.036	0.644	4.99	1.13	11.13	2.249	0.891	0
	Amundsen	2492.55	59.48	5.53	10.54	0.716	0.832	0.286	5.41	2.01	12.71	1.75	0.728	0
30--3-4	Ness	2833.77	80.94	9.2	1.545	0.483	0.904	0.839	1.726	0.999	3.003	0.085	0.277	0
		2867.55	80.84	8.61	2.053	0.544	0.0142	0.314	2.021	1.057	3.67	0.112	0.753	0
	Etive	2874.8	81.65	4.017	6.27	0.618	0.053	0.394	1.324	1.095	4.04	0.123	0.421	0
		2888.75	58.18	6.89	13.12	0.742	0	0.231	5.93	2.74	10.25	1.062	0.863	0
	Drake	2951.7	62.82	4.583	12.03	6.731	0.64	0.402	3.26	1.85	7.21	0.073	0.4	0
		2958.6	20.09	2.56	5.79	0	55.45	0	4.26	2.3	6.99	0.198	0	2.37
		2959.8	55.51	5.28	7.37	21.86	1.64	0.471	2.85	1.08	3.73	0.036	0.163	0
	Cook	3088.75	69.11	9.01	5.86	7.626	0	0.515	1.261	1.389	4.51	0.637	0.089	0
		3102.22	39.68	6.28	4.997	35.24	0	1.85	2.8	1.533	6.31	0.85	0.462	0
		3108.55	62.85	10.88	6.29	0.558	0	2.66	7.24	2.56	5.8	0.261	0.898	0
		3113.87	63.39	10.1	6.77	1.538	0	0.17	6.56	3.4	7.37	0.182	0.518	0
		3126.9	48.64	12.64	7.73	0.661	1.228	0	13.01	6.65	7.46	0.893	1.081	0
30--3-5	Ness	4061.80	67.16	4.74	5.57	0.78	0.00	0.20	9.83	2.17	8.27	0.10	1.19	0.00
		4086.60	89.90	3.13	0.34	0.32	0.63	0.00	1.09	0.00	4.11	0.13	0.34	0.00
		4112.43	77.11	8.97	2.05	0.55	0.84	0.28	3.64	1.25	4.18	0.33	0.82	0.00
	Etive	4137.60	54.89	5.92	13.16	0.84	0.00	0.14	8.64	3.58	11.18	0.39	1.28	0.00
	Oseberg	4181.43	68.65	4.20	6.51	0.41	0.00	8.80	2.50	1.77	7.01	0.10	0.04	0.00
		4210.34	53.30	3.30	5.33	0.40	0.00	24.49	2.27	1.57	6.22	0.22	0.13	2.77
	Cook	4429.40	62.06	9.13	6.04	1.41	0.00	0.27	7.14	2.43	8.21	2.42	0.90	0.00
		4435.65	60.45	8.56	5.93	1.10	0.00	0.23	8.37	3.58	9.34	1.40	1.04	0.00
		4440.75	63.48	8.48	5.94	0.72	0.00	0.27	8.08	3.42	7.08	1.46	1.07	0.00
		4441.65	75.48	8.90	2.77	0.59	0.00	2.25	2.24	2.34	4.65	0.45	0.33	0.00
		4442.35	51.79	9.44	8.02	0.72	0.00	0.15	12.77	5.54	8.43	1.63	1.51	0.00
		4444.70	62.54	11.23	5.89	0.58	0.00	0.13	7.60	3.28	7.21	0.52	1.05	0.00

Table 8.5 Bulk mineralogical composition of samples obtain through XRD analysis.

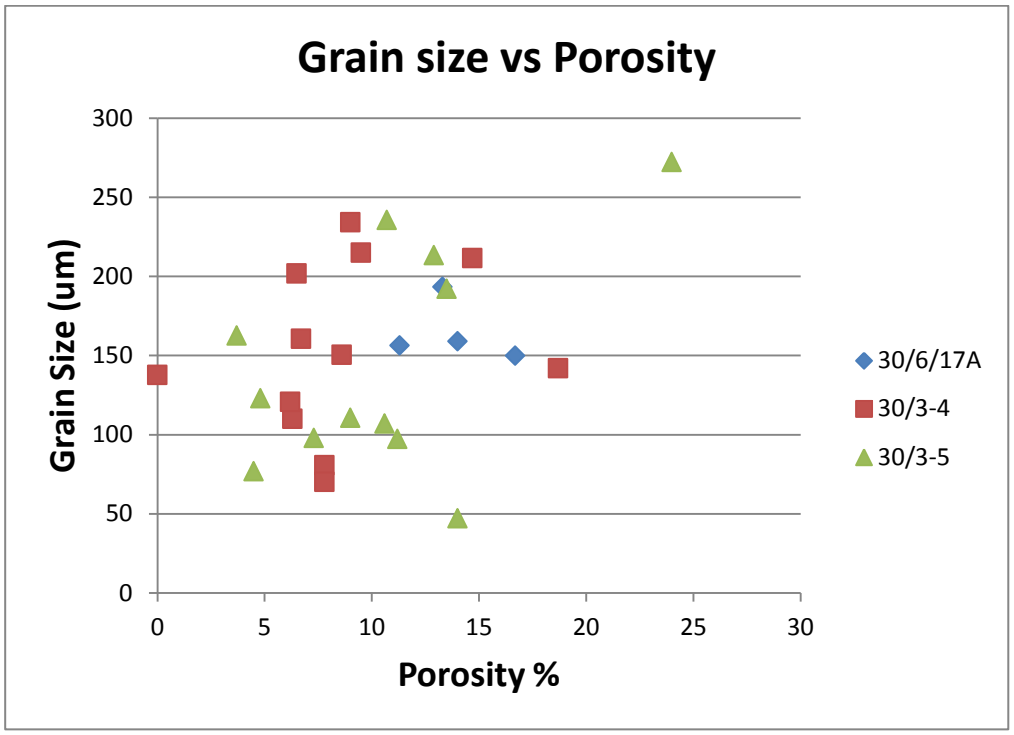

Figure 8.3 Grain size vs porosity cross-plot shows increasing porosity with increasing grain size.

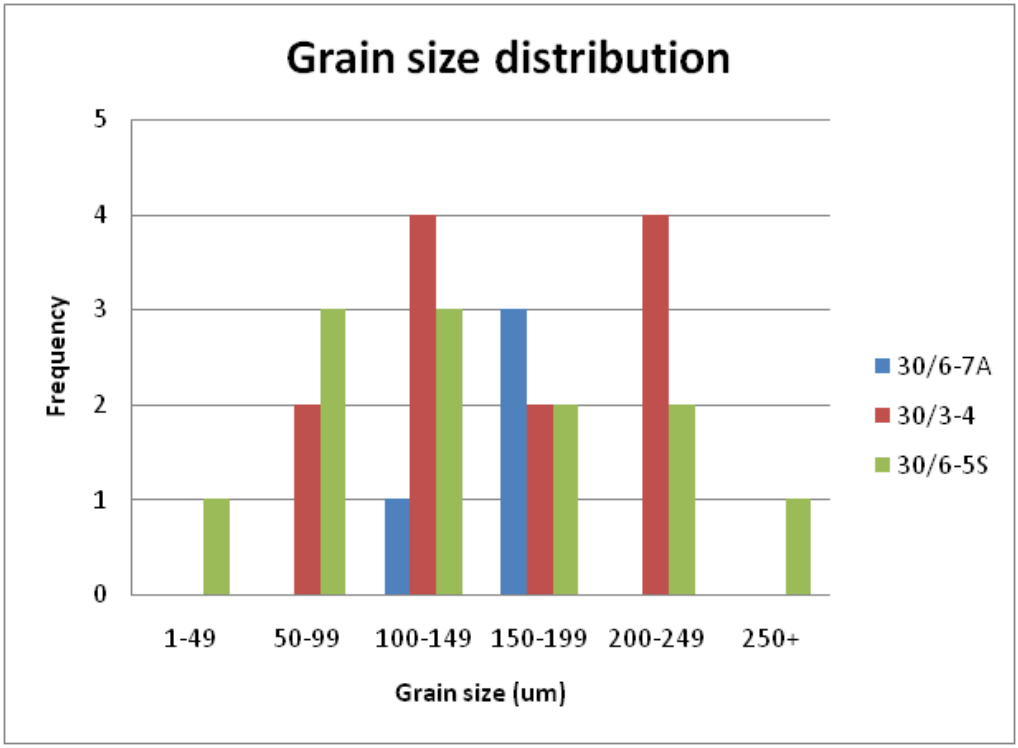

Figure 8.4 Grain size distribution in three studied wells.

8.4 Intergranular volume

Intergranular volume (IGV) is the sum of inter granular porosity, matrix and cements. IGV is considered as a good index of the compaction state of sandstone. It indicates the amount of maximum possible porosity that can be expected in the absence of cement and depositional matrix (Bloch et al., 2002, Paxton et al., 2002). Inter granular volume (IGV) is determined after the porosity loss by mechanical compaction and prior to the start of chemical compaction (Bjørlykke and Jahren, 2010).

Paxton et al. (2002) showed in his study that IGV of sands declines rapidly due to mechanical compaction from about 40-42% at the surface to approximately 28% at 1500 meters depth. IGV continues to decrease slowly between 1500-2500 to 26% when framework becomes more stable. It also showed that grain compaction is limited in rigid grain sandstones which imply that occurrence and distribution of deep porosity is dependent upon the availability and volume of pore filling cement. Therefore, deep, porous sandstones are less cemented rather than being under compacted.

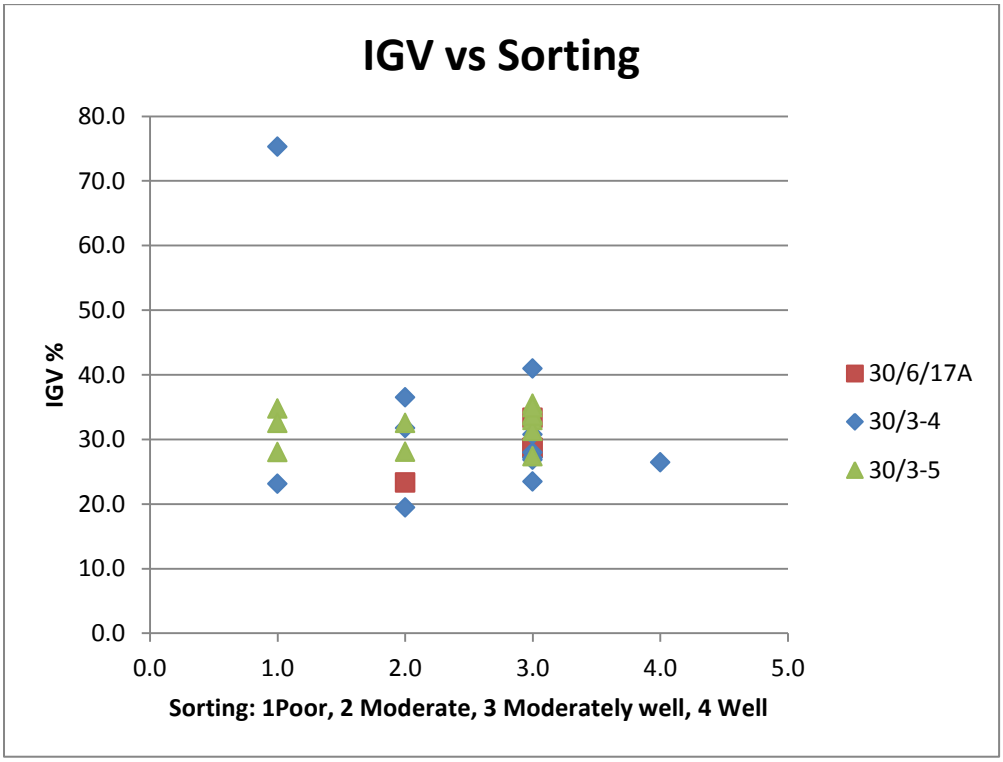

Figure 8.5 IGV plotted against Sorting, moderate to moderately well sorted samples are in majority.

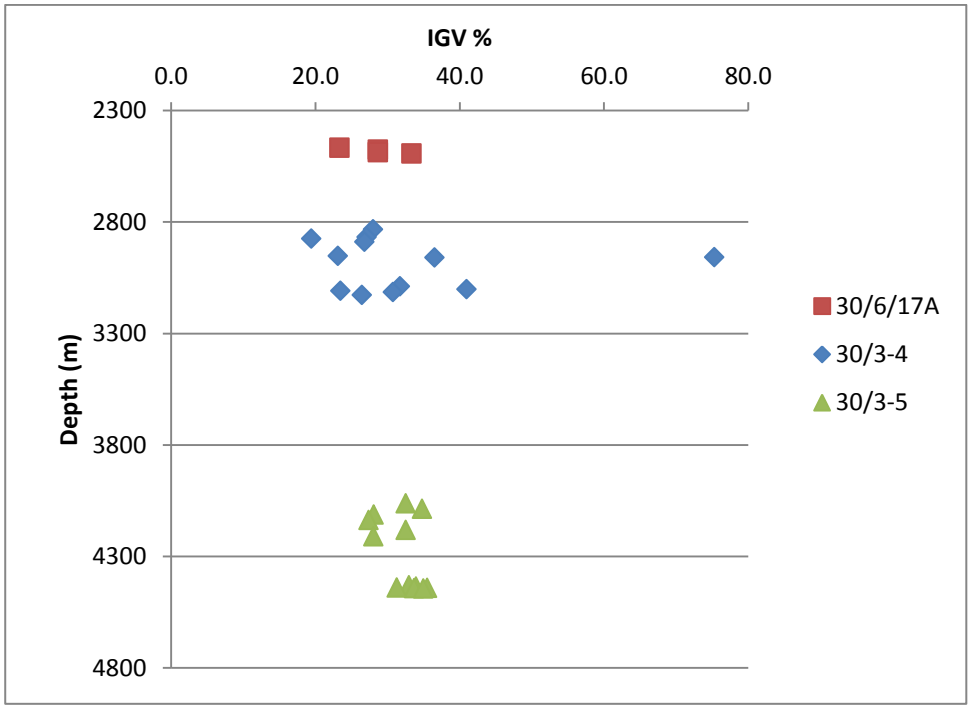

Figure 8.6 IGV vs. Depth cross plot.

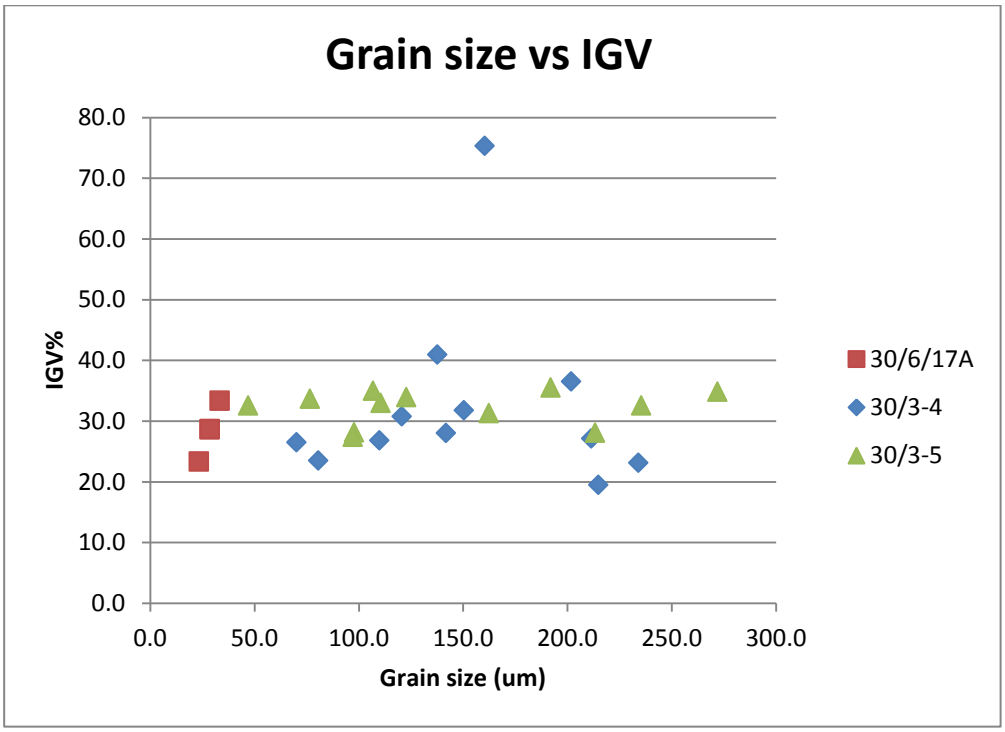

Figure 8.7Grain size vs. IGV cross plot does not show any significant trend.

XRD results from well 30/6-17A (Oseberg area) are mentioned below in Figure 8.8; it can be observed that there is very little change in mineralogical composition of samples except one sample at depth 2475.8 meters has more siderite than others.

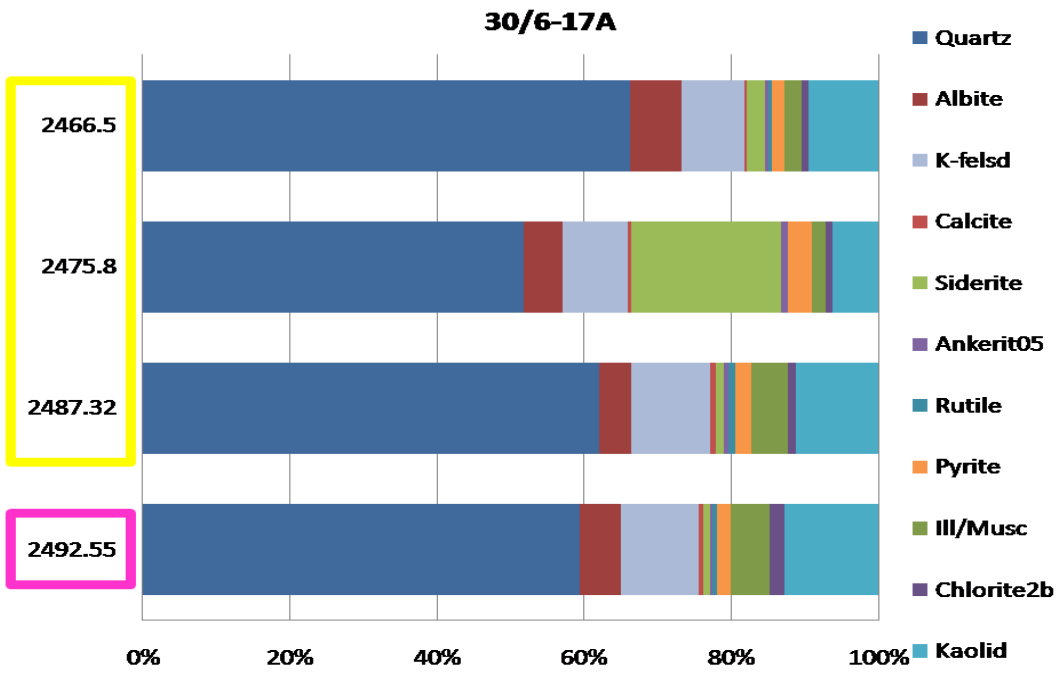

Figure 8.8 XRD results of well 30/6-17A from Oseberg area (coloured squares represent the formations mentioned in Table 8.1)

In Figure 8.9 and 8.10, it can be seen that quartz content is more or less constant in samples from the same formation (marked by distinct coloured squares) except sample at 2958.60 meters depth, which has significant amount of siderite cement. This sample shows 75% of IGV due to siderite cementation. One sample at 3102.22 meters depth exhibits almost zero porosity in thin section due to relatively high amount of calcite cement. This high cement can be formed by the re-crystallization of bioclasts or aragonite grains during diagenesis, which were in contact with sand grains at the time of deposition.

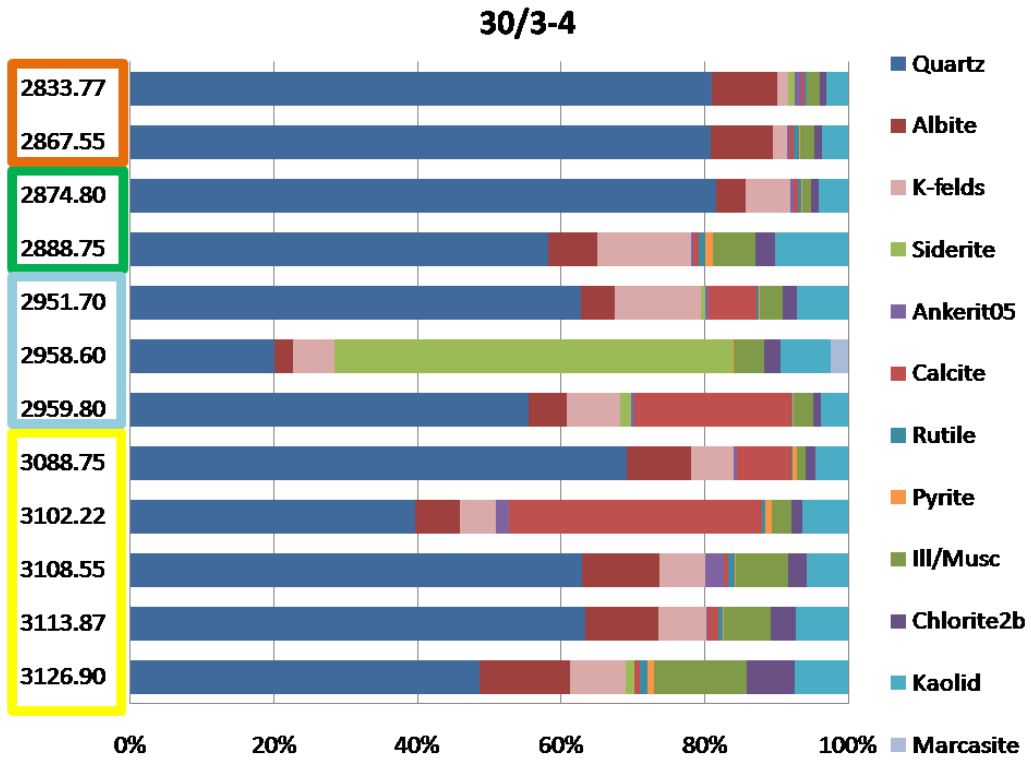

Figure 8.9 XRD results of well 30/3-4 from Veslefrikk area.

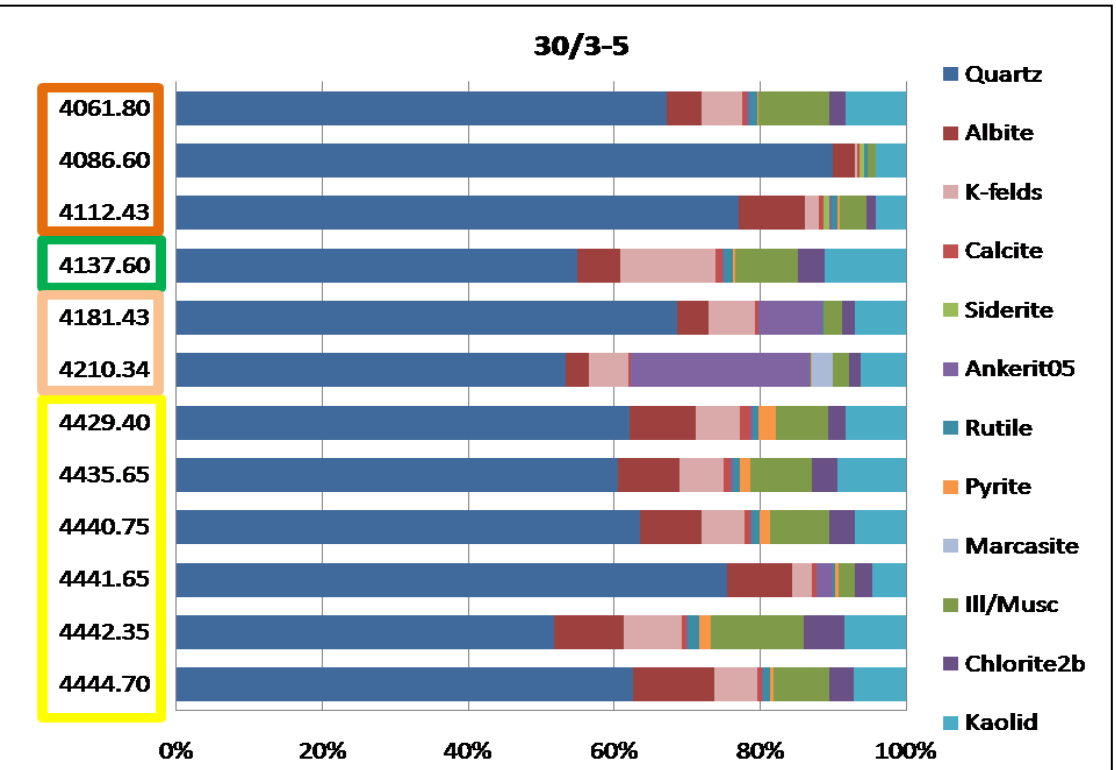

Figure 8.10 XRD results of well 30/3-5 from Veslefrikk area.

8.5 SEM Petrography

Authigenic clays (kaolinite, chlorite), quartz overgrowths, heavy minerals such as rutile, apatite and pyrite were observed in almost all the samples along with other rock forming minerals. Stacked booklets and vermiculite structure of kaolinite grains indicated authigenic origin. In almost all the samples kaolinite acted as porefilling mineral.

Chlorite was observed at depths more than 2800 meters and it varied significantly in morphology. Partial and complete chlorite coating was observed Cook Formation in wells 30/3-4 and 30/3-5 (Veslefrikk area). In Oseberg area, only quartz and siderite cement was observed and chlorite coating was not found.

Fibrous illite was observed in few samples along with authigenic kaolinite and sometimes with chlorite as well. It acted as pore filling mineral in most of the cases (Figure 8.12b). It was found in minor amounts and mostly around leaching K-feldspar grains.

Carbonate cement was also found in minor amounts in some samples but in well 30/3-4, in Cook Formation at a depth of 3102 meters, carbonate cement found around 35% and destroyed almost all the porosity (Figure 8.11). In optical microscope, carbonate cement was easily identified because of its distinct cleavage planes and colour.

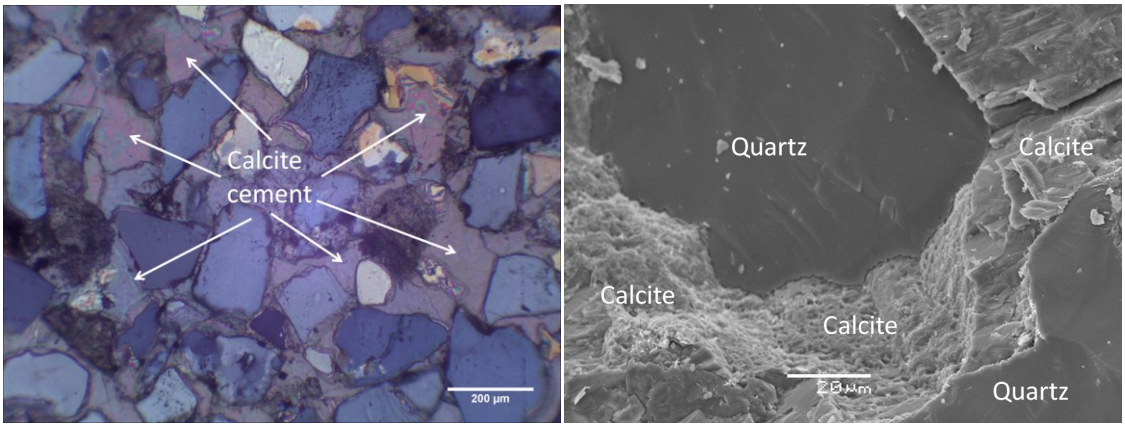

Figure 8.11 High amount of calcite cement occupied all the available porosity (30/3-4, 3102.2m). Left: Optical microscope image; right: BSE image.

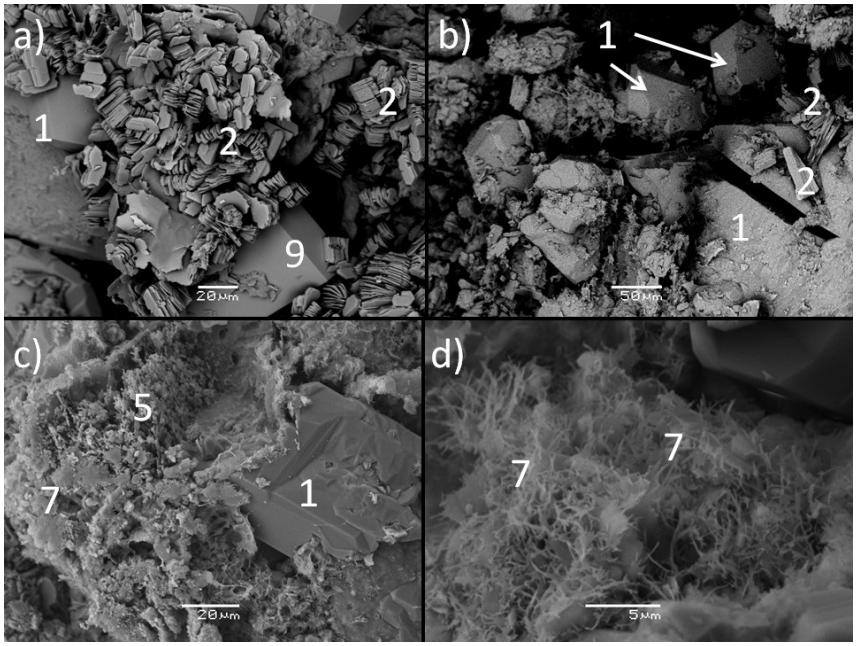

Figure 8.12 a) and b) are both authigenic kaolinite can be observed with quartz overgrowths (30/3-5S, 4086.60m,). c) Leached out K-feldspar and adjacent illite can be seen with quartz overgrowth (30/3-5S, 4061.8m). d) Fibrous authigenic illite can be observed (30/3-5S, 4086.6m).

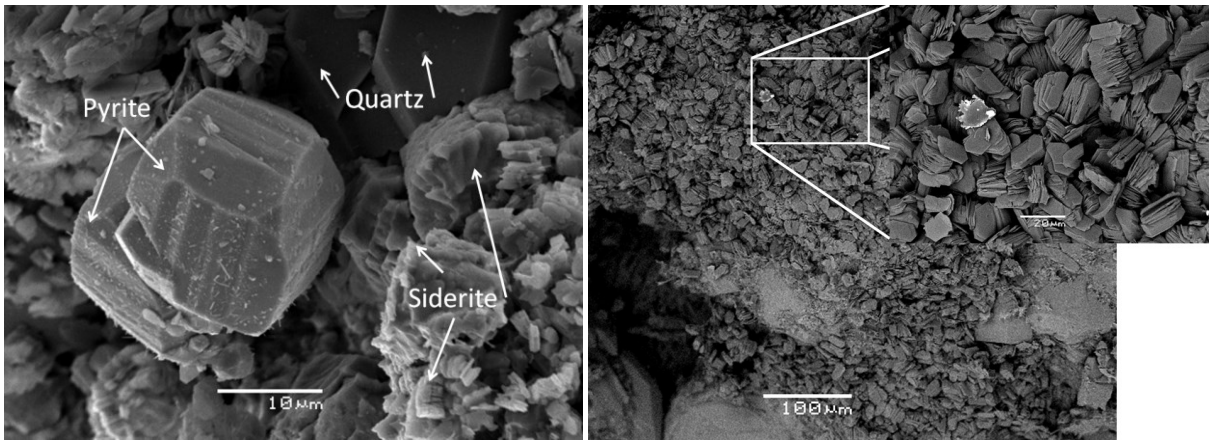

Figure 8.13 Pyrite grain attached to siderite (30/6-17A, 2492.55m). Authigenic pore filling clays (right) (30/3-5S, 4181.43 m)

Heavy minerals like zircon ($ZrSiO_2$) in Figure 8.14, barite ($BaSO_4$), pyrite (FeS_2) in Figure 8.13, rutile (TiO_2), and siderite ($FeCO_3$) in (Figure 8.13) were found mostly attached to clay matrix.

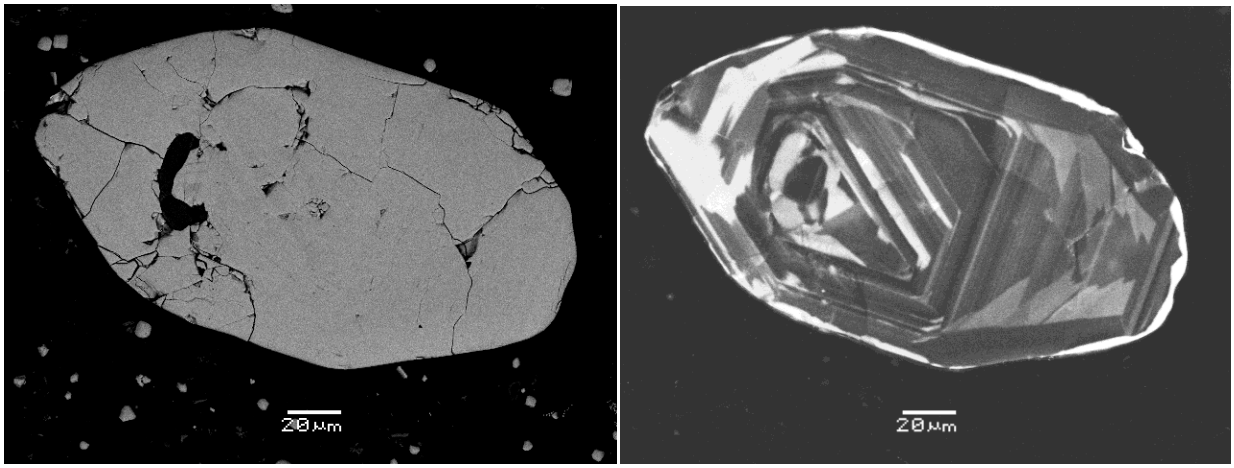

Figure 8.14 Zircon in backscattered electron (BSE) image (left) and in cathodoluminescence (CL) image (right) (30/6-17A, 2487.32m).

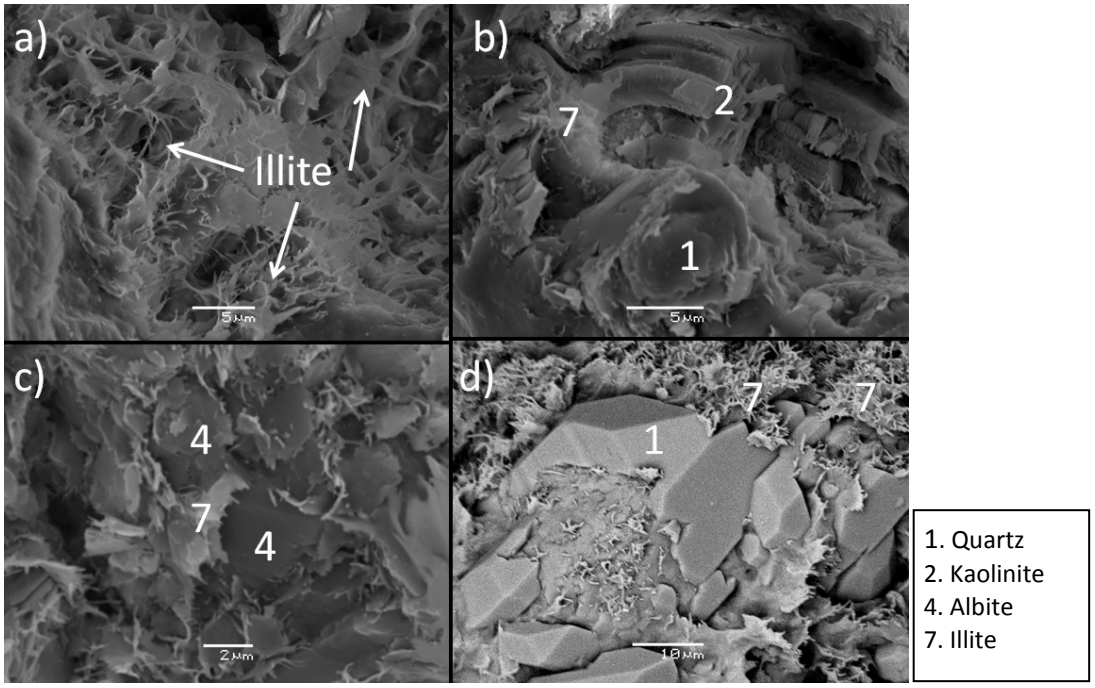

Figure 8.15 a) Authigenic illite, b) Authigenic chlorite, quartz and illite, c) Albite grains are coated with illite fibre (a, b, c are form 30/3-5S, 4061.8m), d) Quartz overgrowth surrounded by illite fibres. (30/3-5S, 4086.6m).

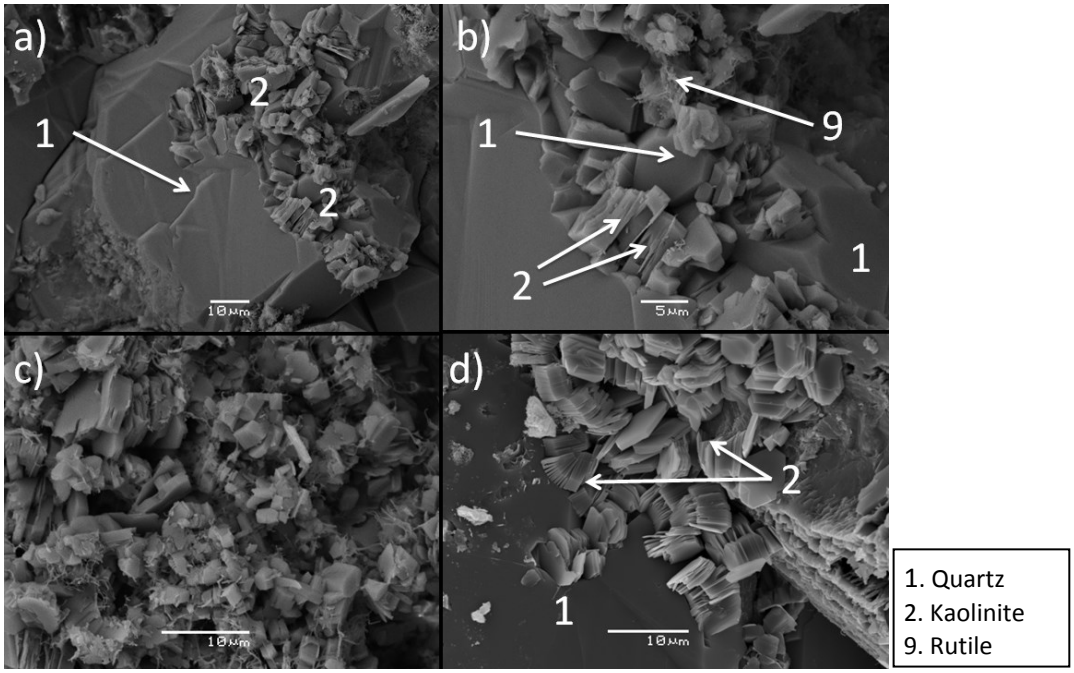

Figure 8.16 a) Quartz overgrowth is enclosing pre-existing kaolinite grains, b) Zoom up of a) (30/3-5S, 4112.43m), c) Illite fibres can be seen growing between kaolinite booklet shape grains (30/3-5S, 4112.43m), d) Quartz overgrowth prevailing in spite of kaolinite presence (30/3-5S, 4137.6m) .

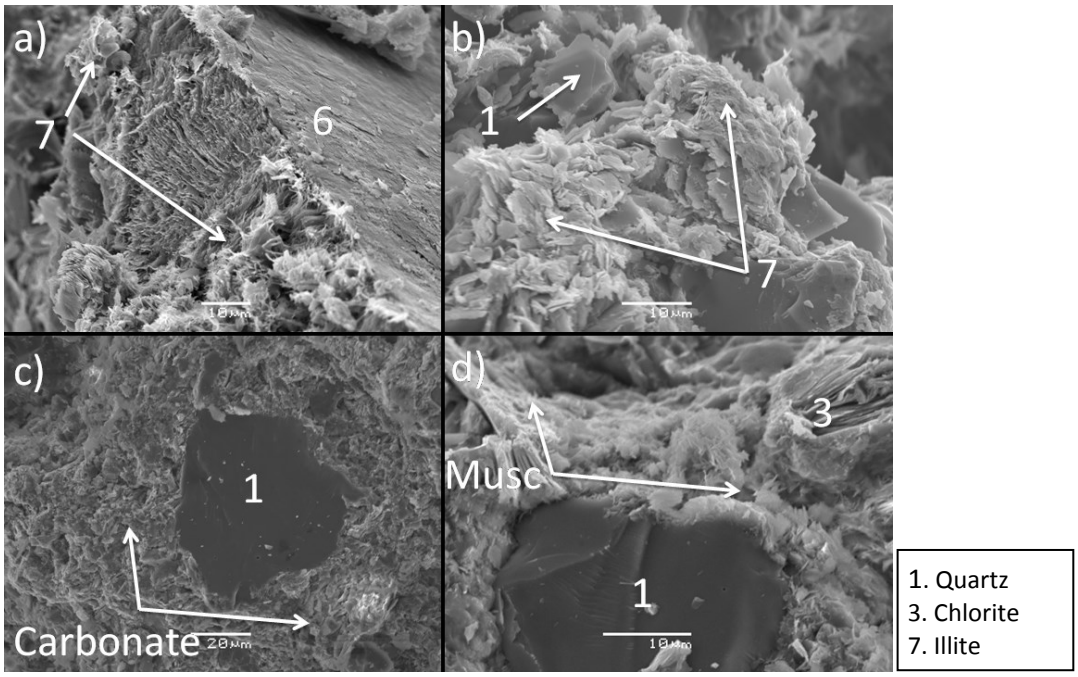

Figure 8.17 a) Illite attached to muscovite, (30/3-5S, 4137.60m) b) illite with quartz (in 30/3-4, 2958.6m), c) Quartz grain is completely surrounded by carbonate cement (30/3-4, 2958.6m), d) Quartz grain covered by muscovite and chlorite (30/3-4, 3126.9m).

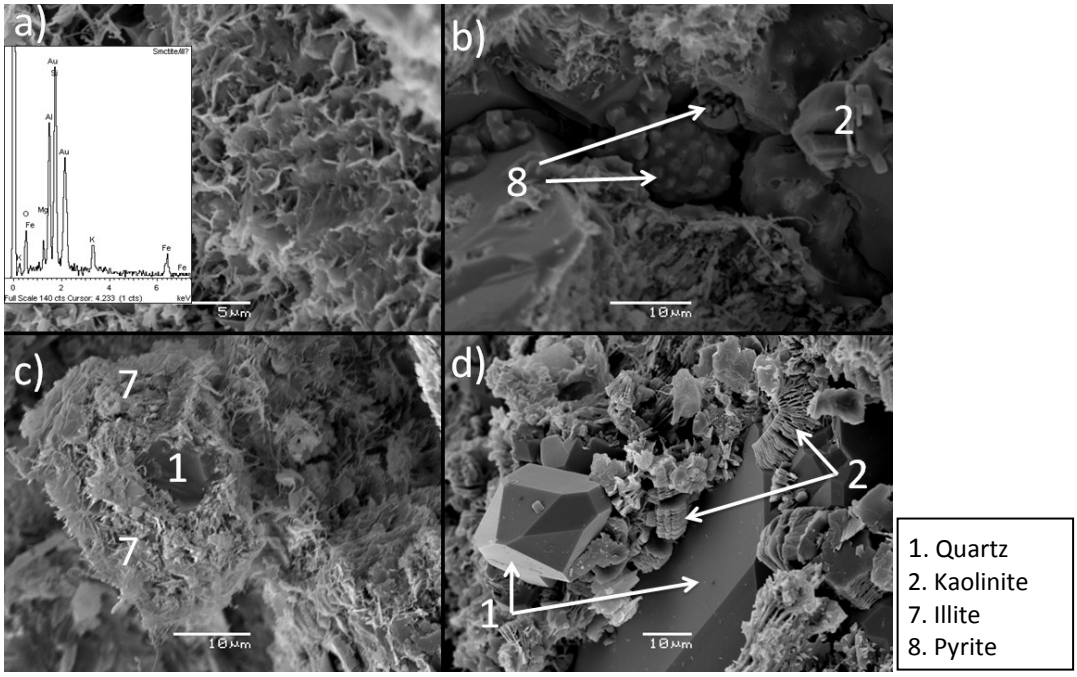

Figure 8.18 a) Transition between illite and smectite, (30/3-4, 3113.87m) b) Pyrite and kaolinite (30/3-4, 3113.87m), c) Quartz grain is completely coated by thick illite fibres (30/3-4, 3113.87m), d) Authigenic kaolinite with typical prismatic quartz overgrowths (30/3-4, 3126.9m).

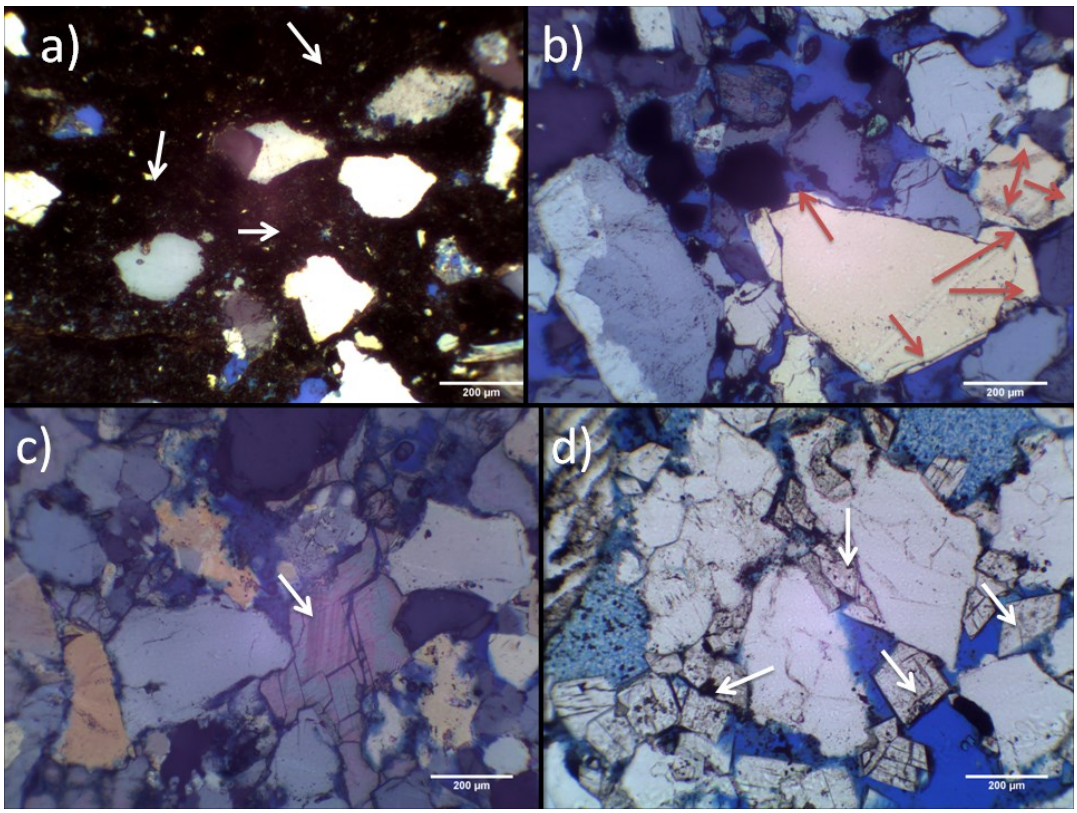

Figure 8.19 a) Matrix (siderite cement) supported texture explain unusually high IGV, (30/3-4, 2958.6m) b) Quartz overgrowths cans be seen along the rims of grains shown by orange arrows, (30/3-4, 2867.55m), c) White arrow points out towards porefilling calcite grains, (30/3-5S, 4210.4m), d) White arrows pointing calcite grains existing more like porefilling grains (30/3-4, 2959.8m).

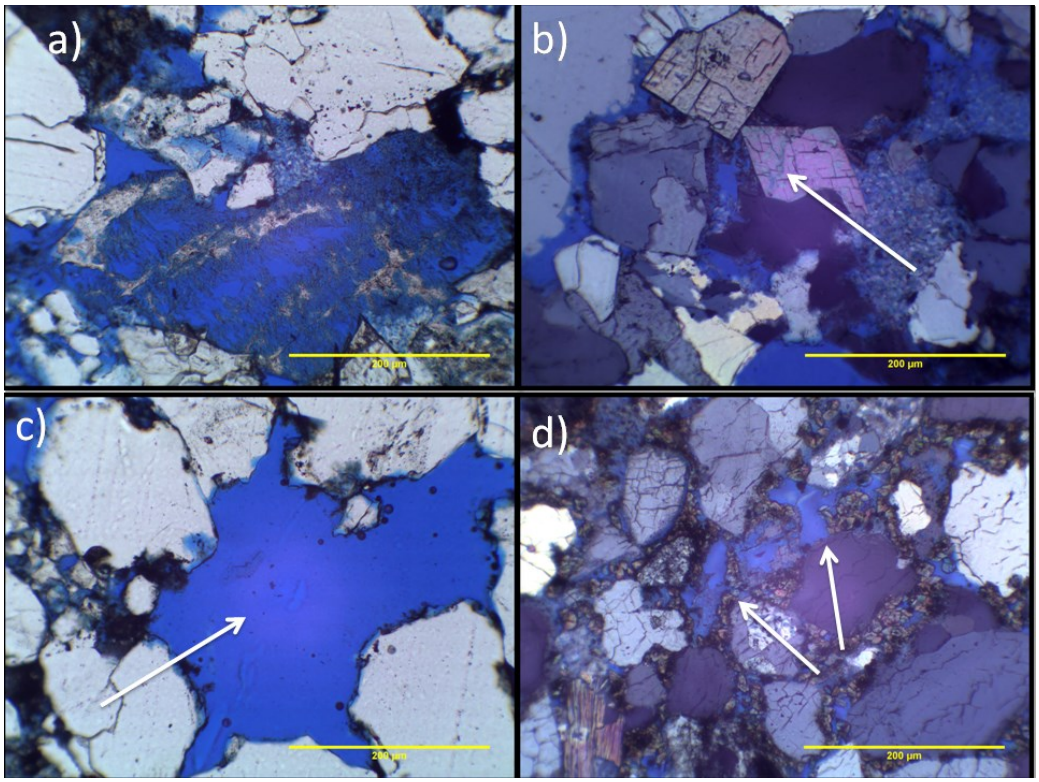

Figure 8.20 a) Secondary porosity by dissolution of a grain can be seen, b) Ankerite crystal shown by arrow (30/3-5S, 4181.43m), c) White arrow points out towards large pore space, (30/6-17A, 4086.6m), d) White arrows pointing towards secondary porosity (30/6-17A, 2475.8m).

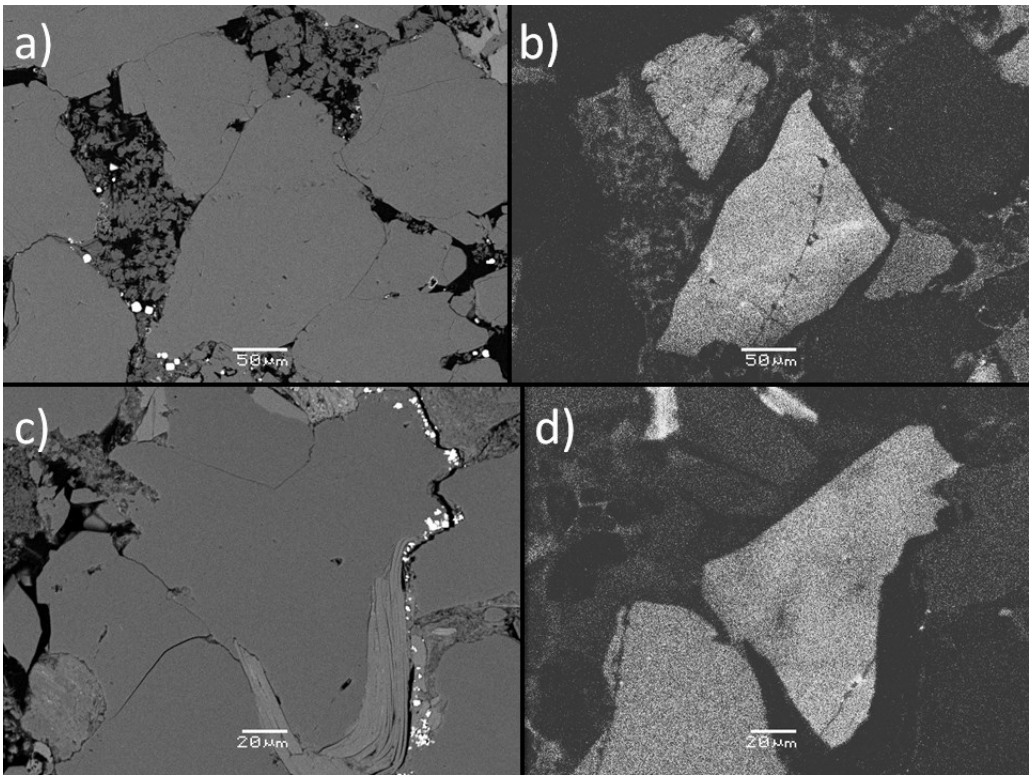

Figure 8.21 a) BSE image show quartz grains and porefilling kaolinite, b) CL image of the same area reveals the bright detrital grains (30/6-17A, 2487.32m), c) BSE image show quartz overgrowth, d) CL image exposes the detrital bright grains and gives an idea about original IGV (30/3-4, 3113.8m).

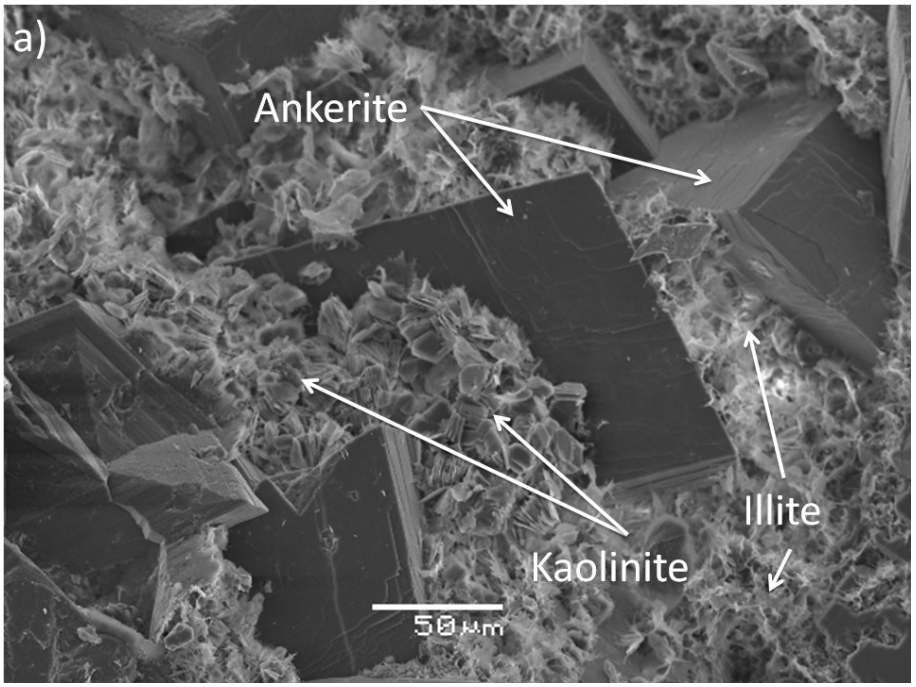

Figure 8.22Ankerite crystals in kaolinite and illite matrix (30/3-4, 4210.34m).

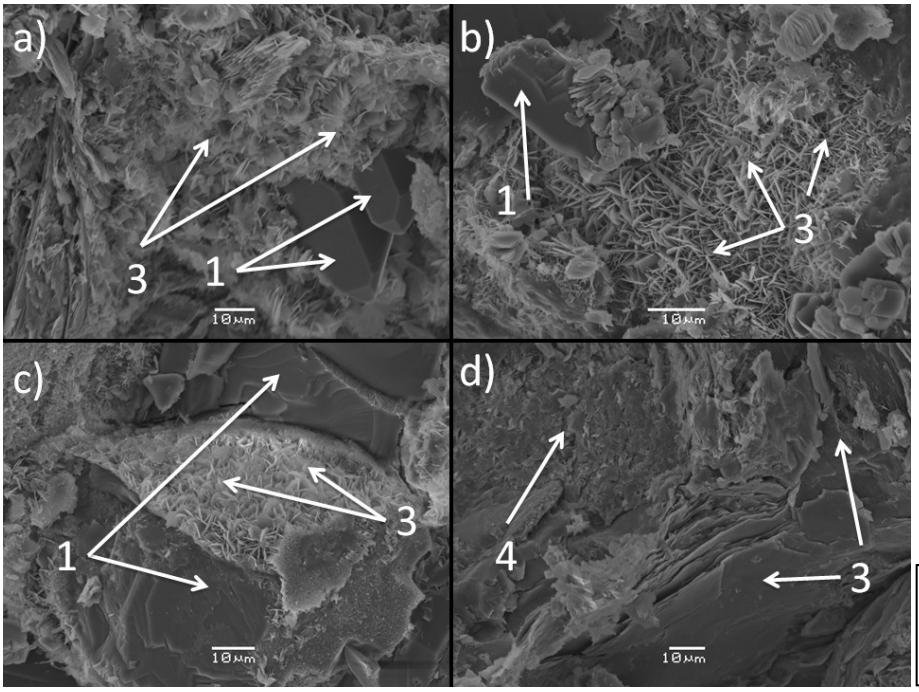

Figure 8.23 a) Quartz over growth can be seen in spite of chlorite coatings (30/3-5S, 4440.75m), b) Flaky chlorite grains can be seen (30/3-5S, 4440.75m), c) Partial coating of quartz grains (30/3-5S, 4441.65m), d) Sheet-like form of chlorite with albite (30/3-5S, 4442.35m).

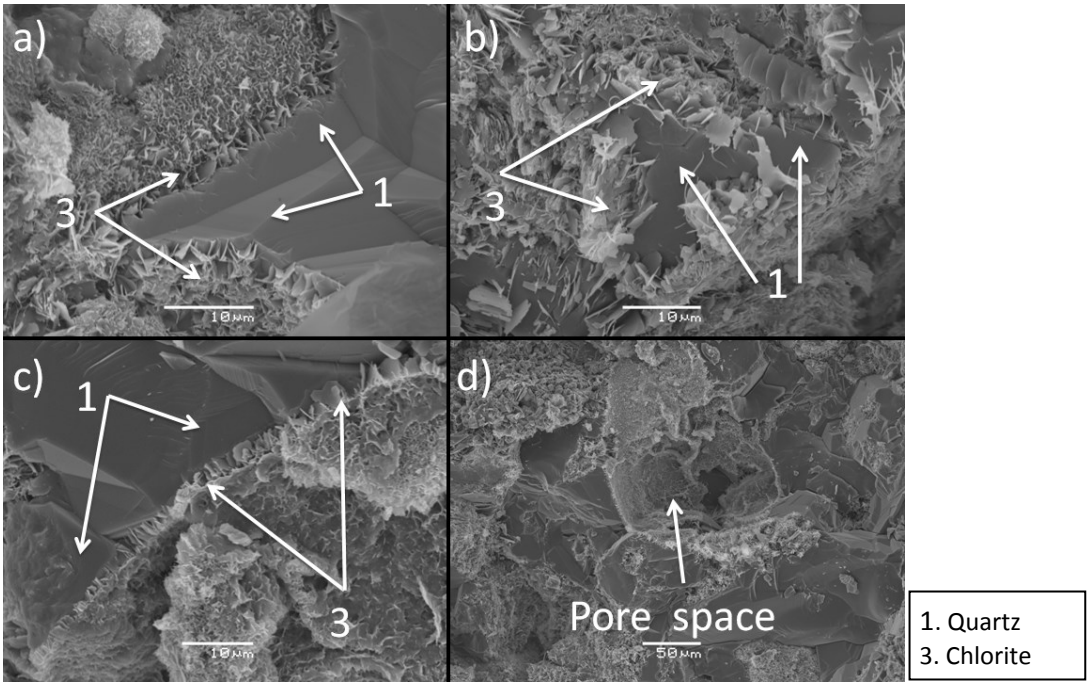

Figure 8.24 a) Quartz over growth can be seen growing into chlorite (30/3-5S, 4444.70m), b) and c) Flaky chlorite grains are covering the surface of quartz grains (30/3-5S, 4444.70m), d) Pore can be seen chlorite coated form inside (30/3-5S, 4444.70m).

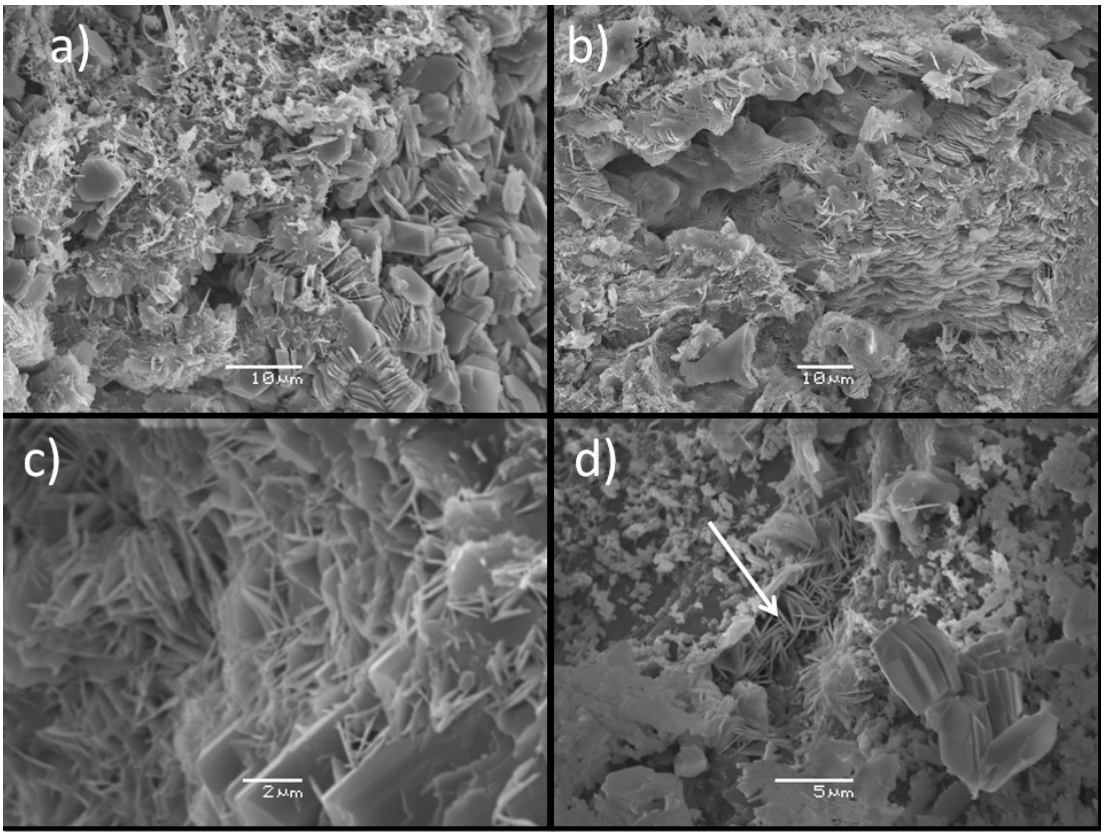

Figure 8.25 a) Mixture of kaolinite, chlorite and illite (30/3-4, 3108.55m), b) Aggregate of chlorite grains (30/3-4, 3108.55m), c) Flaky chlorite grains (30/3-4, 3088.75m), d) Flaky chlorite is visible through grain contact (30/3-4, 3088.75m).

9. Discussion

9.1 Introduction

In this chapter, results from chapters 6, 7, and 8 will be discussed to understand the relationship between chlorite coatings and geological processes involved. Focus of this chapter will be on Cook Formation. Chlorite coating was found in wells 30/3-4 and 30/3-5S in Veslefrikk area. It has been observed in Section 8.5 that chlorite exist in deeper parts of Cook Formation. Chlorite significantly coats detrital grains to preserve them from further cementation and eventually loosing porosity. Chlorite coating was visible in SEM stub images (Figure 8.23 and 8.24), but was not visible in petrographic microscope, possibly because of very small size. In well 30/6-17A (Oseberg area) only quartz cementation was observed.

9.2 Depositional environment of Cook Formation

Cook Formation consists of sand stone packages with wide range of depositional settings in different parts of the basin as explained in section 0. Depositional environments were interpreted on the basis of core images and wireline logs as described in section 1.1. Cook Formation showed coarsening upward trend in both areas with slight variation. In Oseberg area, facies analysis suggested the depositional environment as upper shoreface deposits, whereas tidally influenced prograding deltaic environment was observed in Veslefrikk area. In well 30/3-4 of Veslefrikk, subtidal features like wavy, lenticular and flaser beddings (Facies B4/B3) were observed at the bottom of Cook Formation, they further transformed into bioturbated tidal flat sandstones (Facies B3/B2). These facies transformed into coarser and cleaner, fine to medium grain, brown sandstone units. These units show cycles of mud drapes and wave ripples (Facies B1), indicating a relatively high energy setting with tidal influence, possibly tidal channel deposits. This facies was also found in second well of Veslefrikk (i.e. 30/3-5S, Facies C2), but contained slightly thinner mud drapes and light grey colour. Mud drapes get thinner and fewer in the upper part of Cook Formation in this well. At the top (Facies C1) sand cycles are thick and mud drapes and wave ripples are thinner, suggesting a more or less similar setting like Facies B1 and C2 but closer to shoreface. In both wells, Cook Formation has more or less similar thickness i.e. 45 and 49

meters in 30/3-4 and 30/3-5S, respectively. Over all, Cook Formation has a shallowing upward depositional setting.

In Oseberg area Facies A2 was found in the lower part of Cook Formation as fine grain porous sandstone with few thin layers of mud. In the upper part Facies A1 was fine to medium grain, more porous and cleaner sandstone. No organic fragments, roots or plant fragments were observed, indicating the distance from continental area and reworking of the sediments. Cook Formation was found as 28m thick sandstone interval and interpreted as shoreface deposits.

This interpretation is similar to Livbjerg and Mjøs (1989), they divided Cook Formation in three units i.e. A: prograding subtidal sand body, C: offshore ridge and B: thin mudstone bed separating A and C. However, during this study only upper shoreface sandstone unit was found which is closely related to C unit. Thickness of Cook Formation reduces from Veslefrikk towards Oseberg area which could indicate that progradation took place from Veslefrikk area (north of Oseberg).

9.3 Petrography

Samples were analysed by point counting under optical microscope for porosity, cementation, IGV calculation, mineralogical composition, determination of the degree of cementation, and mechanical and chemical compaction effects. Only grain to grain contacts were included for IGV and porosity calculations in point counting, while mud drapes were ignored. IGV ranged between 19.4% - 41% with an outlier being 75.3%. Average IGV in all three wells was calculated about 32% with one sample being abnormally high. Sample at depth 2958.6 meters in well 30/3-4 showed very high amount (61%) of carbonate cement leading in overestimated calculation of IGV i.e. 75% in thin section (Figure 8.a). These results were also conformed later in XRD analysis which showed about 55% siderite in the sample (Table 8.5). This high IGV put this sandstone in fluid state with very little grain to grain contact. Generally, grain supported sands are deposited with an IGV range between 40-42%. In thin section image (Figure 8.a), it can be seen that grains are not in contact with each other they are rather in a suspended state within carbonate cement (siderite in this case). It could be postulated that grain supporting carbonates were dissolved and replaced or transformed into porefilling cement.

9.3.1 Porosity observations

A normal trend of porosity and carbonate proportion can be seen in Figure 9.1. It is noticeable that high carbonate cement is related to low porosity values, and vice versa. Carbonate grains dissolve in early phase of diagenesis and their precipitation and re-crystallisation can occupy available pore spaces, ultimately reducing the reservoir quality.

Except in well 30/3-4, Cook Formation in other two wells appears to have little or no carbonate cement. In Oseberg area, only one sample has significant siderite cement but it has not depleted porosity. It could be due to the reason that carbonate grains are in dissolving state and creating secondary porosity (Figure 8.20). Presence of siderite cement is also observed by Marjanac and Steel (1997) in the upper part of Cook Formation.

In Veslefrikk area, Cook Formation has high amounts of carbonate cement in one sample of well 30/3-4 at 3102 meters depth, calcite cement has occupied all the pore spaces hence reducing the porosity to zero (Figure 8.11). Siderite cementation can reduce the area available for quartz cementation (which is a permanent porosity occupier) in early stages of diagenesis. In later stages of diagenesis, siderite cement can dissolve partially or completely producing secondary porosity which can be available for hydrocarbons, migrating into the reservoir. This type of model is observed by Rossi et al. (2001) in fluvio-deltaic sandstones of Jurassic age Khatatba Formation of Egypt

Oseberg Formation (Middle Jurassic) has carbonate cement (sample 4181.43) as it is observed by Walderhaug and Bjørkum (1992) and as well as in this study. Porosity in this sample is still available in the form of primary and secondary porosity as seen in Figure 8.20a.

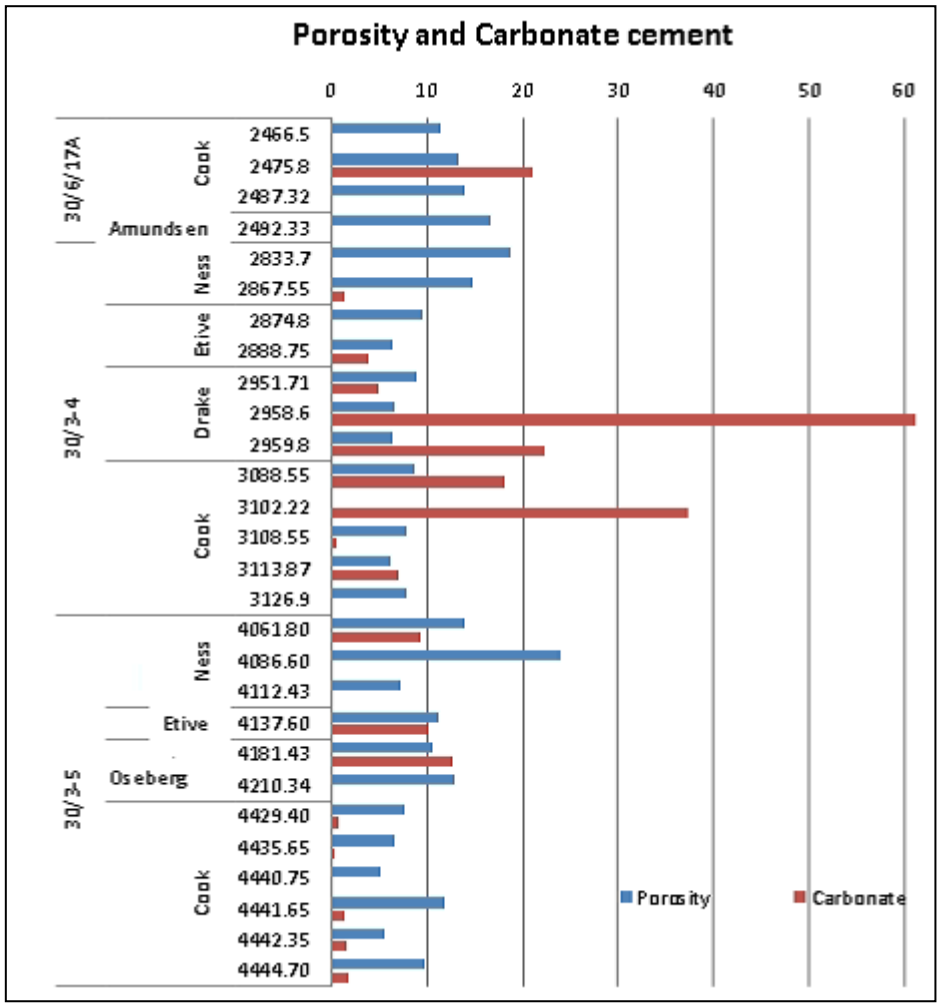

Figure 9.1 Carbonate cement and porosity proportions in study wells.

9.3.2 Grain size

Grain size analyses showed most of the sandstones are fine grained. Average grain size of Cook Formation in Veslefrikk and Oseberg area was 120 and 169 microns, respectively. Cook Formation showed an upward coarsening trend in all the wells which is vaguely observed in Table 8.3 and 8.4. In well 30/3-4 coarsening upward trend can be seen by looking at the average grain size data, whereas in 30/3-5S and 30/6-30/6-17A this trend is not that obvious. The reason could be that the grain size analysis was performed on thin sections which represent very small part of a large scale trend. For a representative grain size analysis more than 50 grains should have been measured for each thin section. This overall coarsening upward trend was a collection of small coarsening upward cycles in Cook Formation. Some

samples may be taken from a depth representative of coarser grain size on a large scale but sample itself belong to the bottom of small coarsening upward cycle. Most important reason could be that samples were not selected on the basis of grain size but for the possibility of the presence of chlorite coatings.

9.4 Mineralogy

Cook Formation sandstones are classified as subarkosic to arenites (Figure 8.1) of a cratonic interior to transitional continental provenance (Figure 8.2). Angular to sub angular grains showed textural immaturity of sandstones. Mineralogy remained more or less similar within formation except few exceptions of carbonate cement. Increasing porosity trend was observed with increasing grain size (Figure 8.3). Most of the samples were moderately to well sorted which correspond to relatively high porosity and permeability of reservoir (Beard and Weyl, 1973).

9.5 Clay mineralogy

Most common and abundant clay mineral found in Cook Formation in both areas was kaolinite. Illite and chlorite were found in similar proportions after kaolinite (Figure 9.2). For Clay mineral XRD analysis, five samples (due to lack of time) were selected from Cook Formation on the basis of high chlorite proportion. It should be considered that these clay minerals are a fraction of total clay present in each sample, and their proportion is an estimated value acquired form Newmod(II) after matching the experimental XRD pattern with standards provided in software.

9.5.1 Chlorite

Chlorite mineral present in the samples could be both detrital and authigenic in origin. In Cook Formation it found as flaky coats over the detrital grain surfaces (Figure 8.23, 8.24 and 8.25), indicating authigenic origin. In some places it also appeared as sheet-like forms (Figure 8.17d, Figure 8.23d).

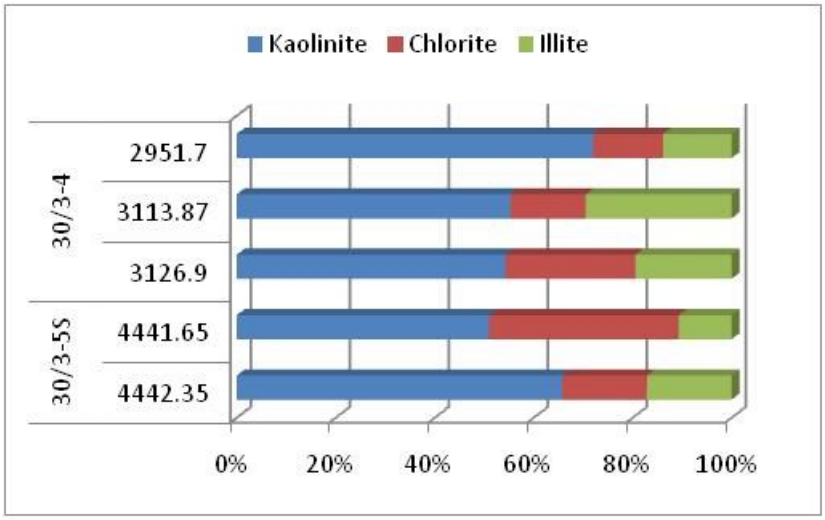

Figure 9.2 Clay mineralogy of chlorite coated samples.

9.5.1.1 Chlorite coating and precursor

Chlorite coating was found in samples of Cook Formation of the Veslefrikk area which was interpreted as shallow deltaic depositional setting. Flaky chlorite structures were found in the middle part of Cook Formation in patches and between kaolinite matrixes, occasionally with illite (Figure 8.25). This chlorite proportion kept on growing with depth and transformed into partial grain coating. Around the base of Cook Formation in Veslefrikk, chlorite coats covered significant area on detrital grain surfaces (Figure 8.23) inhibiting quartz overgrowths and preserving porosity.

Chlorite requires an iron-rich precursor to form grain coats. In the presence of an iron rich clay precursor attached to the detrital grain in form of a rim, above 90-120°C, chlorite coatings can form. Precursor is a prerequisite for chlorite coating. This precursor is actually depositional environment dependent and it determines the amount and extent of coating. Aagaard et al. (2000) suggested that the precursor of chlorite coating forms in early diagenesis and chlorite starts to re-crystallise at intermediate depth.

Precursor must be covering all the surface of the grain, otherwise quartz precipitation can start from the smallest available surface of detrital grain. Uplift of the reservoir can destroy its preserved porosity, as soon as the reservoir enters into mechanical compaction regime and low temperatures i.e. 70°C, the smallest fracture or uncoated surface of the grain

can become the source of quartz cementation. Early introduction of iron-rich clay precursor and rapid burial until 90°C temperature zone is ideal scenario for the formation of chlorite coating.

Matlack et al. (1989) suggested that grain coatings are formed when water with clay suspensions passes through pores of sand and deposits a significant amount of suspended clay on sand grains. Cook Formation in Veslefrikk area is interpreted as tidal and shallow marine, prograding delta setting, justifying the presence of clay in mineral assemblage. Sand bodies formed in this setting could get subaerially exposed due to low tide or fluctuation in the sea level. Freshly depositing sands are more permeable and porous making it possible for meteoric water to percolate and deposit suspended detrital clays. These clays can stick to the grain surfaces and later act as a precursor for chlorite coating. Cook Formation in Veslefrikk has porefilling, disoriented clay, indicating some influence of meteoric water. Another possible explanation could be the stormy condition, in which fine clays could become suspension in water due to agitation and this water can transport the clay suspension into already submerged sand bodies such as compound dunes sand bars, turbidites and low stand fans etc. However, evidence of subaerial exposure such as, mud cracks or root marks were not found in any of the cores of Cook Formation.

Samples were rich with mud drapes. Mud drapes are very fine clay layers deposited in a sand body during relatively long low energy intervals (tidal times). These mud drapes can act as a source for precursor in tidal environments. Another possibility of clay rims can be the fecal material of organisms living in continuously depositing sediments. Needham et al. (2005) produced biogenic clay rims from the fecal material of burrowing organisms. Biogenic rims strongly resembled with inherited and infiltrated clay rims. This could suggest that grain coating chlorite can be the ultimate consequence of sediment ingestion and excretion by the sediment dwelling organisms (Needham et al., 2005).

Depositional setting of Cook Formation in Veslefrikk area appears to be favourable for the formation of chlorite grain coats. Cook Formation has temperature above 119°C in both wells (Table 6.1), which would have been much lower in the geological past. Since no signs of subaerial exposure were found during core analysis, two possibilities for the introduction of iron rich clay precursor in the system are considered: the fluvio-deltaic deposition of iron rich clay in Cook Formation (Ehrenberg, 1993); and/or through biogenic means, as

bioturbation is observed in the lower part of Cook Formation in 30/3-4. In well 30/3-5S, cores were not available below 4445 meters depth, but considering the similar depositional trends of Cook Formation in both wells, possibility of biogenic source of clay rims cannot be ruled out.

Considering the depositional environment of Cook Formation, it can be suggested that the source of clay precursor can be biogenic activity to some extent but mainly it is by mechanical infiltration of clay particles into sand bodies. In Veslefrikk area, precursor was suggested to be berthierine by Ehrenberg (1993). Formation of chlorite coating possibly took place after the conversion of precursor clay rims into berthierine between 65°C to 100°C (Aagaard et al., 2000). Increasing temperature (between 80°C-100°C) due to further burial caused precipitation of chlorite. Chlorite formed as a coating material where berthierine rims were present and preserved porosity from quartz overgrowths. Effectiveness of chlorite coats depend upon the distribution and continuity of berthierine rims on detrital grains.

In Oseberg area chlorite coating was not found which could be due to the absence of precursor. Precursor may not be present due to reworking of the sediments, as it is interpreted as upper shoreface depositional setting. Precursor rims might have eroded from the grain surfaces during reworking of the sediments (Wilson, 1992) and/or reworking had been started before precursor was attached to the grains. Extent of reworking can be estimated by comparing the amount of porefilling kaolinite in the sample. Aagaard et al. (2000) also noticed the absence of well-developed chlorite coatings in this area.

9.5.1.2 Chlorite coating and porosity

Samples which showed chlorite coatings in SEM were analysed through XRD clay analysis (Figure 9.2). Chlorite proportion from total clay fractions are plotted with porosity (Figure 9.3), indicating a relationship between the two.

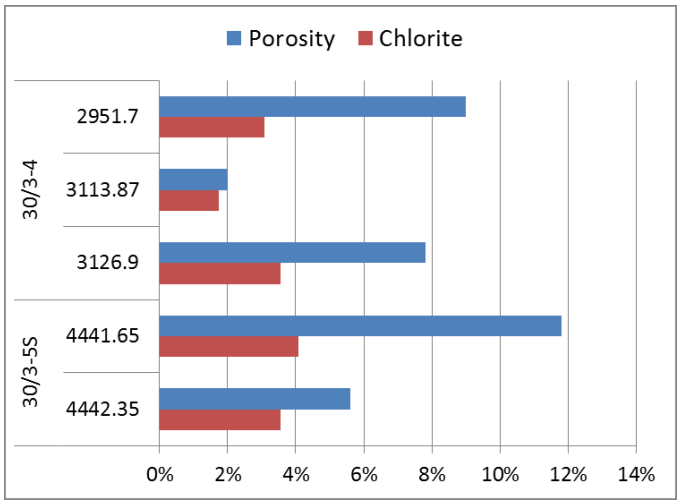

Figure 9.3 High porosity and chlorite content in Cook Formation.

In the Figure 9.3 (above), all samples have sufficient amount of chlorite to form grain coatings and preserve porosity, but from the data it looks like chlorite was not effective in preserving porosity in some samples. For example, sample 3113.87 and 4442.35 have similar amount of chlorite but low porosities compared to others samples. This is possibly because chlorite is present in sample but not in the form of coatings which could be related to the fact that these sandstone samples are finer grained than the other samples. It can be seen in Table 8.3 and 8.4 that these two samples have smaller average grain size than the other samples and large proportions of silts as well. Silt can act like a porefilling material in fine grain sandstones. Water with clay suspensions would be less mobile in fine sandstones compared to coarse grain sandstones. Mobility of clay suspensions is necessary for an even distribution of clay as the precursor of chlorite coating; otherwise, the clay suspension may preferentially end up as mud drapes. In coarse grain sandstones, clay suspension can flow easily due to large pore spaces enhancing the possibility of ending up as a clay precursor on grain surfaces. The suggested process also indicates that clay precursor was introduced after the final deposition of the sand.

9.5.2 Kaolinite

Both detrital and authigenic kaolinite were encountered in Cook Formation, however, amount of authigenic kaolinite was dominant on all other clay minerals. Vermicular, stacked-booklets, and well defined sharp edges (euhedral) were observed suggesting its authigenic

origin (Wilson et al., 2014), which was most likely a product of the dissolution and leaching of feldspar grains (Figure 8.12a and 8.13). Detrital kaolinite was observed as porefilling aggregates of disoriented small grains. Kaolinite ranged from 4% to 13% in all the samples but in Cook Formation it appeared to be consistently between 6-9% indicating similarities of depositional processes. Vermicular kaolinite was observed as a source of illite. In Oseberg area, porefilling kaolinite proportion was relatively low suggesting reworking of sediments.

9.5.3 Illite

Illite was found as fibrous mineral, mostly attached to kaolinite matrix. This morphology of illite is regarded as the representative of earliest stages of illite formation (Wilson et al., 2014). It was found in a constant proportion throughout samples both in bulk and clay proportions. Illite can be formed by two mechanisms i.e. by replacement of smectite, or by replacement of kaolinite (Bjørlykke and Aagaard, 1992). Since, no illite after smectite was found in any of the samples, kaolinite is the possible source for illite. This is also supported by SEM observations which show illite growing in between the vermicular book-stack grins of kaolinite. However, illite was not observed as a coating mineral. Temperature required to form illite from kaolinite is 130°C, which was not achieved in well 30/3-5S, but it is very close to it in well 30/3-4. Kaolinite requires potassium to produce illite, but not much K-feldspar was observed in the samples, most of the originally K-feldspar grains found are albitized.

9.6 Cook Formation as a reservoir

Hydrocarbon reservoirs are influenced by various factors ranging from micro to macro level. Most important factors include depositional environment, mechanical compaction, and burial diagenesis. Depending upon the combined influence of these factors, porosity, and permeability of a reservoir is developed or destroyed. A combination of these two parameters determines the quality of a reservoir.

9.6.1 Depositional environment

Cook Formation was deposited in a range of depositional settings, however in Veslefrikk, it was characterised as tidally influenced prograding delta setting. Identified

facies (Table 7.2) represent poor (Facies B3 and B4), moderate (Facies B1, B2, C1, and C2) and good (Facies A1 and A2) reservoir quality. Facies B4 was mainly mudstone with thin layers of very fine sandstones, making it a bad or poor reservoir due to rather little expected porosity and almost negligible permeability. Facies B3 was overlying facies B4. Facies B3 contained more sand then B4 but was intensely bioturbated. Bioturbation reduces the permeability of the reservoir, making it a bad medium for hydrocarbon mobility. Medium to fine grained relatively cleaner sandstones (Facies B1, B2, C1, and C3) were observed to have good porosity, occasional thin layer and drapes of mud were found which can affect the permeability of reservoir. Carbonate cementation was another issue with these sandstones decreasing their reservoir quality. These sandstones were classified as moderate to poor reservoirs.

Cook Formation of Oseberg area was observed to have medium to fine grained, occasionally cemented, porous sandstones (Facies A1 and A2). In this area Cook, Formation consists of well sorted grains, fewer and thinner mud layers and no bioturbation. These properties place it in good reservoir category. High porosity in this area could be due to well sorted grains and minor quartz cementation. Since, permeability of sandstones was not measured during this study; reservoir quality is an estimate of observed porosity.

9.6.2 Mechanical compaction

Lander and Walderhaug (1999) suggested that reservoir quality of quartz-rich sandstones is controlled by mechanical compaction and quartz cementation. Porosity starts to decrease right after deposition due to mechanical compaction, making it the main porosity destroying mechanism in most cases. Cook Formation consists on moderately to well sorted sandstones, with angular to sub angular grains. Mechanical compaction appears to have a high to moderate affect on Cook Formation which can be reflected by IGV values (Table 8.1) ranging from 23% to 41%. High values of IGV indicate carbonate cementation. The effect of mechanical compaction stops as soon as quartz cementation starts which provides stability to grain contacts and stops re-orientation. In Cook Formation, more than 2% quartz cement was observed in many samples, which is considered sufficient to stop mechanical compaction by Bjørlykke and Jahren (2010).

9.6.3 Diagenetic processes

Diagenetic processes can play an important role in creating or destroying porosities in sandstones. After mechanical compaction, cements are considered to be the most effective porosity destroying factors in most cases.

The effect of kaolinite was considered as neutral to bad depending upon its proportion. Porosity was observed to be low in samples where kaolinite was in high proportions. Because of the shape and form of kaolinite, it was considered to be of authigenic origin indicating the leaching of feldspar through meteoric water. Kaolinite can produce illite at temperatures around 130°C if there is some potassium available in the system. Illite can also be produced from smectite at lower temperature (70°C). Authigenic illite can destroy permeability of the reservoir due to its fibrous form. However, illite was found only in negligible amounts in Cook Formation indicating absence or very little quantity of smectite and potassium during deposition.

Chlorite was formed by precursor clay at temperatures between 65°C to 100°C. It was observed as coating and porefilling mineral. Over all, it has a good influence on reservoir quality of Cook Formation, where it formed continuous coatings over detrital grains and inhibited quartz cementation. In samples where it was found as porefilling mineral its affect was observed as bad to neutral. In Figure 9.3 it can be noticed that chlorite acted as porosity enhancing material in some samples, while in others it could not preserve porosity.

This diagenetic scenario took place in steps from deposition until the development of reservoir. During and after the deposition of sands, mechanical infiltration of iron-rich clay took place. At low temperatures (less than 70°C) berthierine rims around detrital grains formed, along with mechanical compaction and grain reorientation. Leaching and dissolution of feldspar through meteoric water produced authigenic kaolinite and secondary porosity. As the temperature rose above 70°C, precipitation of quartz overgrowths started. Berthierine started to precipitate as chlorite coatings with increasing burial depths and temperatures.

10. Conclusions

1. Depositional environment of Cook Formation is suggested to be tidal, prograding delta setting in Veslefrikk and upper shoreface in Oseberg. Shallow marine environments with fine to coarse grains sand (given that reworking of the grains is not too vigorous) are proposed to be optimal locations of chlorite coatings such as in Veslefrikk.
2. Chlorite proved to be more efficient in preserving the porosity in fine to medium grain sandstones, while in fine to very fine sandstones it was not that effective. This could be due to the restricted mobility of water and limited mechanical infiltration of clay precursor. Mechanical infiltration mainly, and bioturbation to minor extent are proposed clay precursor producing mechanisms in Veslefrikk.
3. Cook Formation maintained porosity feasible to act as a reservoir at depths more than 3000 metres and temperatures ranging from 118°C to 138°C in Veslefrikk area. This is because of the presence chlorite coatings which inhibited quartz overgrowths by covering the surface of detrital grains. Chlorite coatings were observed to be less than 10 micron thick.
4. It was observed during this study that reservoir properties of Cook Formation depend largely upon the inhibition of quartz overgrowths and carbonate cementation. Carbonate cement can dissolve and create secondary porosity during diagenesis, but for the inhibition of quartz cementation, well developed chlorite coating played a vital part.
5. Carbonate cement and porefilling kaolinite were observed as porosity destroying elements. Quartz overgrowths were mostly found in struggle with chlorite coatings; still it occupied some amount of porosity.
6. Samples from Oseberg area showed high porosities mostly because of well sorted grains due to reworking. Chlorite coats or precursors were not observed. Siderite cement was observed as porosity destroying element in this area.
7. Based on the results of this study, Cook Formation is considered as moderate to good reservoir. However, it is reasonable to conclude that it is a heterogeneous sandstone body in terms of reservoir qualities.

11. References

AAGAARD, P., JAHREN, J. S., HARSTAD, A. O., NILSEN, O. & RAMM, M. 2000. Formation of grain-coating chlorite in sandstones. Laboratory synthesized vs. natural occurrences. *Clay Minerals,* 35**,** 261-261.

AASE, N. E., BJORKUM, P. A. & NADEAU, P. H. 1996. The effect of grain-coating microquartz on preservation of reservoir porosity. *AAPG bulletin,* 80**,** 1654-1673.

AJDUKIEWICZ, J. M. & LANDER, R. H. 2010. Sandstone reservoir quality prediction: The state of the art. *AAPG Bulletin,* 94**,** 1083-1091.

BADLEY, M. E., PRICE, J. D., RAMBECH DAHL, C. & AGDESTEIN, T. 1988. The structural evolution of the northern Viking Graben and its bearing upon extensional modes of basin formation. *Journal of the Geological Society,* 145**,** 455-472.

BEARD, D. & WEYL, P. 1973. Influence of texture on porosity and permeability of unconsolidated sand. *AAPG bulletin,* 57**,** 349-369.

BERGER, A., GIER, S. & KROIS, P. 2009. Porosity-preserving chlorite cements in shallow-marine volcaniclastic sandstones: Evidence from Cretaceous sandstones of the Sawan gas field, Pakistan. *AAPG bulletin,* 93**,** 595-615.

BJØRLYKKE, K. & AAGAARD, P. 1992. *Clay minerals in North Sea sandstones*, SEPM Society for Sedimentary Geology.

BJØRLYKKE, K. & JAHREN, J. 2010. Sandstones and Sandstone Reservoirs. *Petroleum Geoscience.* Springer Berlin Heidelberg.

BJØRLYKKE, K., NEDKVITNE, T., RAMM, M. & SAIGAL, G. C. 1992. Diagenetic processes in the Brent Group (Middle Jurassic) reservoirs of the North Sea: an overview. *Geological Society, London, Special Publications,* 61**,** 263-287.

BLOCH, S., LANDER, R. H. & BONNEL, L. 2002. Anomalously high porosity and permeability in deeply buried sandstone reservoirs: Origin and predictability. *AAPG bulletin,* 86**,** 301-328.

BLOTT, S. J. & PYE, K. 2001. GRADISTAT: a grain size distribution and statistics package for the analysis of unconsolidated sediments. *Earth Surface Processes and Landforms,* 26**,** 1237-1248.

BRENNAND, T. P., VAN HOORN, B., JAMES, K. H. & GLENNIE, K. W. 1998. Historical Review of North Sea Exploration. *Petroleum Geology of the North Sea.* Blackwell Science Ltd.

CANT, D. 1992. Subsurface facies analysis. *Facies Models: Response to Sea level Change (Walker, RG; James, NP***,** 195-218.

CHARNOCK, M. A., KRISTIANSEN, I. L., RYSETH, A. & FENTON, J. P. G. 2001. Sequence Stratigraphy of the Lower Jurassic Dunlin Group, Northern North Sea. *In:* OLE, J. M. & TOM, D. (eds.) *Norwegian Petroleum Society Special Publications.* Elsevier.

CHRISTIANSSON, P., FALEIDE, J. I. & BERGE, A. M. 2000. Crustal structure in the northern North Sea: an integrated geophysical study. *Geological Society, London, Special Publications,* 167**,** 15-40.

CHUHAN, F. A., KJELDSTAD, A., BJØRLYKKE, K. & HØEG, K. 2002. Porosity loss in sand by grain crushing—experimental evidence and relevance to reservoir quality. *Marine and Petroleum Geology,* 19**,** 39-53.

COLEMAN, J. M. & PRIOR, D. B. 1982. Deltaic Environments of Deposition. *Sandstone Depositional Environments: AAPG Memoir 31***,** 139.

DALRYMPLE, M. 2001. Fluvial reservoir architecture in the Statfjord Formation (northern North Sea) augmented by outcrop analogue statistics. *Petroleum Geoscience,* 7**,** 115-122.

DICKINSON, W. R., BEARD, L. S., BRAKENRIDGE, G. R., ERJAVEC, J. L., FERGUSON, R. C., INMAN, K. F., KNEPP, R. A., LINDBERG, F. A. & RYBERG, P. T. 1983. Provenance of North American Phanerozoic sandstones in relation to tectonic setting. *Geological Society of America Bulletin,* 94**,** 222-235.

DOWEY, P. J., HODGSON, D. M. & WORDEN, R. H. 2012. Pre-requisites, processes, and prediction of chlorite grain coatings in petroleum reservoirs: A review of subsurface examples. *Marine and Petroleum Geology,* 32**,** 63-75.

DREYER, T. & WIIG, M. 1995. Reservoir architecture of the Cook Formation on the Gullfaks Field based on sequence stratigraphic concepts. *In:* R.J. STEEL, V. L. F. E. P. J. & MATHIEU, C. (eds.) *Norwegian Petroleum Society Special Publications.* Elsevier.

EDMONDS, D. A. & SLINGERLAND, R. L. 2007. Mechanics of river mouth bar formation: Implications for the morphodynamics of delta distributary networks. *Journal of Geophysical Research: Earth Surface,* 112**,** n/a-n/a.

EHRENBERG, S. 1993. Preservation of anomalously high porosity in deeply buried sandstones by grain-coating chlorite: examples from the Norwegian continental shelf. *AAPG Bulletin,* 77**,** 1260-1286.

FALEIDE, J. I. & BERGE, A. M. 2000. The geometries and deep structure of the northern North Sea rift system. *Dynamics of the Norwegian Margin,* 167**,** 41.

FJELDSKAAR, W., TER VOORDE, M., JOHANSEN, H., CHRISTIANSSON, P., FALEIDE, J. I. & CLOETINGH, S. A. P. L. 2004. Numerical simulation of rifting in the northern Viking Graben: the mutual effect of modelling parameters. *Tectonophysics,* 382**,** 189-212.

FOLK, R. L. 1951. Stages of textural maturity in sedimentary rocks. *Journal of Sedimentary Research,* 21**,** 127-130.

FOLK, R. L. 1980. *Petrology of sedimentary rocks*, Hemphill Publishing Company.

FOLK, R. L. & WARD, W. C. 1957. Brazos River bar: a study in the significance of grain size parameters. *Journal of Sedimentary Research,* 27.

FOLKESTAD, A., VESELOVSKY, Z. & ROBERTS, P. 2012. Utilising borehole image logs to interpret delta to estuarine system: A case study of the subsurface Lower Jurassic Cook Formation in the Norwegian northern North Sea. *Marine and Petroleum Geology,* 29**,** 255-275.

GABRIELSEN, R., FÆRSETH, R., STEEL, R., IDIL, S. & KLØVJAN, O. 1990. Architectural styles of basin fill in the northern Viking Graben. *Tectonic evolution of the North Sea rifts,* 181**,** 158-179.

GLENNIE, K. & UNDERHILL, J. 1998. Origin, development and evolution of structural styles. *Petroleum Geology of the North Sea: Basic Concepts and Recent Advances, Fourth Edition***,** 42-84.

HESLOP, K. & HESLOP, A. 2003. Interpretation of Shaly Sands. *LPS DiaLog,* 15**,** 2003.

LANDER, R. H., LARESE, R. E. & BONNELL, L. M. 2008. Toward more accurate quartz cement models: The importance of euhedral versus noneuhedral growth rates. *AAPG Bulletin,* 92**,** 1537-1563.

LANDER, R. H. & WALDERHAUG, O. 1999. Predicting porosity through simulating sandstone compaction and quartz cementation. *AAPG bulletin,* 83**,** 433-449.

LIVBJERG, F. & MJØS, R. 1989. The Cook Formation, an offshore sand ridge in the Oseberg area, northern North Sea. *In:* COLLINSON, J. D. (ed.) *Correlation in Hydrocarbon Exploration.* Springer Netherlands.

LUNDEGARD, P. D. 1994. Mixing zone origin of ^{13}C-depleted calcite cement: Oseberg Formation sandstones (Middle Jurassic), Veslefrikk Field, Norway. *Geochimica et Cosmochimica Acta,* 58.

LYNGSIE, S. B., THYBO, H. & RASMUSSEN, T. M. 2006. Regional geological and tectonic structures of the North Sea area from potential field modelling. *Tectonophysics,* 413**,** 147-170.

MARCHAND, A. M., SMALLEY, P. C., HASZELDINE, R. S. & FALLICK, A. E. 2002. Note on the importance of hydrocarbon fill for reservoir quality prediction in sandstones. *AAPG bulletin,* 86**,** 1561-1572.

MARCUSSEN, Ø., MAAST, T. E., MONDOL, N. H., JAHREN, J. & BJØRLYKKE, K. 2010. Changes in physical properties of a reservoir sandstone as a function of burial depth – The Etive Formation, northern North Sea. *Marine and Petroleum Geology,* 27**,** 1725-1735.

MARJANAC, T. & STEEL, R. J. 1997. Dunlin Group sequence stratigraphy in the northern North sea: a model for Cook Sandstone deposition. *AAPG bulletin,* 81**,** 276-292.

MATLACK, K. S., HOUSEKNECHT, D. W. & APPLIN, K. R. 1989. Emplacement of clay into sand by infiltration. *Journal of Sedimentary Research,* 59.

MCCUBBIN, D. G. 1982. Barrier-Island and Strand-Plain Facies. *Sandstone Depositional Environments: AAPG Memoir 31***,** 247.

MORAD, S. 2009. *Carbonate Cementation in Sandstones: Distribution Patterns and Geochemical Evolution (Special Publication 26 of the IAS)*, John Wiley & Sons.

MUTO, T. & STEEL, R. J. 1997. The Middle Jurassic Oseberg Delta, northern North Sea: a sedimentological and sequence stratigraphic interpretation. *AAPG bulletin,* 81**,** 1070-1086.

NEEDHAM, S. J., WORDEN, R. H. & MCILROY, D. 2005. Experimental Production of Clay Rims by Macrobiotic Sediment Ingestion and Excretion Processes. *Journal of Sedimentary Research,* 75**,** 1028-1037.

NORLEX. 2015. *Norwegian Interactive Offshore Stratigraphic Lexicon* [Online]. Available: http://www.nhm2.uio.no/norlexlite/N_Viking_Graben.html [Accessed 22, May 2015].

NORWEGIAN PETROLEUM DIRECTORATE. 2013. *Recoverable resources* [Online]. Available: http://npd.no/Global/Engelsk/3-Publications/Facts/Facts2014/Facts_2014_nett_.pdf [Accessed January 12, 2015].

NORWEGIAN PETROLEUM DIRECTORATE. 2014. *Veslefrikk* [Online]. Available: http://www.npd.no/en/publications/facts/facts-2013/chapter-10/veslefrikk/ [Accessed November 04, 2014].

NYSTUEN, J. P. & FÄLT, L.-M. 1995. Upper Triassic-Lower Jurassic reservoir rocks in the Tampen Spur area, Norwegian North Sea. *In:* HANSLIEN, S. (ed.) *Norwegian Petroleum Society Special Publications*. Elsevier.

PAXTON, S., SZABO, J., AJDUKIEWICZ, J. & KLIMENTIDIS, R. 2002. Construction of an intergranular volume compaction curve for evaluating and predicting compaction and porosity loss in rigid-grain sandstone reservoirs. *AAPG bulletin,* 86**,** 2047-2067.

RIDER, M. H. 2002. *The geological interpretation of well logs*, Rider-French Consulting Ltd.

ROE, S. & STEEL, R. 1985. SEDIMENTATION, SEA-LEVEL RISE AND TECTONICS AT THE TRIASSIC-JURASSIC BOUNDARY (STATFJORD FORMATION), TAMPEN SPUR, NORTHERN NORTH-SEA. *Journal of Petroleum Geology,* 8**,** 163-186.

ROSSI, C., MARFIL, R., RAMSEYER, K. & PERMANYER, A. 2001. Facies-Related Diagenesis and Multiphase Siderite Cementation and Dissolution in the Reservoir Sandstones of the Khatatba Formation, Egypt's Western Desert. *Journal of Sedimentary Research,* 71**,** 459-472.

RUPKE, L., SCHMALHOLZ, S., SCHMID, D. & PODLADCHIKOV, Y. 2008. Automated thermotectonostratigraphic basin reconstruction: Viking Graben case study. *Aapg Bulletin,* 92**,** 309-326.

SAIGAL, G. & BJØRLYKKE, K. 1987. Carbonate cements in clastic reservoir rocks from offshore Norway—relationships between isotopic composition, textural development and burial depth. *Geological Society, London, Special Publications,* 36**,** 313-324.

SHINN, E. A. & ROBBIN, D. M. 1983. Mechanical and chemical compaction in fine-grained shallow-water limestones. *Journal of Sedimentary Research,* 53.

SLATT, R. M. 2013. Chapter 6 - Geologic Controls on Reservoir Quality. *In:* ROGER, M. S. (ed.) *Developments in Petroleum Science.* Elsevier.

STATOIL. 2013. *Veslefrikk* [Online]. Available: http://www.statoil.com/en/ouroperations/explorationprod/ncs/veslefrikk/pages/default.aspx [Accessed November 05 2014].

STEEL, R. Triassic–Jurassic megasequence stratigraphy in the Northern North Sea: rift to post-rift evolution. Geological Society, London, Petroleum Geology Conference series, 1993. Geological Society of London, 299-315.

STORVOLL, V., BJØRLYKKE, K., KARLSEN, D. & SAIGAL, G. 2002. Porosity preservation in reservoir sandstones due to grain-coating illite: a study of the Jurassic Garn Formation from the Kristin and Lavrans fields, offshore Mid-Norway. *Marine and Petroleum Geology,* 19**,** 767-781.

SUN, Z.-X., SUN, Z.-L., YAO, J., WU, M.-L., LIU, J.-R., DOU, Z. & PEI, C.-R. 2014. Porosity preservation due to authigenic chlorite coatings in deeply buried Upper Triassic Xujiahe Formation sandstones, Sichuan Basin, Western China. *Journal of Petroleum Geology,* 37**,** 251-267.

TAYLOR, T. R., GILES, M. R., HATHON, L. A., DIGGS, T. N., BRAUNSDORF, N. R., BIRBIGLIA, G. V., KITTRIDGE, M. G., MACAULAY, C. I. & ESPEJO, I. S. 2010. Sandstone diagenesis and reservoir quality prediction: Models, myths, and reality. *AAPG bulletin,* 94**,** 1093-1132.

UNDERHILL, J. R. 1998. Jurassic. *In:* GLENNIE, K. W. (ed.) *Petroleum Geology of the North Sea: Basic Concepts and Recent Advances.* Oxford, UK.: Blackwell Science Ltd.

VOLLSET, J. & DORÉ, A. G. 1984. *A revised Triassic and Jurassic lithostratigraphic nomenclature for the Norwegian North Sea*, Norwegian Petroleum Directorate.

WALDERHAUG, O. 1990. A fluid inclusion study of quartz-cemented sandstones from offshore mid-Norway; possible evidence for continued quartz cementation during oil emplacement. *Journal of Sedimentary Research,* 60**,** 203-210.

WALDERHAUG, O. & BJØRKUM, P. A. 1992. Effect of meteoric water flow on calcite cementation in the Middle Jurassic Oseberg Formation, well 30/3-2, Veslefrikk Field, Norwegian North Sea. *Marine and Petroleum Geology,* 9**,** 308-318.

WEIMER, R. J., HOWARD, J. D. & LINDSAY, D. R. 1982. Tidal flats and associated tidal channels. *Sandstone Depositional Environments: American Association of Petroleum Geologists, Memoir,* 31**,** 191-245.

WELTON, J. E. 2003. *SEM petrology atlas*, American Association of Petroleum Geologists Tulsa^ eOklahoma Oklahoma.

WILSON, M. D. 1992. Inherited grain-rimming clays in sandstones from eolian and shelf environments: their origin and control on reservoir properties.

WILSON, M. J., WILSON, L. & PATEY, I. 2014. The influence of individual clay minerals on formation damage of reservoir sandstones: a critical review with some new insights. *Clay Minerals,* 49**,** 147-164.

ZIEGLER, P. 1982. Geological Atlas of Central and Western Europe. *Shell International Petroleum, Maatschappij BV, Amsterdam*.

12. Appendices

Appendix A: Sedimentological logs

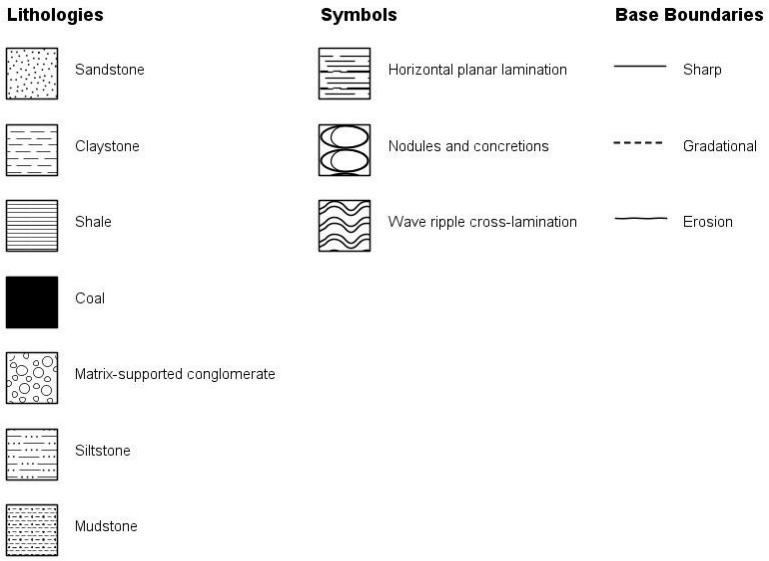

Figure 12.1 Symbols legend.

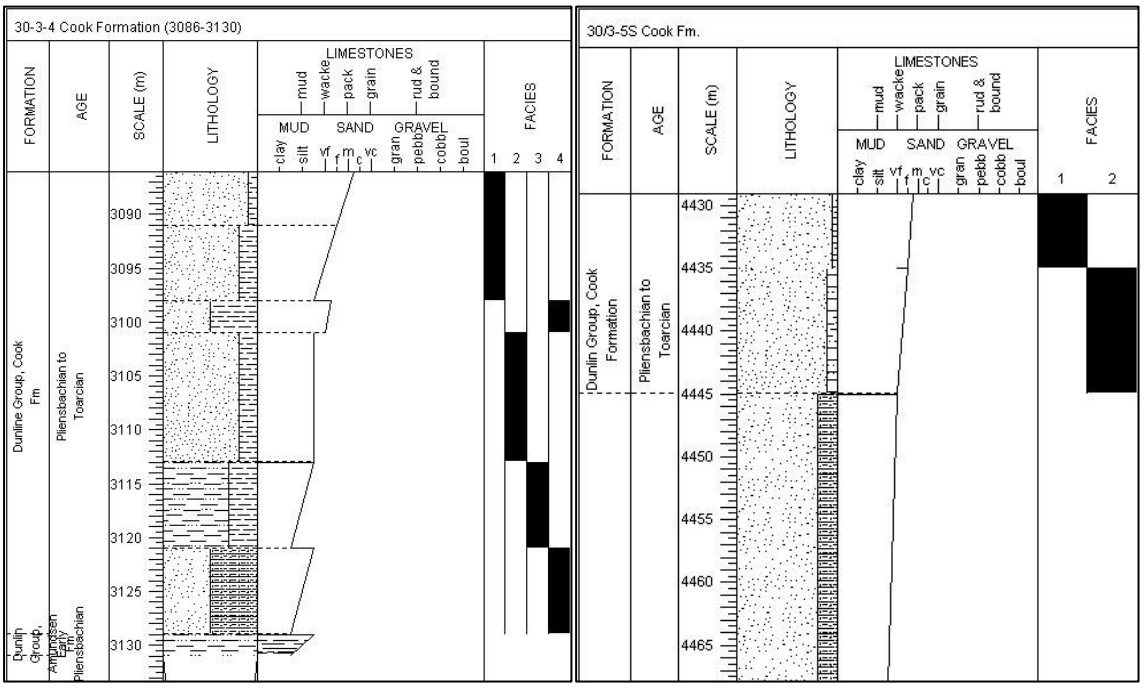

Figure 12.2 Left: core description sedimentary log of Cook Formation in well 30/3-4. Facies 1,2,3,4 represent B1, B2, B3, B4, respectively. Right: Cook Formation in well 30/3-5S, facies 1 and 2 represent C1 and C2, respectively. Below the depth of 4445 meters, log is made on the basis of electrical logs. Core description logs of Brent Group can be seen on the next page.

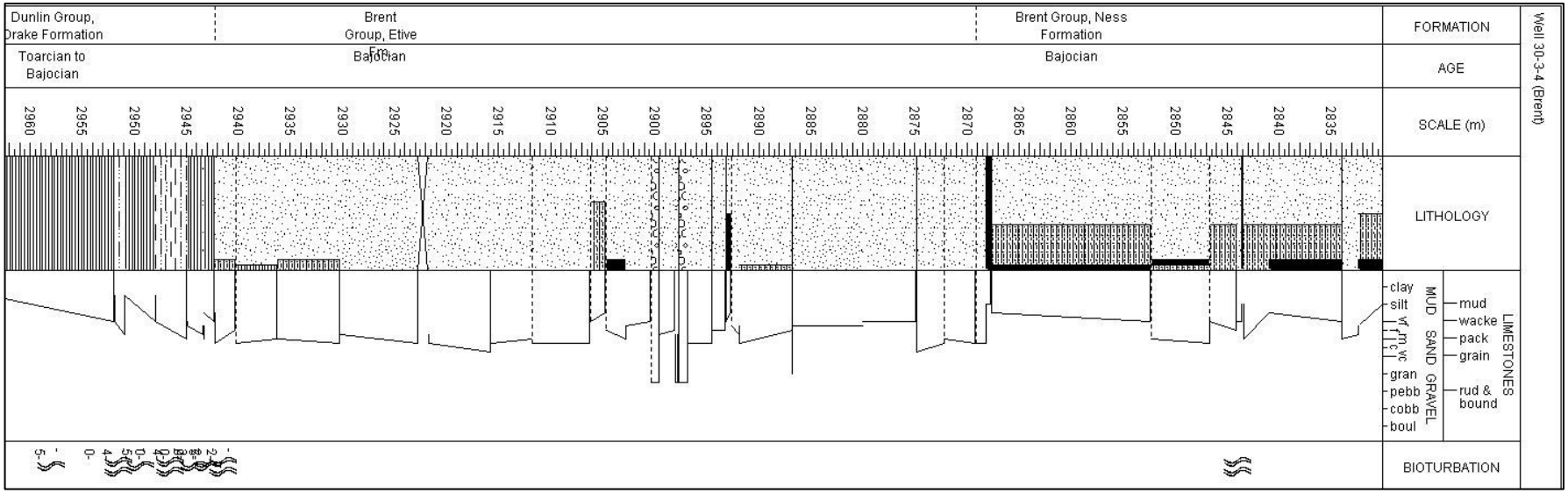
Dunlin Group, Drake Formation
Brent Group, Etive Fm
Brent Group, Ness Formation
Toarcian to Bajocian
Bajocian
Bajocian
FORMATION
AGE
SCALE (m)
LITHOLOGY
clay
silt
vf f m c vc
gran
pebb
cobb
boul
MUD
SAND
GRAVEL
mud
wacke
pack
grain
rud & bound
LIMESTONES
BIOTURBATION
Well 30-3-4 (Brent)

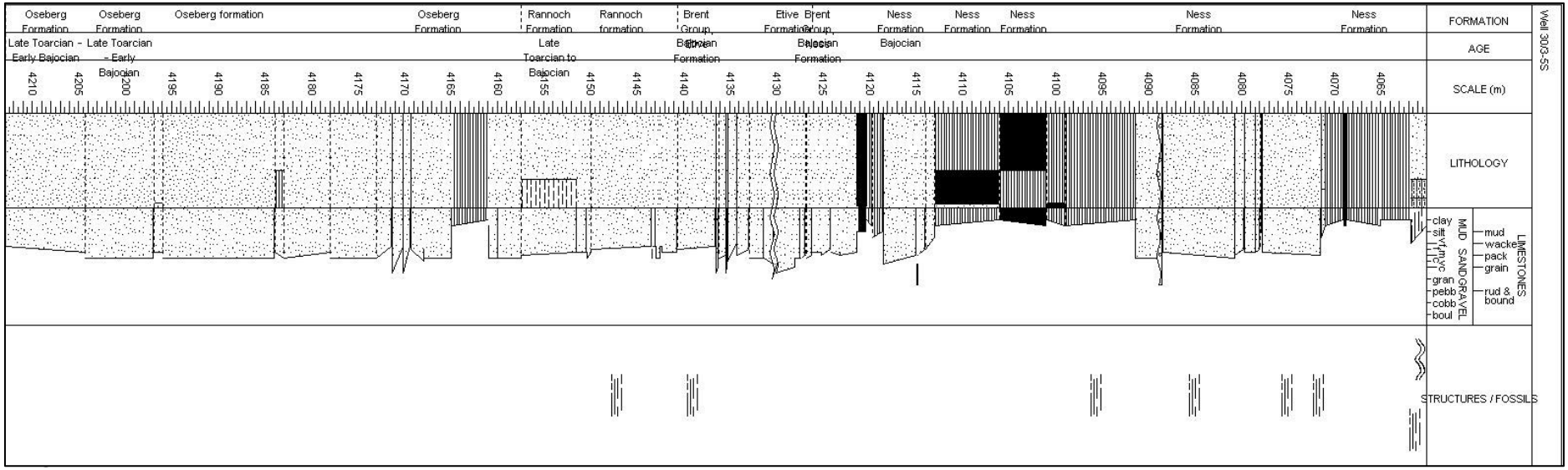
Oseberg Formation
Oseberg Formation
Oseberg formation
Oseberg Formation
Rannoch Formation
Rannoch formation
Brent Group, Etive Formation
Etive Formation
Brent Group, Ness Formation
Ness Formation
Ness Formation
Ness Formation
Ness Formation
Ness Formation
Late Toarcian - Early Bajocian
Late Toarcian - Early Bajocian
Late Toarcian to Bajocian
Bajocian
Bajocian
FORMATION
AGE
SCALE (m)
LITHOLOGY
clay
silt
vf f m c vc
gran
pebb
cobb
boul
MUD
SAND
GRAVEL
mud
wacke
pack
grain
rud & bound
LIMESTONES
STRUCTURES / FOSSILS
Well 30/3-5S

Appendix B: Chlorite composition and TVD for samples from well 30/3-5S

Sample	O	Mg	Al	Si	Fe
	27.38	9.47	14.66	21.53	26.96
3126.9	30.13	17.38	15.61	19.67	17.22
	29.18	15.13	16.24	19.97	19.47
	27.05	11.41	13.83	19.04	28.68
3113.87	25.37	4.82	16.29	21.26	32.26
	27.86	8.61	14.17	21.72	26.37
4442.35	27	9.38	14.22	21.49	27.91
	25.57	6.85	13.79	20.61	33.18
4444.7	25.86	6.08	14.8	18.87	34.38
	24.13	5.67	16.04	19.41	34.63
	24.8	6.01	16.28	19.33	33.58

Table 12.1 Average weight percentage of Chlorite grains acquired from SEM.

Measured Depth (mMD)	True Vertical Depth (TVD)
4061.80	2952.00
4086.60	2967.00
4112.43	2986.00
4137.60	3003.00
4181.43	3031.12
4210.34	3050.00
4429.40	3191.14
4435.65	3195.00
4440.75	3198.00
4441.65	3199.66
4442.35	3200.00
4444.70	3201.00

Table 12.2 Measured depths and corresponding true vertical depths of samples in well 30/3-5S.